What do climate projections say about future droughts in Alabama and the Apalachicola-Chattahoochee-Flint River Basin?

by

Nischal Mishra

A thesis submitted to the Graduate Faculty of
Auburn University
in partial fulfillment of the
requirements for the Degree of
Master of Science

Auburn, Alabama
August 1, 2015

Keywords: drought, drought indices, climate change, groundwater, Standardized Precipitation Index, Standardized Precipitation Evapotranspiration Index

Approved by

Puneet Srivastava, Chair, Butler-Cunningham Eminent Scholar and Professor of Biosystems Engineering
Latif Kalin, Professor, School of Forestry and Wildlife Sciences
Ming-Kuo Lee, Robert B. Cook Professor, Department of Geosciences

Abstract

Droughts, often considered the costliest natural disaster, are triggered by severe shortage of water, mainly in the form of precipitation. The Southeast US has been affected by frequent severe droughts in recent years and this calls for a more pragmatic approach to better manage its consequences. The primary objective of this study was to analyze how droughts in Alabama and ACF River Basin will change in future as a result of projected climate change. Commonly used drought indices were computed to quantify the change in droughts.

Historical and future droughts were quantified by the means of Standardized Precipitation Index (SPI) and Standardized Precipitation Evapotranspiration Index (SPEI) and the change in frequency, severity and spatial extent of future droughts were studied using Severity-Area-Frequency (SAF) curves. Precipitation and temperature data, regionally downscaled for the Southeast US for high emission scenario (A2), from three General Circulation Models, Hadley Centre Coupled Model Version 3 (HadCM3), Geophysical Fluid Dynamics Laboratory (GFDL) Model and Community Climate System Model (CCSM), from the Third Coupled Model Inter-comparison Project (CMIP3) archive were used for this study. Data from 1969 to 1999 were used for historical simulation and that from 2039 to 2069 were used for future projections.

The study showed that droughts similar to ones in the past would be observed frequently in future as well. In Alabama, SPI from GFDL and HadCM3 models indicated increasing frequency of droughts with more severity and increased spatial extent in the future. SPI from CCSM model indicated decreased severity of droughts in the future spread over similar area as in the past. This model indicated decreased occurrences of severe and extreme droughts but increased occurrences of moderate

droughts. Similar conclusions were drawn about droughts in the ACF River Basin as well from the respective models and indices.

SPI was also correlated with groundwater levels in the Lower ACF River Basin to determine if it could be used to monitor groundwater conditions in the region. The index, when calculated at timescales between 9 and 12 months, showed strong correlation with groundwater levels in many groundwater wells in the region. The results suggested that it can be used as a tool to monitor groundwater conditions and hydrologic droughts in the Lower ACF River Basin.

The results of this research can be used by policymakers to plan ahead of time for better preparation of drought years. If droughts can be projected well ahead of time, their consequences can be tackled more appropriately. The results will also help us understand expected changes in droughts in the Southeast US and would help us prepare better to mitigate the economic, social and environmental effects of droughts.

Table of Contents

List of Figures

List of Tables

List of Abbreviations

ACF	Apalachicola-Chattahoochee-Flint
AMO	Atlantic Multidecadal Oscillation
AMS	American Meteorological Society
ASCE	American Society of Civil Engineers
CAED	Center for Agribusiness & Economic Development
CCSM	Community Climate System Model
CMIP3	Third Coupled Model Inter-comparison Project
COAPS	Center for Ocean-Atmospheric Prediction Studies
ENSO	El Niño Southern Oscillation
FAO	Food and Agriculture Organization
GCM	General Circulation Models
GDP	Gross Domestic Product
GFDL	Geophysical Fluid Dynamics Laboratory
HadCM3	Hadley Centre Coupled Model Version 3
IPCC	Intergovernmental Panel on Climate Change
NCA	National Climate Assessment
NCAR	National Center for Atmospheric Research

NCDC	National Climatic Data Center
NDMC	National Drought Mitigation Center
NOAA	National Oceanic and Atmospheric Administration
NSF	National Science Foundation
PDO	Pacific Decadal Oscillation
PDSI	Palmer's Drought Severity Index
PET	Potential evapotranspiration
RSM	Regional Spectral Model
SAD	Severity-Area-Duration
SAF	Severity-Area-Frequency
sc-PDSI	Self-calibrating Palmer's Drought Severity Index
SPEI	Standardized Precipitation Evapotranspiration Index
SPI	Standardized Precipitation Index
SRES	Special Report on Emission Scenarios
US	United States
USCoE	United States Army Corps of Engineers
USDA	United States Department of Agriculture
USGS	United States Geological Survey
WMO	World Meteorological Organization

Chapter 1

Introduction

1.1 Background

Water is a crucial resource for sustenance of life on earth. Although almost 71 percent of earth is covered by water, only about 2.5 percent is fresh water and only about 1 percent of this fresh water is available for human consumption (Gleick, 1993). The increasing population and decreasing water supply over the past few decades have stressed available water resources resulting in the need for better water treatment and management practices. The proper management of water resources often influences social, economic and environmental growth of a society. Water hazards cause disruption in water management plans, often halting growth in affected area. Drought is one natural hazard triggered by the shortage of water resources and affects the ecosystem and the economy of the region where it occurs.

Drought, although simple in definition, has proven to be a natural hazard that has been very complex to understand. It can broadly be defined as a shortage in water supply but its causes and implications are not just confined to lack of availability of water. They can be relatively short or long, local or widespread, and the degree of severity varies for each occurrence. Droughts have often been claimed to be the costliest natural hazard. Even a minor drought event can bring immense losses. Since 1900, droughts have caused deaths of more than 11 million people and have affected more than 2 billion people, which is more than by any other physical hazard (FAO, 2013). Although they cannot be prevented, their temporal and spatial identification would enable stakeholders and water users to specifically identify the impacts they

may cause. Also, the policymakers and decision makers would be able to make better plans for drought mitigation.

Shortage of precipitation or snow generally triggers droughts. However, different components of the water cycle and other climatic phenomena influence the characteristics of droughts in the affected region. Certain human activities often ignite droughts. Cutting of trees reduce the soil's capacity to hold water, hence, making it dry. Construction of dams can reduce streamflow causing droughts downstream. Decreased snow pack and glaciers cause droughts in regions where they are the sources of water supply. The land and sea surface temperatures and the atmospheric circulation patterns affect the precipitation in a region. To put it in a nutshell, droughts can often be a outcome of a number of causes.

The severity and impact of droughts usually depend on their causes and the region where they occur. Their impacts last for a longer time and over large areas compared to the impacts from other natural hazards. These impacts, unlike those of floods, show up only after some time and are often more far reaching than one might expect. As droughts limit the water supply in a region, they affect all activities that are dependent on water resources. It often leads to reduction in agricultural production, loss in biodiversity, and increase in soil erosion. This ultimately results into competition among consumers for food and water resources and imbalances in the ecosystem of the region they occur.

In the United States, droughts have been one of the most detrimental natural disasters ever since climatic data have been recorded. Tree ring studies indicate that long and extreme drought events have occurred since as early as the thirteenth century (Weakly, 1965). Although the Great Plains region is considered to be the region that is most susceptible to droughts, they are just as common across the Southeast and the Southwest too. The drought of 2011 affected the southern states of Texas,

New Mexico and Oklahoma the most. Arizona, Kansas, Arkansas, Mississippi, Alabama, Georgia, Florida, South Carolina and North Carolina were among the other affected states. Droughts in the United States have led to increase in the price of food and commodities all across the country. According to a recent study (by Professor Timothy Richards of Arizona State University), the California Drought of 2014 was expected to significantly increase the prices of avocados, lettuce, berries, broccoli, grapes, melon, packaged salad, peppers and tomatoes. United States Drought Monitor predicts that the drought is affecting about 52 million people across California, Texas and Oklahoma (as of April 1, 2015).

Droughts have been known to be occurring since ages and will continue to occur in the future. The recurrence of droughts in the Southeast United States has been a major economic, social and environmental problem for the region. Although there have been efforts to mitigate the consequences, a number of problems have prevented it from being tackled.

The repercussions of climate change can be better managed if we make better choices today. By forecasting droughts with climate models and enforcement of better management practices by governing bodies, droughts will not have catastrophic repercussions or irreversible consequences. Water resource managers and policymakers rely on novel studies that pertain to the present and projected future world scenarios to overcome the obstacles arising from new challenges.

1.2 Problem Statement

The Southeast US has a variable climatic condition and it experiences different kinds of weather and climate events. The future projections of natural disasters like droughts and thunderstorms cannot be done with certainty. Even though this region generally has abundant water, it is highly susceptible to droughts as most of the water resources demand is met by winter precipitation (especially in Alabama and Georgia)

and lack of it immediately causes water troubles. However, Florida receives most of its water because of tropical storms that mostly occur in July and August.

Droughts have been one of the major causes of economic downturn in the region. NCDC (2011) states that the region has experienced the most billion-dollar natural disasters than any other region in United States. Loss of more than \$1 billion was caused because of the major Georgia drought of 2007-2008 and it led to federal lawsuits regarding release of water from Lake Lanier which supplies water to the city of Atlanta (NOAA, 2013).

Droughts have been more frequent and severe in the region since 1980s and this changing nature of droughts forces us to explore them more deeply. Analysis of droughts using projected climate data can provide insight about how climate change will change drought characteristics in the region. There is a significant gap in studies pertaining to changes in droughts in the Southeast US because of climate change. This study intends to bridge this gap so that policymakers and water resource managers can have an insight to the enormity of problems droughts can cause in the future.

1.3 Thesis Objectives

The goal of this study is quantify what the commonly used drought indices say about future droughts in Alabama and the Apalachicola-Chattahoochee-Flint River Basin. The objectives of this thesis are:

1. Analyze the changes in frequency, severity and spatial extent of droughts in Alabama using Severity-Area-Frequency Curves.

2. Analyze the changes in frequency, severity and spatial extent of droughts in the Apalachicola-Chattahoochee-Flint River Basin using Severity-Area-Frequency Curves.

3. Determine the applicability of Standardized Precipitation Index for monitoring groundwater conditions in the lower Apalachicola-Chattahoochee-Flint (ACF) River Basin.

Chapter 2

Review of Literature

2.1 The Hydrologic Cycle

Water is a limited renewable resource. It circles the earth's ocean, atmosphere, and land in various forms through different physical processes. It moves through various pathways, including precipitation in the form of rain and snow, percolation or seepage in rivers and streams, and comes back to the atmosphere through evaporation and transpiration. Water keeps changing its forms between solid, liquid and gas phase constantly. Although about 70 percent of the earth's surface is water, only about 2.5 percent of this is freshwater (Postel et al. 1996). The circulation of this water is critical to sustenance of life on Earth (Jackson et al., 2001) and it accounts for the largest volumetric flow of any material in the biosphere (Chahine 1992).
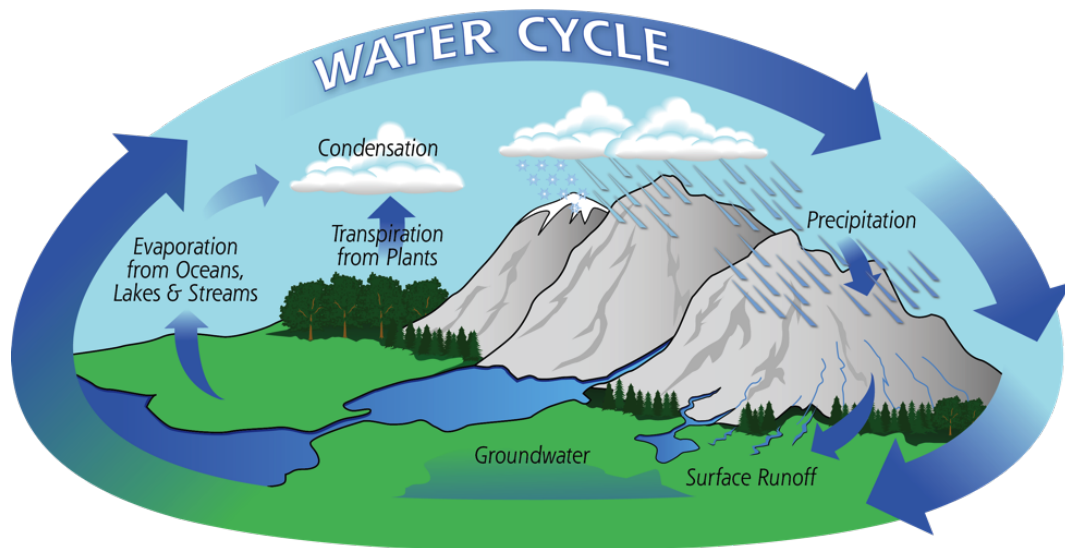
Figure 2.1: Pathways through which water circles the earth.
Source: `http://pmm.nasa.gov/education/water-cycle`

Huntington (2005) showed intensification of the water cycle because of climate change. Change in the usual pattern of water cycle in a region can cause an increase in the frequency of extreme weather events. An increased volume of water in rivers causes flood. Similarly, lack of water availability causes droughts. Drought is an effect, and not merely the cause, of an imbalanced water cycle.

2.2 Droughts

Droughts are basically a consequence of aberrations in the normal pattern of water cycle. They are natural hazards that are predominantly caused by the lack of precipitation. The common conception is that droughts are abnormal climatic condition. However, droughts are normal climatic events that occur periodically (Glantz 2003) and are a characteristic feature of the North American climate. Natural hazards such as floods and earthquakes show immediate damage, whereas, droughts usually show their effect slowly. They are often called a creeping phenomenon (Gillette 1950) due to this fact. The definition of droughts is subjective because their effects vary based on region and climate. Droughts vary from aridity in the sense that aridity is a permanent climatic feature and are limited to climate regions that receive low rainfall (Wilhite, 1993).

Unlike other extreme disasters like flood, droughts are more widespread and continue for a longer period of time. Hence, the spatial and temporal identification of these events become extremely complicated. The difficulty to determine the onset, duration, magnitude and spatial extent of any drought event (Burton et al., 1978; Cordery and McCall, 2000; Wilhite, 2001) complicates things even more. Numerous efforts have been made to better understand this phenomenon clearly so that we can be better prepared for their effects.

2.3 Kinds of Droughts

Wilhite and Glantz (1985) suggested classification of droughts as meteorological, hydrological, agricultural or socioeconomic based on their causes and effects. American Meteorological Society officially accepted this classification and brought it into use in 1997.

2.3.1 Meteorological Droughts

Meteorological droughts are those that occur due to immediate result of lack of precipitation. They are considered to occur when the rainfall in a region decreases 25 percent below the normal precipitation of the region. The lack of precipitation could either be a consequence of reduction in total amount of rainfall, reduction in the intensity of rainfall or even the timing of rainfall. As the variation in rainfall across regions is significant, this kind of drought is region specific. Their start and end can often be abrupt.

2.3.2 Agricultural Droughts

Agricultural droughts occur when the top level of the soil surface (root zone) dries and cannot supply enough water to the plant for its growth. It usually occurs during the growing season. It is defined by the amount of water available in soil for a crop to grow properly. Such droughts also depend on the water holding capacity of the soil, as soils with low water holding capacity are more susceptible to agricultural droughts. A reduction in agricultural production and biomass are immediate effects of such kind of droughts.

2.3.3 Hydrological Droughts

Hydrological droughts occur when the surface and subsurface water supply is diminished by reduction in precipitation over long periods of time. As a result of this

kind of droughts, water levels in most of the components (streams, lakes, reservoirs, etc.) are seen to decrease. Such droughts often lead to decrease in wetlands and wildlife habitat.

2.3.4 Socioeconomic Droughts

Socioeconomic droughts are those wherein the three other droughts instigate an imbalance in the supply and demand of economic goods. These are the droughts that arise from decreased water supply which affect the production and consumption in a society. Policymakers are most concerned about droughts of this category.

2.4 Effects of Droughts

In most cases, the effects of droughts are quantified in terms of the loss suffered by the society and its economy. There has been a significant increase in the number of drought occurrences and their severity over the past few decades in America (Wilhite and Hayes, 1998; Changnon et al., 2000). Fifty-eight weather-related disasters affected United States between 1980 and 2003, and they caused a total loss of about $349 billion (Ross and Lott, 2003). Droughts accounted for 10 (17.2 percent) of these events and about $144 billion (41.2 percent) of the losses (Ross and Lott, 2003). USDA declared a natural disaster in about 71 percent of United States at the peak of the drought of 2012. About 81 percent of the contiguous United States was under abnormal drought conditions during this time, which caused an estimated loss of $30 billion. In 2011, about 80 percent of the total area of Texas was under exceptional drought (Center for Climate and Energy Solutions, Last accessed June 12th, 2015). In consideration of the fact that droughts can prove to be extremely detrimental economically, they are often called the costliest economic disaster (Cook et al., 2007).

All kinds of droughts are usually triggered by scanty rainfall (Wilhite and Glantz, 1985). However, various other factors like climate conditions, available water capacity of soil, population of the region, etc. influence and often exacerbates droughts. The effects of droughts progress in the order of meteorological, agricultural, hydrological and socioeconomic droughts.

2.5   Droughts in the Southeast USA

Southeast US has experienced frequent droughts that are usually attributed to climate variability cycles. Droughts in the region are normally a result of reduced winter precipitation. The recharge of water resources in the southeastern US is dependent on winter precipitation and hence, dry winter conditions (La Niña) has a big role in causing droughts in the region. The La Niña conditions that persisted in the region in 1998 and 1999 were connected to the drought in immediate years that lasted till 2001 in Georgia. Again, the major Georgia drought of 2007 was linked to the La Niña conditions that persisted in 2006. Droughts have been a major problem since early 1980s causing massive losses in agricultural production and affecting water usage in the region.

Even though southeastern United States does not experience intense droughts like those in Central and Western US, they often instigate serious water troubles that last from months to years (Seager et al., 2009). Although droughts in the Southeast, even as long as two years are relatively short when compared to those in the west, they undoubtedly bring about huge economic losses (Manuel 2008). The 2007 drought in Georgia caused a loss of about $1.3 billion worth of agricultural output (CAED, 2007).

Droughts have often been associated with regional conflicts about water-usage between the states of Alabama, Georgia and Florida (Ruhl, 2005). The rapidly growing population in the Southeast US will only increase the water-related problems (Seager et al., 2009).

2.6   Drought Indices

Any parameter, which possesses the capability to signal the occurrence of droughts or their effects are called drought indicators. The amount of rainfall, streamflow level, groundwater level, availability of snow packs, etc. are drought indicators. Droughts are usually characterized in terms of their severity, duration, intensity and spatial extent. Drought index is a calculated value which can measure and quantify droughts according to their characteristics. According to World Meteorological Organization (1992), drought index is an index, which is related to some of the cumulative effects of a prolonged, and abnormal moisture deficiency. Drought indices are developed using various drought indicators. The fact that droughts don't have a universal definition makes it difficult for them to be measured in a universal way and for a universal drought index to be developed (Heim 2002).

Friedman (1957) enlisted four fundamental criteria for any index to be classified as a drought index. First, the timescale should be appropriate to the problem at hand. Second, the index should be a quantitative measure of large-scale and long-continuing drought conditions. Third, the index should be applicable to the problem being studied, and fourth, a long accurate past record of the index should be available or computable. Lastly, a fifth criterion exists for indices used in operational drought monitoring. It states that the index should be able to be computed on a near-real-time basis. This criterion will not be applicable to drought studies that depend on paleoclimatic data (e.g., indices based on glacier and lake sediments, tree ring studies, etc.).

Almost all drought indices use precipitation data either solely or in conjunction with other variables (WMO, 1975a; Tannehill, 1947). Munger's Index and Kincer's Index were two of the early drought indices both of which depended on precipitation (Heim, 2002). Many other indices evolved over time, which took into account other variables like temperature and soil moisture. With the intent of providing drought information to governing entities, National Drought Mitigation Center (NDMC) has been consistently maintaining a National Drought Risk Atlas across contiguous USA. This web-based tool can be used to visualize and assess droughts across the USA. NDMC has been using 5 drought indices in the Drought Risk Atlas to monitor droughts across America. They are Standardized Precipitation Index (SPI), Standardized Precipitation Evapotranspiration Index (SPEI), Palmer's Drought Severity Index (PDSI) and Self-calibrating Palmer's Drought Severity Index (sc-PDSI) and Deciles.

To avoid the drawbacks arising from the variable and unpredictable nature of droughts, ample priority has been given to devise drought indices that can tell researchers more about droughts. Many studies (Wells et al., 2004; González and Valdés, 2004; Keyantash and Dracup, 2004; Tsakiris et al., 2007) have been conducted either to develop new drought indices or to ameliorate the ones that are being used currently.

2.6.1 Palmer's Drought Severity Index (PDSI)

Palmer's Drought Severity Index (PDSI), devised by Palmer, 1965, is based on a simple two-layered water bucket-type balance model. It has been continuously used as a tool for monitoring and assessing droughts. It uses available water capacity of the soil apart from precipitation and evapotranspiration. Its values usually range between -4 and +4.

Although PDSI proved to be a remarkable index for its ability to assess and monitor droughts, it has several drawbacks (Alley, 1984; Karl, 1986; Soulé, 1992; Akinremi et al, 1996; Weber and Nkemdirim, 1998). The use of 68 terms in calculation of PDSI (Soulé 1992) makes its calculation sophisticated. Although many of the drawbacks of PDSI were overcome by the self-calibrating PDSI, its computation is very tedious. The most significant drawback of PDSI and sc-PDSI is that both use a fixed timescale (Vicente-Serrano, 2007). The timescale used by PDSI in its computation is about 9 months (Guttman, 1998) and it prevents identification of droughts of shorter timescales. Also, PDSI hasn't been used to study the effect of climate change on droughts, most likely because of the difficulty in quantifying the change in available water capacity of soil due to climate change.

2.6.2 Self-calibrating Palmer's Drought Severity Index (sc-PDSI)

Self-calibrating Palmer's Drought Severity Index (sc-PDSI) was developed by Wells et al., 2004 to fix the drawbacks of PDSI. It is different from PDSI only because it uses location-specific climate characteristic coefficient and duration factor in its computation. In PDSI, the values initially computed by Palmer, 1965 are used for these parameters for any given location. Hence, the index is spatially more comparable and more consistent than PDSI.

Most of the drawbacks of PDSI were taken care of by sc-PDSI (Wells and Goddard, 2004). However, sc-PDSI decreases significantly with increased temperatures, thereby indicating severe and frequent droughts (Vicente-Serrano et al., 2007). Also, it uses separate climate characteristic coefficients and duration factors for each points and hence it is tedious to compute those at each and every grid point for a high resolution dataset. SPEI is highly correlated to sc-PDSI and given its vivid advantages over sc-PDSI, Vicente-Serrano et al. (2007) suggested its use over sc-PDSI.

2.6.3   Standardized Precipitation Index (SPI)

McKee et al. (1993) developed the SPI. The index has been widely praised for its ability to predict severity of droughts. The analysis on several drought indices done by Keyantash and Dracup (2002) concluded the superior ability of SPI to correctly forecast the severity of droughts in spatial as well as temporal terms. Unlike PDSI, SPI is spatially and temporally comparable (Guttman, 1998; Hayes et al., 1999). Its relative ease of calculation makes it able to be calculated on real time basis hence, making it an invaluable tool for drought management.

The normalization of SPI makes it an index that is equally capable of monitoring wet spells just like dry spells. Depending on the timescale for which it is calculated, it can be used to deduce conclusions on various aspects of the hydrological cycle. Short timescales (2-3 months) can be used to draw conclusions about soil moisture and streamflow, whereas, long timescales (12 to 24 months) can be used to draw conclusions about groundwater levels (Hayes et al., 1999).

SPI was developed in such a way that it could better account for the moisture supply than PDSI. As it is a multiscalar index, SPI can quantify droughts at different timescales. It is determined by computing the probability of observed precipitation at any given location for any chosen duration and hence, is simply a statistical index. The World Meteorological Organization accepted SPI as the reference drought index because of all its qualities (Vicente-Serrano et al., 2011).

Even though the SPI is a relatively new index, it has been used either in research or operational mode in more than 60 countries. It has been growing in popularity in the US with more and more studies using it every day. Some countries where it has been used so far are Spain (Lana et al., 2001; Vicente-Serrano et al., 2007), India (Pai et al., 2011; Chaudhari and Dadhwal, 2004), South Korea (Min et al., 2003), Turkey (Komuscu, 1999), Greece (Livada and Assimakopoulos, 2006), Hungary (Domonkos, 2003), Germany (Khadr et al., 2009), China (Wu et al., 2001; Zhang et al., 2009),

Mexico (Giddings et al., 2005) and Poland (Łabedzki, 2007). Because of its pragmatic applications, Guttman (1999) suggested SPI to be made the primary drought index and to be considered at least on equal level with the Palmer indices.

The calculated SPI values can vary according to the process used to normalize the data. National Drought Mitigation Center uses gamma distribution for this normalization. However, Guttman (1999) concluded that the Pearson Type 3 distribution is the best probability distribution function to use for the computation of SPI. Initially, an incomplete gamma distribution was used in the computation of SPI (McKee et al., 1993 and 1995).

Positive SPI values indicate moist conditions and negative values indicate drought conditions (Edwards and McKee, 1997). SPI values are influenced by the number of years of data available. At least 30 years of data is desired for calculating the SPI. The criticism faced by SPI is mostly because it's solely based on precipitation data (Vicente-Serrano et al., 2007). However, several studies (Chang and Cleopa, 1991; Heim, 2002) suggest that precipitation is the driving force in the identification of onset, severity, and end of droughts.

The SPI is often considered to be a comparatively better index than the PDSI (Guttman, 1998; Steinemann, 2003; Paulo and Pereira, 2007) not just because of its relative ease to calculate but also because of its capability to detect droughts early (Wu et al., 2001). SPI successfully identified the start and severity of the 1996 drought in Texas at least a month before PDSI. PDSI and SPI were observed to be highly correlated for timescales of 5 to 12 months and strongest correlation was observed around 6 months (Hayes et al., 1999).

2.6.4 Standardized Precipitation Evapotranspiration Index (SPEI)

Even with a few flaws, the PDSI always did a reasonably good job of forecasting droughts because it was sensitive to the evapotranspiration and the available water

in the soil apart from precipitation. SPEI is basically a modification of SPI. It was developed with the intention of adding one more dimension of water cycle (evapo-transpiration) while still keeping the calculation easy and maintaining the multiscalar nature SPI possessed so that it could overcome the flaws of PDSI (Vicente-Serrano, 2007).

Even though the SPEI is in its nascent stage, it has found popularity amongst many researchers and is widely used in studies encompassing from drought monitoring systems and drought impacts (Fuchs et al. 2012; McEvoy et al., 2012; Wolf 2012) to climate change (Wolf and Abatzoglou, 2011; Soo-Jin et al., 2013; Yu et al., 2014). SPEI has also been used to assess the change in frequency and severity of droughts (Yu et al. 2013). Its acceptance is expected to grow over the next few years because of its robustness and ability to monitor droughts of different timescales.

Although the theoretical possible values of both these indices range from $-\infty$ to ∞, the typical values of range from -3 to +3. Depending on the magnitude of these indices, droughts are classified into moderate, severe and extreme.

SPI and SPEI Values	Category
2.00 and above	Extremely Wet
1.50 to 1.99	Very Wet
1.00 to 1.49	Moderately Wet
0.99 to -0.99	Near Normal
-1.50 to -1.99	Very Wet
-2.00 and less	Extremely Wet

Table 2.1: Classification scale for SPI and SPEI values

2.7   Climate Change and Droughts

A general increasing trend in temperature (0.5-2°C) has been witnessed over the world since mid-nineteenth century (Jones and Moberg, 2003). The forecast from climate models indicate significant increase in temperature during this century (Solomon et al. 2007). Also, the precipitation is predicted to decrease as much as 15 percent

in some regions (IPCC, 2007). These changes in climatic parameters are bound to change the characteristics of droughts. With increasing evapotranspiration, the water demand is expected to rise, which will stress the water resources and influence droughts (Sheffield and Wood, 2008). There is no denying that there has been drastic changes in the climate of the Southeast US. The area experiencing moderate to severe droughts during spring, summer and fall has increased by 12, 14 and 9 percent, respectively, in the region since mid-1970s (Karl et al., 2009). However, despite these alarming increases, there is still lack of detailed study relating droughts to climate change in the Southeast US. Several studies (Li et al., 2008; Burke and Brown, 2010; Dai, 2011; Milano et al., 2012) have assessed future drought conditions using projected climate data and different indices. All of these studies have been done at a very coarse resolution and for areas other than the Southeast US. Detailed information on droughts is required to know more about how climate change is influencing droughts in the region. Studies must quantify the spatial variability of droughts at high resolution so that they can be better monitored in the region.

2.8 Climate Change Scenarios

The Special Report on Emission Scenarios (SRES) defined four possible sets of future climate change scenarios, which were driven by population, economy, technology, energy, agriculture and land-use. The scenarios were called A1, A2, B1 and B2. A1 scenario was based on the assumptions of rapid growth of economy, technological innovation and GDP with a balanced energy sector and proper management of resources. A2 scenario was based on the assumptions of rapid population growth, slow technological innovation, low growth of GDP, energy demands fulfilled by fossil fuels and irrational use of resources. B1 scenario was contingent on the assumptions that population growth would be low, GDP growth and technological innovation would be rapid, renewable resources would be used to fulfill energy demands and biodiversity

17

and resources would be conserved. B2 scenario was contingent on the assumptions of intermediate growth of GDP, population and technology in a mixed energy scenario and conservation of resources.

Climate change projected according to A2 emission scenario presents a changed world wherein most of the conditions are different from the present world. Figure 2.2 depicts how various climate change emission scenarios project the global surface warming to change.
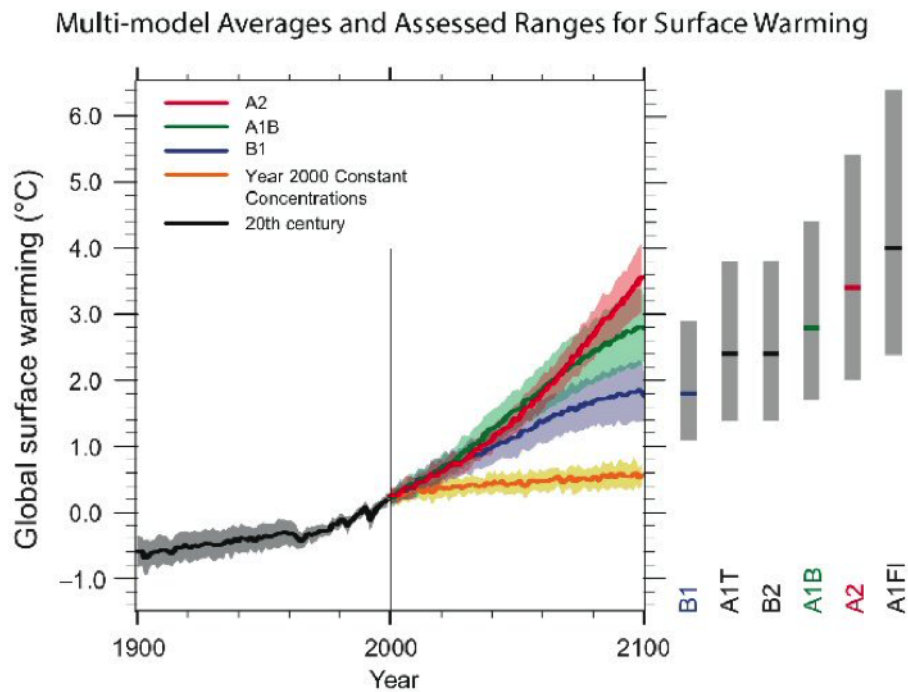
Figure 2.2: Surface warming projections according to different emission scenarios. Source: http://www.narccap.ucar.edu/about/emissions.html

2.9 General Circulation Models

The forecast from various climate change scenarios are based on the assumptions that temperature will increase and precipitation will decrease in the future (IPCC, 2007). Coupled Model Inter-comparison Project Phase 3 (CMIP3) dataset was produced from the outputs of more than 20 General Circulation Models (GCMs) from all

18

over the world (Meehl et al., 2007). There exist differences in various model outputs because of the underlying assumptions and methods used by the models.

2.9.1 Community Climate System Model

This model is based at National Center for Atmospheric Research (NCAR) in Boulder, Colorado and is funded by the National Science Foundation (NSF) and Department of Energy. It is a sophisticated model that couples atmosphere, land, ocean and sea ice components (Gent et al., 2009). The model is capable of producing results at multiple spatial resolutions. Collins et al. (2005) provides detailed descriptions on the intricacies of the model.

2.9.2 Geophysical Fluid Dynamics Laboratory Model

In 1995, National Oceanic and Atmospheric Administration (NOAA) introduced the GFDL model. This model is also an atmosphere and ocean coupled model with comparatively simpler formulation of respective processes. Delworth et al. (2002), Dixon et al., (2003) and Bender et al. (2007) provide informative details about the model in depth.

2.9.3 Hadley Center Coupled Model Version 3

This model was developed at the Hadley Center in the United Kingdom by Gordon et al. (2000). The model is based on coupled atmospheric and oceanic interactions wherein the atmospheric component has 19 levels and the oceanic component has 20 levels. The resolution of the atmospheric component is 2.50 degrees latitude by 3.75 degrees longitude thereby producing an output of 96 x 73 grid cells. The resolution of the oceanic component is 1.25 degrees latitude by 1.25 degrees longitude. This high resolution enables proper depiction of oceanic current (Mishra and Singh, 2008).

2.10 Regional Downscaling

GCMs lack the capability to supply information at fine spatial resolutions. Hence, they cannot be used for studies to evaluate impacts at regional scale (Carter et al., 1985). GCMs typically have horizontal spatial resolution between 250 km and 600 km. To enable them to be used for regional climate studies, the results from various GCMs are regionally downscaled at finer resolution using different downscaling procedures. Downscaling can either be statistical or dynamic. Statistical downscaling involves the use of mathematical and statistical functions like regression to relate large climatic features to local climatic features. It can often just be simple interpolation of coarse resolution data. Dynamic downscaling is done using regional climate models with finer spatial resolution that contain detailed regional features like topography (Déqué et al., 2007). Usually, very fine data is required to run hydrological models. Regional downscaling provides fine resolution data and can also provide results for locations without any observations. This allows detailed regional assessment and provide better information.

2.11 Potential Evapotranspiration (PET)

Potential evapotranspiration (PET) is an essential component in computation of certain drought indices. Various methods like Penmann-Monteith, Thornthwaite and Hargreaves can be used to compute PET. Penmann-Monteith method is dependent on many variables like solar radiation, relative humidity, wind speed and temperature. Although it has a tedious computation methodology, it has been widely accepted by major organizations including Food and Agricultural Organization (FAO) and American Society of Civil Engineers (ASCE). Vicente-Serrano (2007) suggests that the method of computation of PET is not of much concern in case of drought indices as the main objective is to make a relative temporal estimation of PET. Furthermore,

the use of both simple and complex methods in calculation of PET resulted in similar values of drought indices (Mavromatis, 2007). However, some studies argue that the method of calculation of PET does impact the drought index values (Sheffield et al., 2012). Yu et al. (2013) used Thornthwaite method in estimating PET to calculate SPEI and assess if the frequency and severity of droughts were changing with climate change. They successfully quantified the increase in frequency and severity of droughts in China using this method.

2.12   Severity-Area-Frequency (SAF) Curves

The shortcomings and dubiety of GCMs coupled with the complex nature of droughts restricts the analysis of droughts on an event basis. Historical and projected droughts can be better analyzed by seeing the variation in respective Severity-Area-Frequency (SAF) curves (Mishra and Singh, 2009). This useful drought assessment technique was proposed by Henriques and Santos (1999). This technique has been improved and used by many others (Akhtari et al., 2008; Mishra and Singh 2009; Alemaw et al., 2013) conducting drought assessment studies. As studies on drought frequency cannot quantitatively link droughts to its other important characteristics, like severity and spatial extent, such studies lack in elaborateness (Mishra and Desai, 2005).

2.13   Thesis Organization

This thesis is primarily centered on the stated objectives. It has a total of six chapters. Chapter 1 is the introduction and it provides an insight and background information on droughts, especially in the context of the United States. It also gives an overview of the problem statement and states the objectives of this study. Chapter 2 is the review of literature. It discusses the written available studies that have been performed before and the findings of those. The chapter provides the basis for choice

of various methods used in the study. The three objectives are presented in Chapters 3, 4, and 5, respectively, with details about the study area, data, methodology and discussion of results. Chapter 6 discusses the findings and conclusions made from this study. Finally, possible future research is stated in Chapter 7.

Chapter 3

Projected future changes in frequency, severity and spatial extent of droughts in

Alabama

3.1 Abstract

Droughts, often considered the costliest natural disaster, are triggered by severe
shortage of water, mainly in the form of precipitation. The Southeast US has been af-
fected by frequent severe droughts in recent years and this calls for a more pragmatic
approach to better manage their consequences. The primary objective of this study
was to analyze how droughts in Alabama would change in future as a result of pro-
jected climate change. Commonly used drought indices were computed to quantify
the changes in droughts.

Historical and future droughts were quantified by the means of Standardized
Precipitation Index (SPI) and Standardized Precipitation Evapotranspiration In-
dex (SPEI) to study the change in frequency, severity and spatial extent of future
droughts. Precipitation and temperature data, regionally downscaled for the South-
east US for high emission scenario (A2) by Regional Spectral Model (RSM) at the
Florida State University (FSU) - Florida Climate Institute (FCI), from three General
Circulation Models, Hadley Centre Coupled Model Version 3 (HadCM3), Geophysical
Fluid Dynamics Laboratory (GFDL) Model and Community Climate System Model
(CCSM), from the Third Coupled Model Inter-comparison Project (CMIP3) archive
were used for this study. Data from 1969 to 1999 were used for historical simulation
and that from 2039 to 2069 were used for future projections.

The Severity-Area-Frequency (SAF) curves for droughts with different recurrence
intervals were analyzed. Both SPI and SPEI from the GFDL and the HadCM3 model

indicated droughts in the future to be more severe, frequent and widespread. The SPI from the CCSM model suggested more moderate droughts in the future but fewer severe and extreme ones. This model also indicates the severity to decrease and the spatial extents to remain similar. The SPEI from CCSM model suggested increased frequency of extreme droughts in the future with the overall severity and spatial extent to be similar to that in the past.

The results of this study provides insight about expected changes in drought characteristics in Alabama. The results can be used by policymakers to plan better for drought years and mitigate the socioeconomic and environmental effects of droughts.

3.2 Introduction

People from different professions define drought in different ways. Meteorologists simply define drought as shortage of precipitation. Agriculturists define drought as scarcity of ample moisture in the soil to sustain crop growth during growing season. Economists define drought as a period wherein shortage of water supply cripples the economy. No matter in which way one may define droughts, they are, without any doubt, one of the most detrimental environmental hazards. Globally, the average annual losses from droughts are as high as $6-$8 billion. Climate change coupled with rampant increase of population has stressed available water resources all around the globe. Water demand has increased substantially in many regions in recent years due to excessive agricultural and industrial expansion. Drought directly affects water and food availability and may often lead to famine, desertification and loss of biodiversity.

United States is not new to the problems surfacing from droughts. The persistence of droughts in many regions in the US is a major setback for its socioeconomic development and ecosystem balance. Many regions are being affected by droughts each year. Almost 81 percent area of contiguous US was under at least abnormally dry condition when the 2012 drought peaked. The total loss from this disaster was

estimated to be around $30 billion. The West, Southwest and the Midwest are the regions in US that are affected by droughts the most. Presumably because of this reason, most studies about North American droughts are based in the semi-arid regions in Western US. Droughts in the Southeast US haven't been studied as much, possibly because the severity of their effects is comparatively smaller in the region. The droughts of 1986-88, 1998-02 and 2006-09 were notably the most severe ones suffered by the Southeast US since record keeping began. The recent droughts reiterate the need of more drought-related studies based in the region. Studies pertaining to droughts in the Southeast will definitely assist in long term regional planning.

The Southeast US is prone to a wide range of extreme weather and climate events. It frequently witnesses natural disasters in the form of severe thunderstorms, floods, tornadoes and droughts. The southeastern droughts are relatively short in duration when compared with those in the Western and the Central US, which can even last for decades. The climate of the southeastern region is highly influenced by its nearness to water bodies apart from the latitude and topography. The effects of climate change in the region have been quantified by different studies and reports (KC et al, 2015; NCA, 2013). As a result of the change in climate in the region, the average temperatures are expected to increase in several places, the air quality is projected to deteriorate and the water resources are predicted to be strained.

Although Alabama usually receives ample yearly precipitation, the vulnerability of several parts of the states to drought cannot be undermined. The economy of Alabama is highly influenced by the agricultural activities in the state. Almost half of its area is used for agriculture. Hence, the effects of droughts can often be immediately visible in the state's economy. Population of Alabama has increased almost by a million since 1980. The demand for water resources is clearly increasing. It is difficult to counter the point that a drought of magnitude similar to that of the 1980s would

affect Alabama equally or more if it occurred today. It is, hence, essential to be prepared against any sort of event that is likely to strike upon us.

Although extreme droughts are rare in the region, their changing characteristics in recent years force us to contemplate more about them. Are droughts going to be more frequent in the future? If yes, how rapidly is the frequency increasing? How widespread would those droughts be? Would they be more severe? Are the droughts a direct consequence of climate change? Are the droughts associated with anomalies in the sea surface temperature or are they caused by unexplained atmospheric abnormalities? There are many questions that need to be answered.

3.3 Objective

Analyze the changes in frequency, severity and spatial extent of droughts in Alabama using Severity-Area-Frequency Curves.

3.4 Study Area

The area under consideration for this study is the state of Alabama. The southeastern state of Alabama is surrounded by Tennessee in the north, Georgia in the east, Mississippi in the west and Florida and the Gulf of Mexico in the South. The total area of the state is 52,419 square miles. It has four physiographic regions: Gulf Coastal Plain, Piedmont Plateau, Ridge and Valley section, and Appalachian Plateau. The highest elevation in the state is Cheaha Mountain at 2407 feet and the lowest point is at sea level. The state frequently experiences natural hazards in the form of hurricanes, floods, tornadoes and droughts.

Droughts in Alabama are usually the outcome of reduced precipitation in winter and spring. On average, Alabama receives about 55 inches of yearly rainfall. In regions close to the Gulf of Mexico, it can often be as high as 65 inches whereas it is usually about 50 inches in the central and west-central parts. Usually, more

Average Annual Rainfall

less than 52 inches
52-56 inches
56-60 inches
60-64 inches
greater than 64 inches

Produced by the Dept. of Geography
College of Arts and Sciences
The University of Alabama
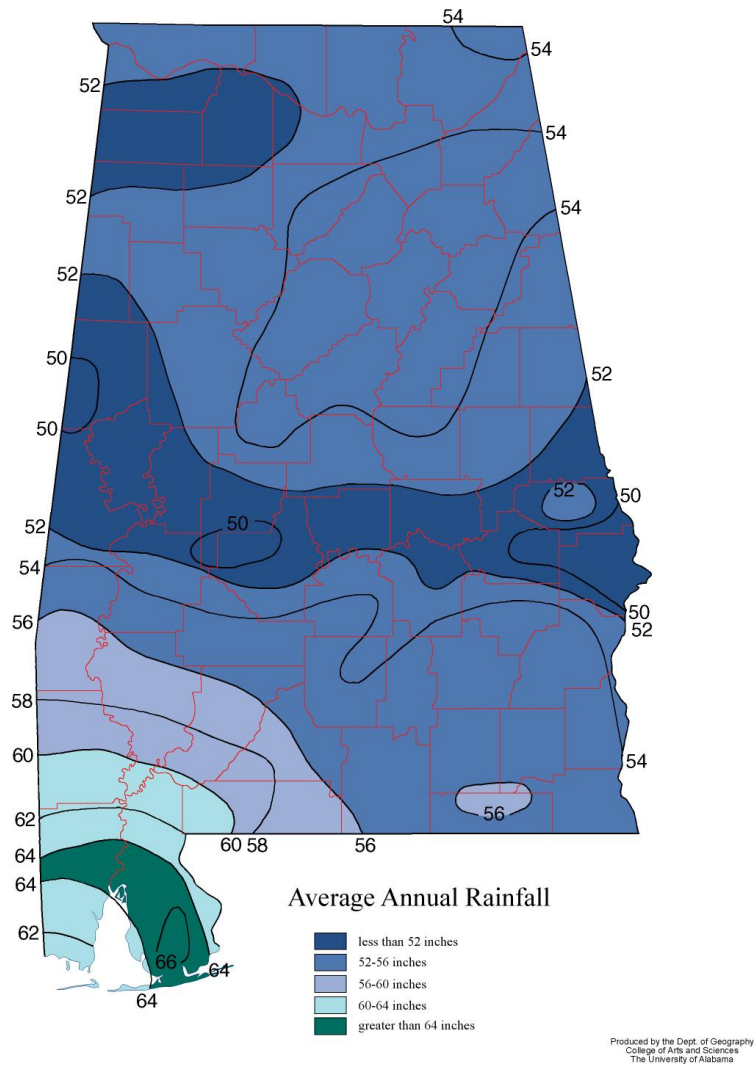
Figure 3.1: The average annual rainfall in Alabama.
Source: Department of Geography, University of Alabama

than half of the total precipitation occurs between the months of December and May. Inadequate precipitation during these months causes insufficient recharge of soil moisture in the region. Summer follows these months and almost no precipitation coupled with excessive evapotranspiration during the summer months causes drying of the soil. The average annual temperature in Alabama is about 64°F. During summer, the average temperature rises to about 90°F increasing water loss to evaporation and transpiration.

60

60

60

62

62

62

64

64

66

66

68

68

Average Annual Temperature, in degrees Fahrenheit

less than 60 degrees
60-62 degrees
62-64 degrees
64-66 degrees
66-68 degrees
greater than 68 degrees

0   5   10   30 Miles
0 5 10 20   30   40 Kilometers

Produced by the Dept. of Geography
College of Arts and Sciences
The University of Alabama
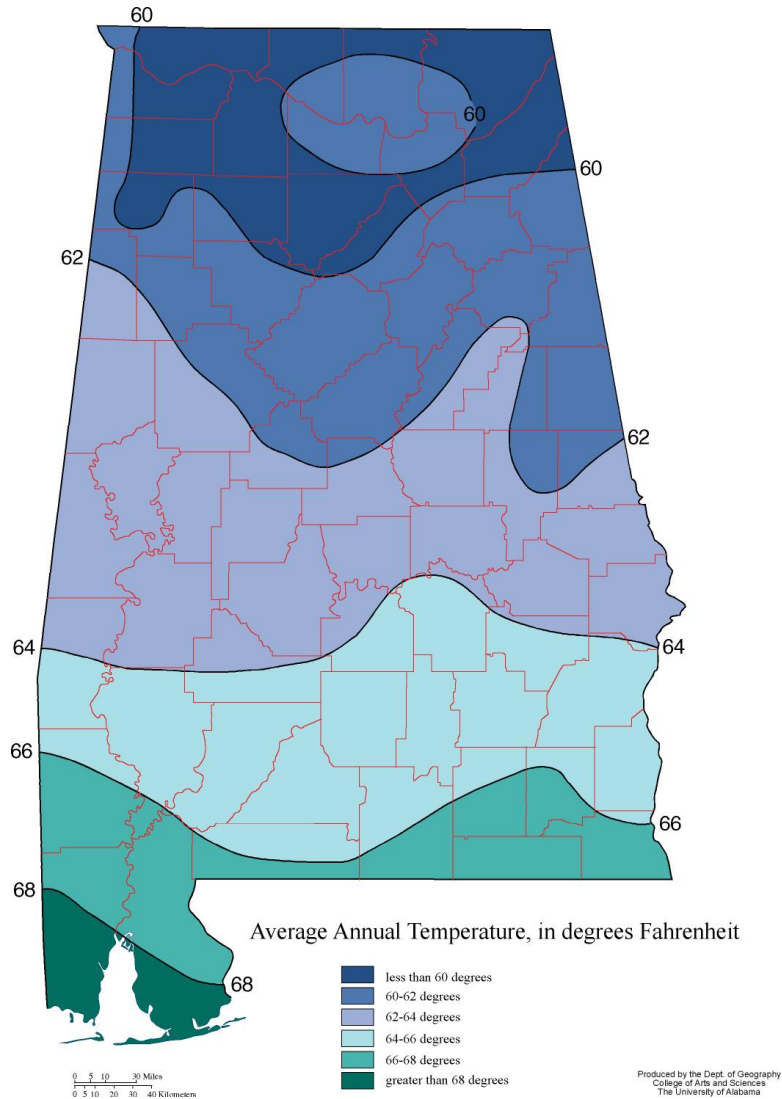
Figure 3.2: The average annual temperature in Alabama.
Source: Department of Geography, University of Alabama

The recording of droughts in Alabama and Georgia were started since the beginning of the twentieth century. It was around this time that droughts started to be quantified by drought indices. Before the droughts of 1980s intensified drought issues in Alabama, the droughts of 1954-55 and 1960-63 were the ones that were most severe and persisted statewide. Besides these, the drought of 1929-32 affected the northeast portion of the state, and those of 1938-45 and 1964-70 affected nearly the entire state (USGS, 1988-89). The severe statewide droughts of the 80s were all a result of reduced precipitation. Some severely affected regions suffered from precipitation deficit

higher than a year's worth of rain. Droughts began to become a major concern in the state only after the occurrence of these droughts. The droughts of 2007 worsened the condition in Alabama and it was considered to be the worst drought in over one hundred years (B. Riley, State of Alabama, Governor's office press release, July 30, 2007). It is evident from the drought patterns that droughts have continuously been increasingly severe.

3.5 Data and Methodology

Many climate variables from three different models were downscaled to 10 km resolution over the Southeast US by the Regional Spectral Model (RSM) at the Florida State University (FSU) - Florida Climate Institute (FCI) with the methods adapted from Kanamitsu et al. (2010). As part of the COAPS (Center for Ocean-Atmospheric Prediction Studies) Land-Atmosphere Regional Ensemble Climate Change Experiment for Southeast US at 10 km resolution (CLAREnCE10), three Coupled Model Inter-comparison Project (CMIP3) coupled General Circulation Models (GCMs) were downscaled for the A2 emissions scenario of the Fourth Assessment Report (IPCC, 2007). The two timeslices used in this study was between 1969 and 1999 for the historical simulations and 2039 and 2069 for the future simulations. The models used were Community Climate System Model (CCSM), Geophysical Fluid Dynamics Laboratory (GFDL) Model and Hadley Centre Coupled Model Version 3 (HadCM3). Precipitation and temperature data were used from these three general circulation models to compute the indices. As the spatial resolution of the data used in this study is 10 km, it was chosen over the data produced by North American Regional Climate Change Assessment Program (NARCCAP), which is at a spatial resolution of 50 km. The resolution of 10 km makes the data ideal for hydrologic assessment over the region.

In this study, droughts were quantified by the use of SPI and SPEI as both possess the capability to monitor and forecast droughts effectively.

3.5.1 Standardized Precipitation Index (SPI)

Long-term precipitation data is required to compute the SPI. Data of at least 30 years is desired. First, the mean and standard deviation for the long record of precipitation at any given location is calculated. The data is transformed into log-normal values to obtain the U-statistic, shape and scale parameter. Using these parameters, the cumulative gamma probability distribution can be calculated. The cumulative probabilities are obtained from this distribution. This probability is further transformed to standardized normal probability distribution using probability transformation techniques suggested by Abramowitz and Stegun (1965). A step-by-step procedure to calculate the index is described in Appendix A.

SPI was computed for timescales of 1, 3, 6 and 12 months using precipitation data from CLAREnCE-10 dataset. A total of 1417 points existed across Alabama for which the time series of SPI values were calculated.

3.5.2 Standardized Precipitation Evapotranspiration Index (SPI)

SPEI calculation procedure is very much similar to that applied in calculating SPI. It takes into account evapotranspiration apart from the precipitation. This index is basically derived based on the moisture value at any given location. The moisture departure is obtained as the difference between the precipitation and potential evapotranspiration. Moisture departure is then transformed into log-logistic probability distribution. This probability distribution is further transformed to standardized normal probability distribution using probability transformation techniques suggested by Abramowitz and Stegun (1965) to obtain the SPEI. A step-by-step procedure to calculate the index is described in Appendix B.

SPEI was computed for timescales of 1, 3, 6 and 12 months using precipitation and temperature data from CLAREnCE-10 dataset. A total of 1417 points existed across Alabama for which the time series of SPEI values were calculated. PET was calculated from temperature using Thornthwaite Method. The difference between precipitation and PET was calculated as the moisture balance, which was used to compute the SPEI.

3.5.3   Potential Evapotranspiration

Potential evapotranspiration (PET) is an important component in calculation of SPEI. The PET is subtracted from the precipitation to obtain the moisture balance. It is the moisture balance that is processed to compute the SPEI. In this study, Thornthwaite method was used to calculate PET. Studies show that Penmann-Monteith is the most reliable method to compute PET. However, Mavromatis (2007) showed that the choice of method for estimation of PET doesn't affect the drought index significantly. The primary idea of this study is to analyze drought events during two time slices. Therefore, the choice of method for PET calculation is not likely to affect the results as the method chosen would equally affect the values during both time slices. The method applied to calculate PET is described in detail in Appendix C.

3.5.4   Severity-Area-Frequency (SAF) Curves

Severity-Area-Frequency (SAF) curves are very effective in analyzing droughts. Although it is a relatively long procedure to construct them, they give detailed and informative description about droughts. Droughts can be compared with standard droughts with specific recurrence intervals to assess their severity, frequency and spatial extent at the same time. To see changes in the frequency and severity of droughts at individual locations, the time series of the index can be studied. However, comparing droughts at individual locations to comment on overall drought characteristics

across a region is not the wisest method. SAF curves make it easier to discern the subtle difference in drought severity across different percentage area while associating them with various return intervals simultaneously.

To construct SAF curves, the drought variable of a suitable timescale (3-SPI, 6-SPI or 12-SPI) must be identified. For the selected drought variable, the drought severity, which is simply the sum of negative values during a dry spell, was calculated. Then, for different areal extent of the droughts, the aggregated mean of drought severity was calculated by taking various areal thresholds into account. The drought severities across various areal extents were all fitted according to a probability distribution. In this study, Extreme Value Type I distribution was used. Then, frequency analysis was performed to generate respective severities across different areal extents for different return intervals. Finally, these severities were plotted against the areal extents to obtain the SAF curves.

3.5.5 Timescale of Indices

SPI and SPEI can be analyzed for different timescales depending on what kind of droughts one wants to quantify and assess. SPI and SPEI from shorter timescales like 2-3 months can provide information about the soil moisture condition or streamflow. Similarly, longer timescales of 12-24 months can be used to assess information about groundwater level. SPI less than -1 indicate drought conditions. Hence, for analysis, all the values of SPI greater than this were omitted. In this study, SPI and SPEI computed using a timescale of 6 months was used to construct SAF curves. This particular drought variable was chosen to analyze general droughts in the region. Droughts usually take up 2-3 months to make a mark and can exist for periods ranging from months to years. Hence, minor temperature fluctuations over a month or two are not likely to instigate a drought. It is, therefore, expected that the timescale of 6 months ensures that all major droughts were covered and minor ones were eliminated

in the analysis. SPI at a timescale of 6 months has been used by many other studies to analyze their results (Reddy and Ganguli, 2012; Tsakiris and Vangelis, 2004).

3.6 Results and Discussion

Droughts in the state were assessed by SPI and SPEI from three GCMs for historical and projected simulations by the means of SAF curves. The results from the respective indices are discussed below:

3.6.1 SPI

The results of SPI from various models are presented below:

CCSM

Initially, the results of SPI from CCSM were used to obtain basic information about drought duration and frequency. The total number of drought incidences at all points across Alabama is shown in Figure 3.3. It shows an increase in moderate droughts whereas a decrease in severe and extreme droughts in the future period being considered. Moderate droughts increased by 10.0 percent, severe droughts decreased by 13.7 percent and extreme droughts decreased by 39.5 percent. However, when the overall occurrence of droughts was considered, droughts were reduced by only 1.5 percent. When the drought durations were compared, it was seen that droughts observed in past lasted as long as 24 months whereas among those in the future, maximum duration was of 12 months.

SAF curves were used to compare the severity of droughts of specific return intervals in the past and future. The historical and future SAF curves are presented in Figure 3.4. It was observed from the curves that for droughts with all return intervals, past droughts are more severe for majority of the area. As the percentage area considered is increased, droughts in past and future tend to be of similar severity.
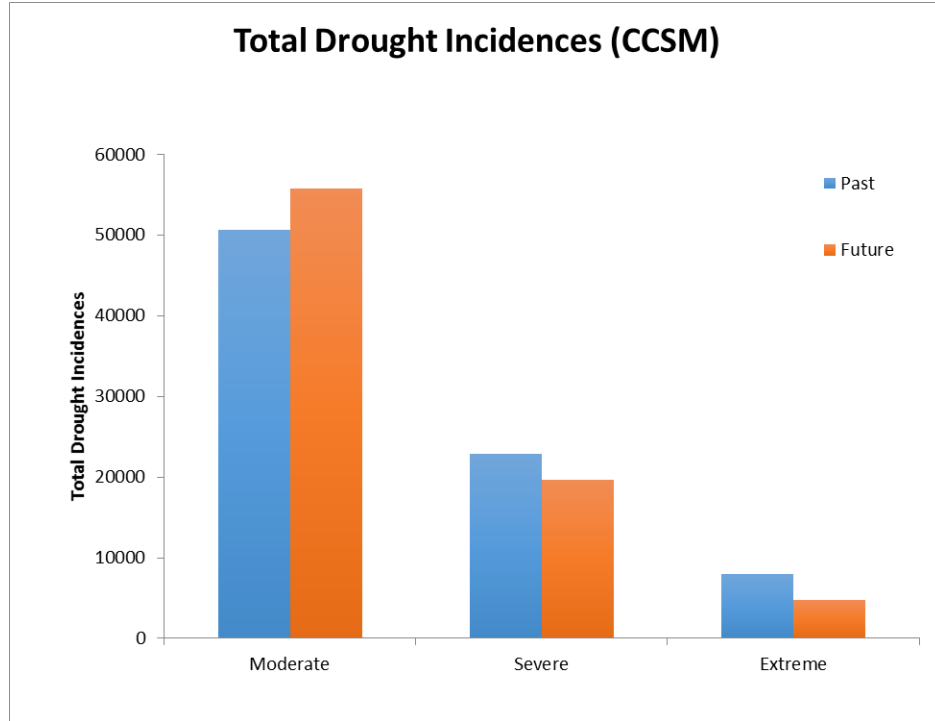
Figure 3.3: Total number of different kind of drought incidences according to SPI from CCSM.

Recurrence Interval	2 years	5 years	10 years	25 years	50 years	75 years	100 years
Percentage Decrease	-10.95	-5.94	-4.63	-3.65	-3.18	-2.97	-2.83

Table 3.1: Average percentage decrease in overall drought severity according to SPI from CCSM.

When smaller percentage area of the state is considered, past droughts usually are of higher severity. On average, droughts with all recurrence intervals decreased in severity. The average decrease in severity for droughts with different recurrence intervals is shown in Table 3.1. It was observed that 2-year droughts in the future would be on average 10.9 percent less severe than the ones in future and 100-year droughts would be 2.8 percent less severe. From the SAF curves, the maximum drought severity can be observed to be around 23.7, spread across 5 percent of the area for a 100-year

6-SPI (CCSM) - Historical and Projected

Figure 3.4: SAF curves for droughts with different recurrence intervals during historical and future periods (SPI from CCSM).

drought in the past. The severity gradually decreases with increase in areal extent being considered.

GFDL

As evident from Figure 3.5, GFDL model indicated that there would be more incidences of all kinds of droughts in the future. Moderate droughts increased by 6.7 percent, severe droughts increased by 8.3 percent and extreme droughts increased by 15.7 percent. On average, the droughts increased by 8.1 percent in the future. The droughts in the future are often as long as 20 months whereas the longest one in the past was of 16 months.

The future droughts were clearly seen to be more severe from the SAF curves shown in Figure 3.6. The SAF curve for droughts with any given recurrence interval in the future was much higher than its corresponding curve in the past. A 50-year

Figure 3.5: Total number of different kind of drought incidences according to SPI from GFDL.

drought in the future almost appears like a 100-year drought in the past. For future droughts, the severity is going to be higher and they are going to be more widespread too. The average increase of severities for droughts of different recurrence intervals

Recurrence Interval	2 years	5 years	10 years	25 years	50 years	75 years	100 years
Percentage Increase	8.01	9.43	9.79	10.09	10.27	10.33	10.38

Table 3.2: Average percentage increase in overall drought severity according to SPI from GFDL.

are presented in Table 3.2. The average percentage increase vary by as much as 8.0 percent for 2 year droughts and 10.4 percent for 100-year droughts. From the SAF curves, the highest severity can be observed to be 27.6 across 5 percent area for a 100-year drought in the future. The overall severity, according to SPI, from GFDL

36

Figure 3.6: SAF curves for droughts with different recurrence intervals during historical and future periods (SPI from GFDL).

was indicated to be higher than that from CCSM. This could either imply more severe droughts or similar droughts spanning a longer duration.

HadCM3

SPI from this model indicated the highest increase in droughts. An increase in the occurrence of all kind of droughts can be seen in Figure 3.7 with moderate droughts increasing by 5.4 percent, severe droughts increasing by 18.6 percent and the extreme droughts increasing by a whopping 74.2 percent. Overall, droughts were seen to increase by 17.3 percent. The longest drought during both periods (past and future) was 15 months.

From the SAF curves shown in Figure 3.8 for SPI from HadCM3, severity of droughts in the future can be observed to be much more severe than those in the past. For any given areal threshold and recurrence interval, droughts in future would
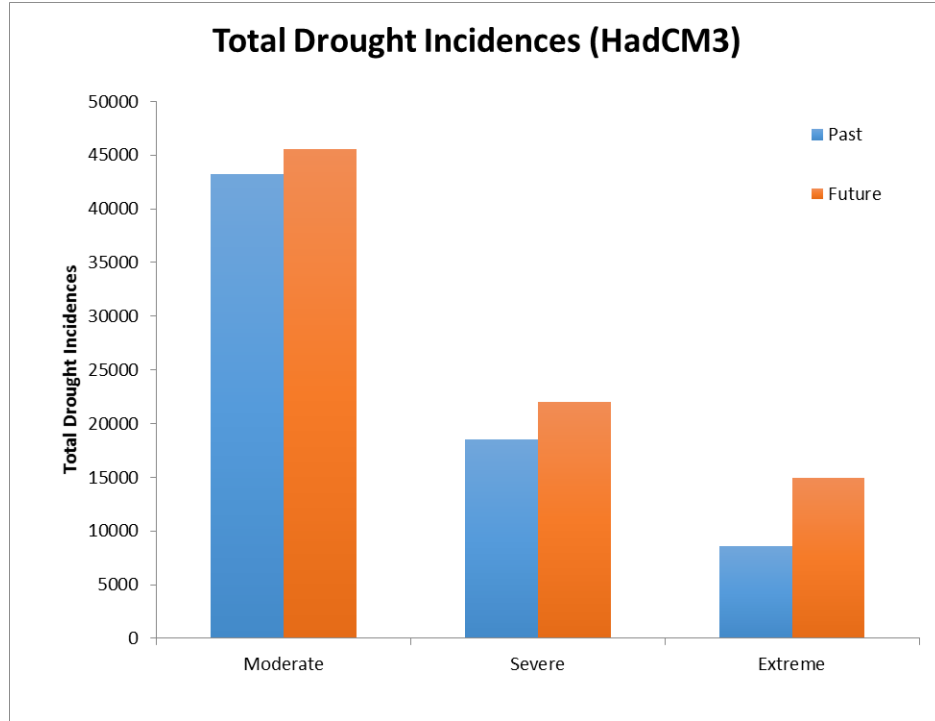
Figure 3.7: Total number of different kind of drought incidences according to SPI from HadCM3.

be substantially more severe than the past ones. It can be seen that even a 50-year drought in the future is going to be more severe than a 100-year drought in the past. The results of this model indicate future droughts to increase in frequency, severity and spatial extent than those in the past. Droughts of all recurrence intervals are expected to increase in severity by more than 20 percent as shown in Table 3.3. Drought severity is expected to increase by 22.8 percent for 2-year droughts and by 23.7 percent for 100-year droughts. However, the severity is still lesser than that

Recurrence Interval	2 years	5 years	10 years	25 years	50 years	75 years	100 years
Percentage Increase	22.77	23.33	23.49	23.60	23.65	23.68	23.69

Table 3.3: Average percentage increase in overall drought severity according to SPI from HadCM3.

Figure 3.8: SAF curves for droughts with different recurrence intervals during historical and future periods (SPI from HadCM3).

indicated by the GFDL model. The maximum severity for a 100-year future drought can be seen to be 25.0 for 5 percent of the area from Figure 3.8.

3.6.2 SPEI

For the analysis of SPEI too, only the values of the index below -1 was considered. The results of SPEI from various models are presented below:

CCSM

The comparison of drought incidences across Alabama with results of SPEI from CCSM is depicted in Figure 3.9. It shows an increase in extreme droughts but a decrease in moderate and severe droughts in the future. Extreme droughts increased substantially by 58.9 percent whereas moderate and severe droughts decreased by 3.5 percent and 8.9 percent, respectively. The total number of droughts decreased by 2.4

percent. The overall change in droughts from SPI as well as SPEI calculated from this model isn't very different from each other. Droughts as long as 19 months can be observed in the future period. In the past period, the longest drought was of 14 months.
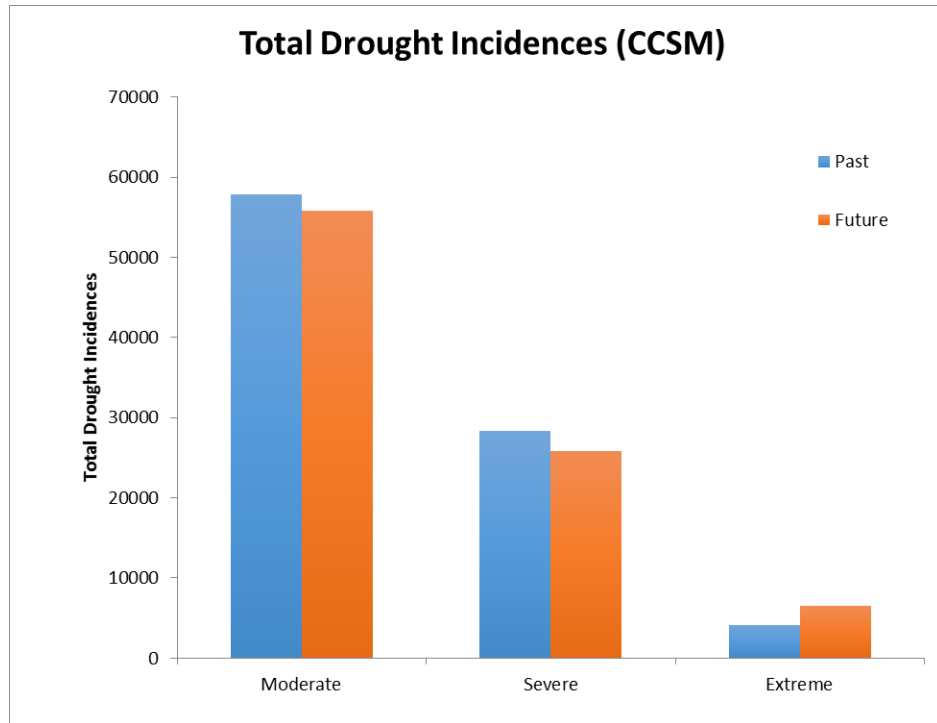
Figure 3.9: Total number of different kind of drought incidences according to SPEI from CCSM.

The SAF curves from the results from this model is shown in Figure 3.10. It can be seen that for droughts of any given recurrence interval in the past and the future appear to be roughly similar. For lower thresholds of area, droughts are slightly more severe in the past whereas for higher thresholds, droughts in future are slightly more severe. As the curves are not significantly different, it can be said that this model doesn't predict droughts to change significantly in the future. Table 3.4 shows average increase or decrease in severity for droughts with different recurrence intervals. The average severity of droughts is expected to decrease by 11.5 percent for 2-year droughts but it is expected to increase by 1.7 percent for 100-year droughts. The SAF curves
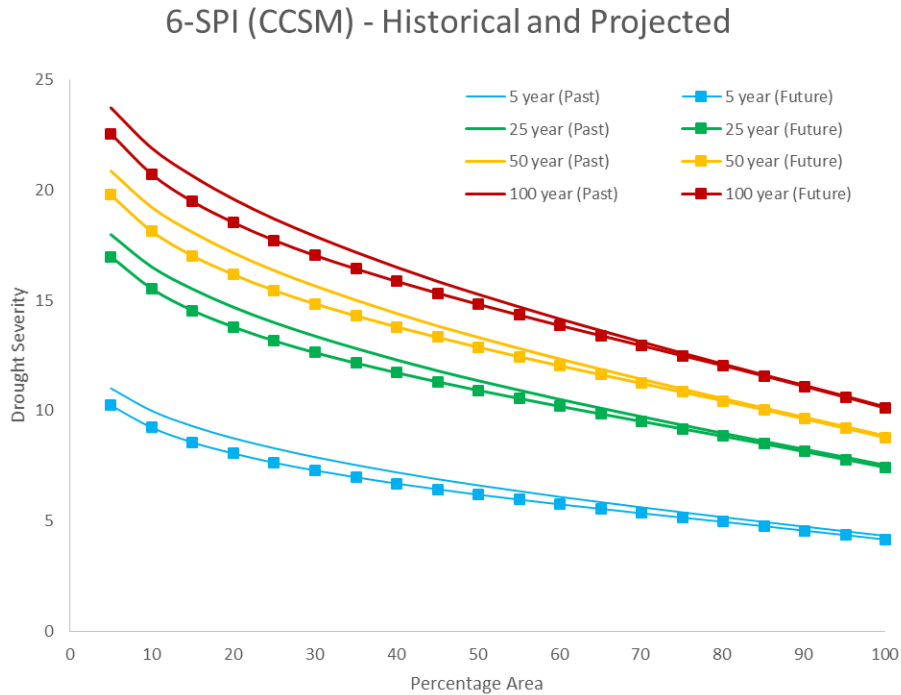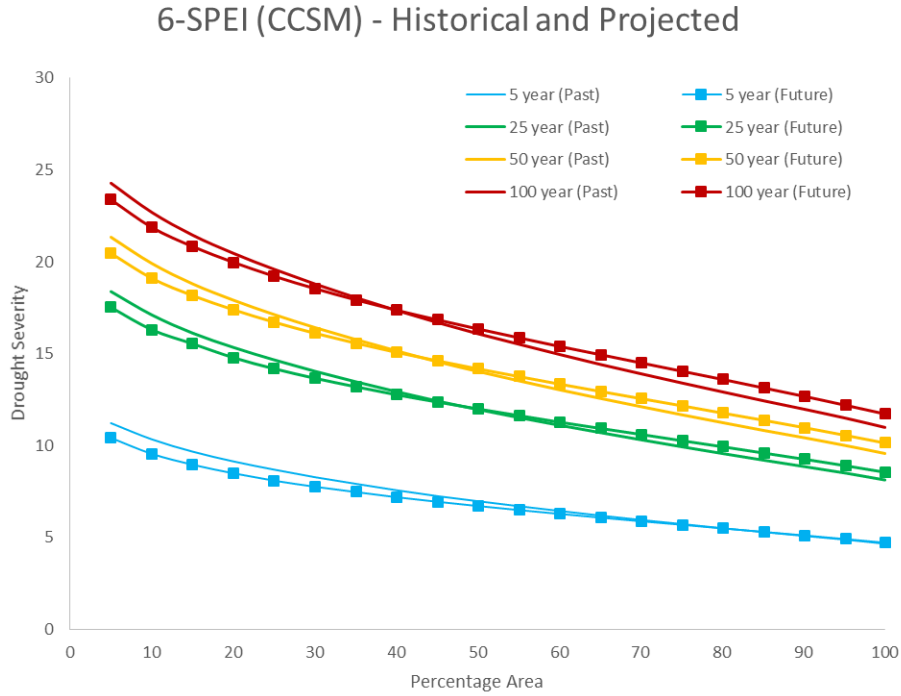
Figure 3.10: SAF curves for droughts with different recurrence intervals during historical and future periods (SPEI from CCSM).

indicate that the maximum severity would be 24.3 for a 100-year drought across 5 percent of the area in the future. This is smaller than the severity values indicated by other models. Both the indices computed from CCSM suggests that climate change won't affect droughts significantly.

Recurrence Interval	2 years	5 years	10 years	25 years	50 years	75 years	100 years
Percentage Increase or Decrease	-11.47	-3.39	-1.26	0.36	1.10	1.44	1.67

Table 3.4: Average increase(+) or decrease (-) in overall drought severity according to SPEI from CCSM.

GFDL

The results from GFDL model indicated increase in moderate and severe droughts whereas a decrease in extreme droughts in the future. This can be observed in Figure 3.11. Moderate droughts increase by 11.6 percent and severe droughts increase by 5.2 percent but extreme droughts decrease by 21.2 percent. In totality, droughts increase by 7.1 percent across the state. The longest drought in the past lasted for 14 months. In the future period, droughts as long as 18 months are projected.
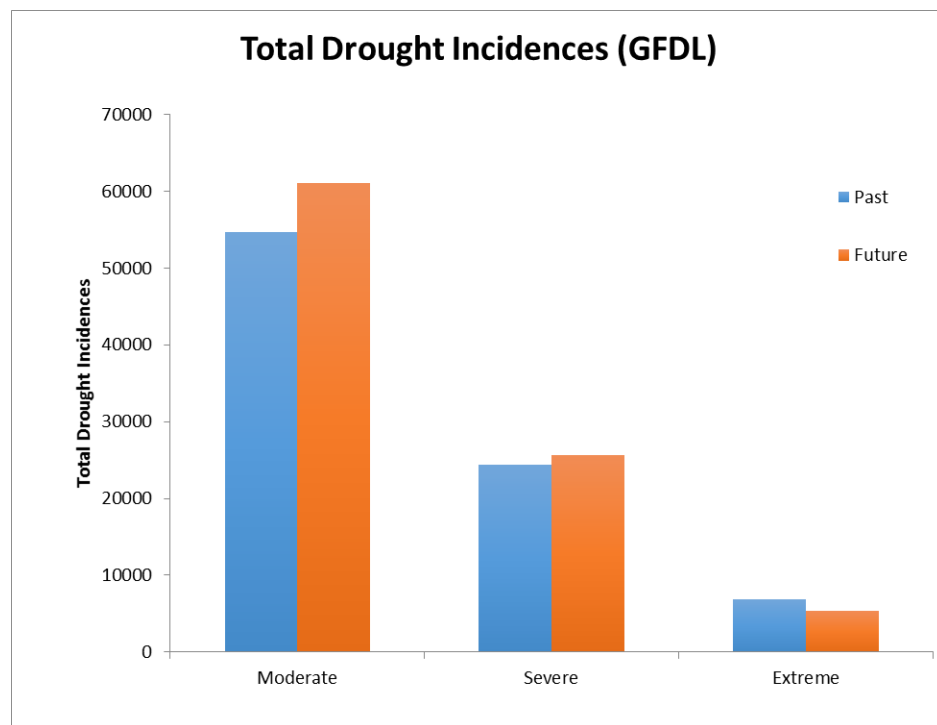
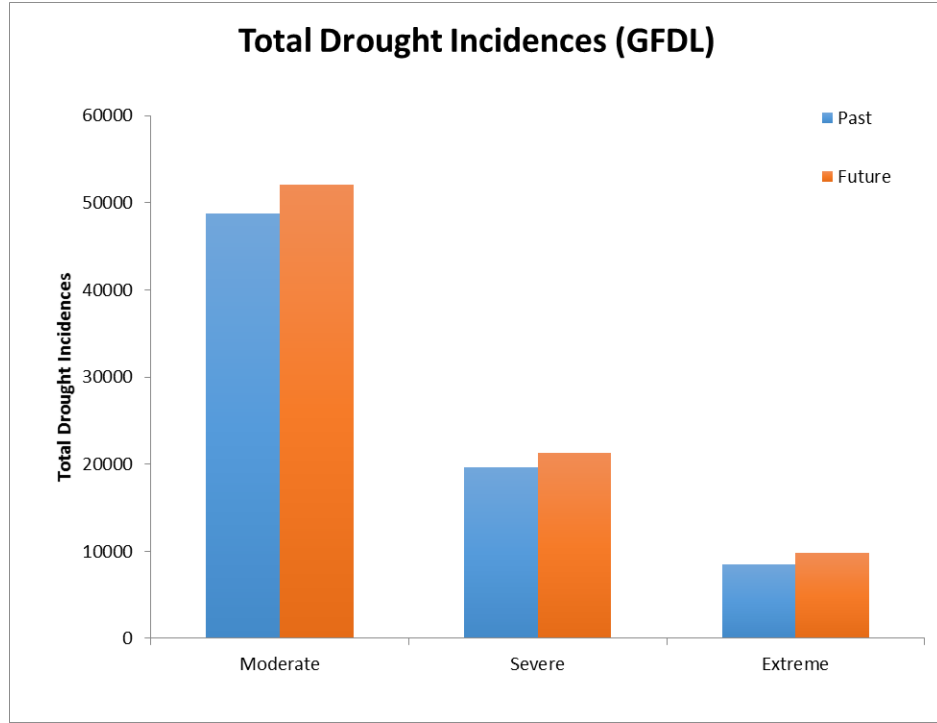
Figure 3.11: Total number of different kind of drought incidences according to SPEI from GFDL.

Droughts in the future are again seen to be more severe from the SAF curves in Figure 3.12. Among the SPEI from various models, this one suggests drought properties to change most significantly in the future. Droughts with all recurrence intervals are distinctly seen to be more severe in the future. Table 3.5 indicate increase in drought severity for droughts with different recurrence intervals. The severity
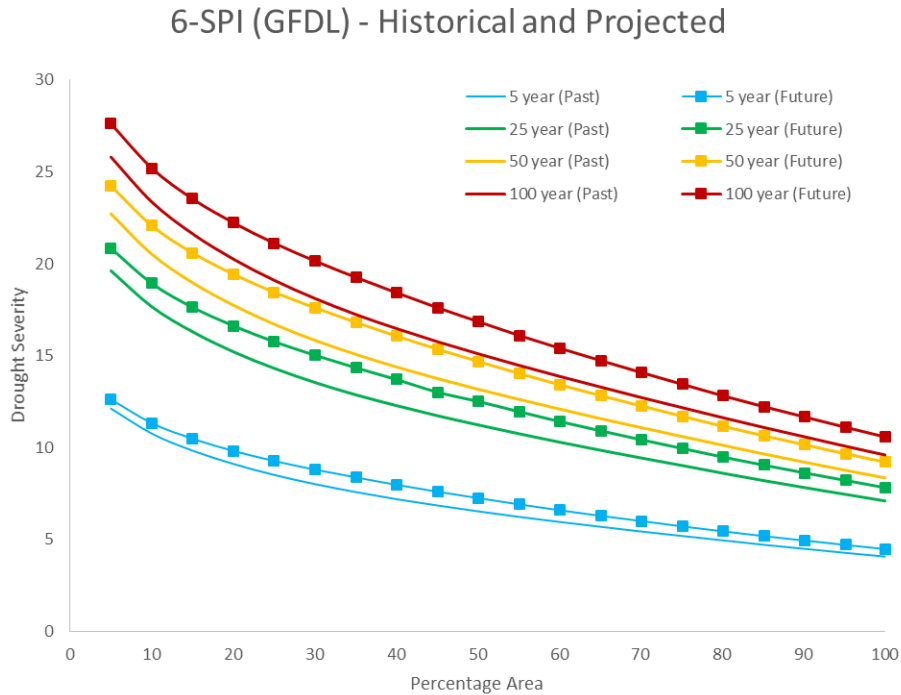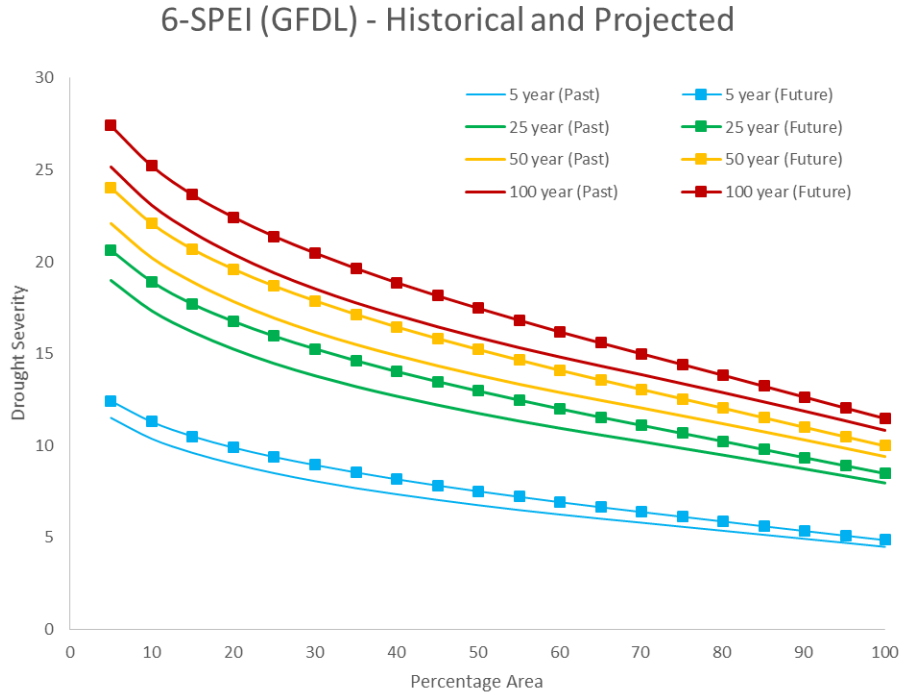
Figure 3.12: SAF curves for droughts with different recurrence intervals during historical and future periods (SPEI from GFDL).

Recurrence Interval	2 years	5 years	10 years	25 years	50 years	75 years	100 years
Percentage Increase	11.77	9.85	9.39	9.05	8.90	8.82	8.78

Table 3.5: Average percentage increase in overall drought severity according to SPEI from GFDL.

increases by 11.8 percent on average for 2-year droughts and by 8.8 percent for 100-year droughts. The maximum severity for a 100-year future drought at 5 percent threshold area is as high as 27.4. As it is evident from Figure 3.12, for any chosen percentage area, future droughts will be more severe and for any chosen severity, future droughts will be more widespread.

HadCM3

HadCM3 indicated an increase in all kinds of droughts. As seen in Figure 3.13, moderate, severe and extreme droughts increased by 6.7 percent, 8.5 percent and 7.6 percent respectively. The total number of drought incidences across Alabama was seen to increase by 7.3 percent. The longest drought in the past period was observed to be of 15 months duration whereas the longest drought was of 14 months in the future time period.
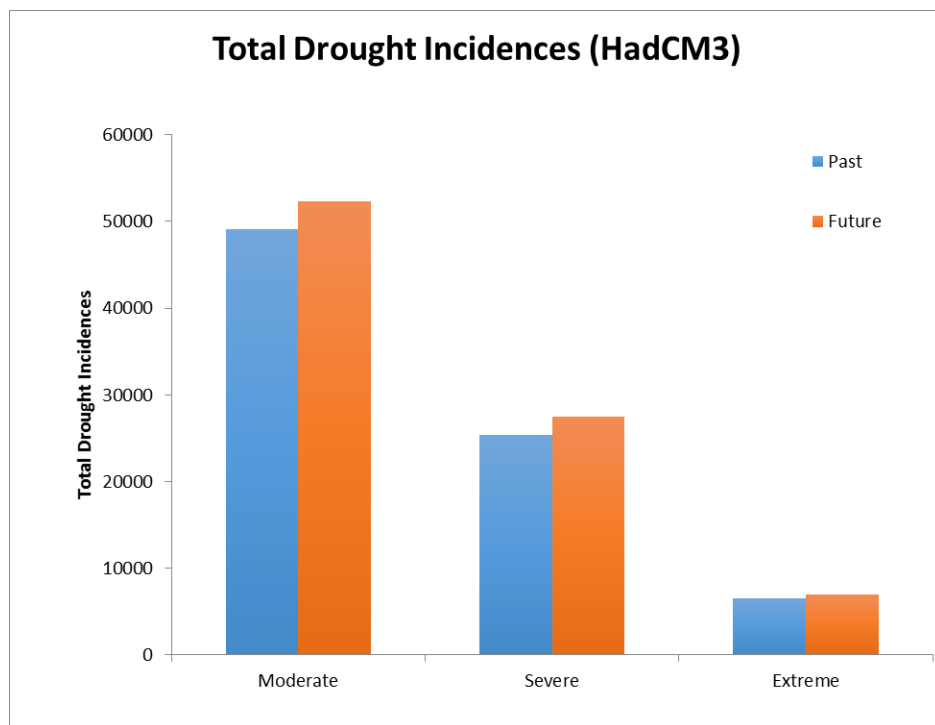
Figure 3.13: Total number of different kind of drought incidences according to SPEI from HadCM3.

Again, the SAF curves in Figure 3.14 indicate future droughts to be more severe than those of the past. However, they don't appear to be as severe as that indicated by the SPI from this model. It can be seen that the future curve for droughts of any recurrence interval is higher than their corresponding curve in the past. This implies droughts in the future will be more severe for any area considered and for any chosen severity, droughts will be more widespread. Table 3.6 summarizes the
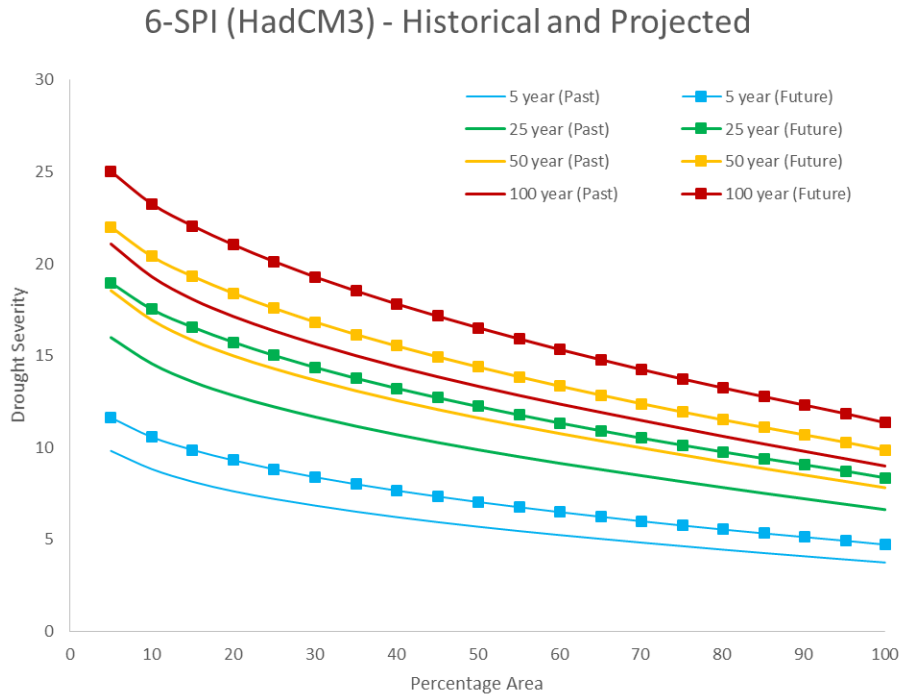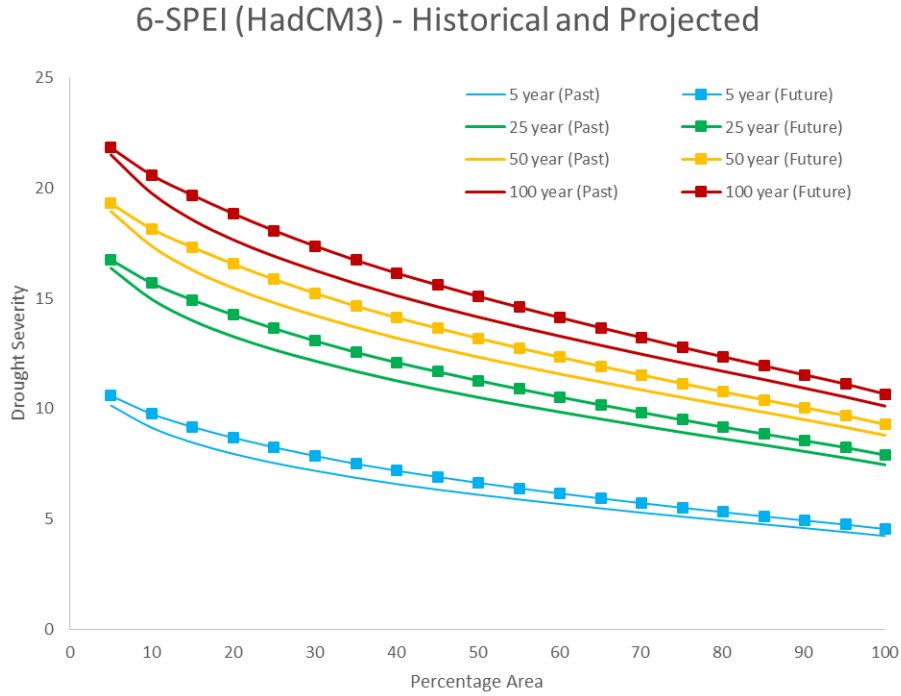
Figure 3.14: SAF curves for droughts with different recurrence intervals during historical and future periods (SPEI from HadCM3).

Recurrence Interval	2 years	5 years	10 years	25 years	50 years	75 years	100 years
Percentage Increase	11.79	8.14	7.18	6.47	6.12	5.96	5.87

Table 3.6: Average percentage increase in overall drought severity according to SPEI from HadCM3.

average percentage increase in drought severities for droughts with different recurrence intervals. 2-year droughts are predicted to increase in severity by about 11.8 percent and 100-year droughts are predicted to increase by 5.9 percent.

3.7 Summary and Conclusion

This study used two common drought indices, SPI and SPEI to quantify the effect of climate change on droughts in Alabama. The indices were analyzed using SAF curves. It is widely known that the effects of climate change can be observed

45

fastest on water resources. Climate change is bound to stress available water resources at any place. As a consequence of limited water supply, the characteristics of droughts are likely to change too because of climate change.

In general, droughts in Alabama are expected to increase in frequency as a result of climate change. The results for two drought indices calculated from two out of three GCMs (GFDL and HadCM3) used in this study showed that droughts in future are expected to be more severe, more frequent and also more widespread in the future than in the past. CCSM model indicates droughts to be similar in both time periods being considered in this study. The increase in severity indicated by this study could imply longer droughts that are moderately severe or relatively shorter droughts that are exceptionally severe.

With droughts increasing in severity by as much as 23.7 percent, there is definitely the need for better preparedness against them. The characteristics of droughts are being influenced by climate change to a certain extent. Our preparedness for the future should be influenced by anticipation of worst droughts in future and far-reaching consequences from those droughts.

The results of this research can be used by policymakers to plan ahead of time for better preparation to the drought years. If droughts can be projected well ahead of time, their consequences can be tackled more appropriately. The results of this study also helps us to understand expected changes in droughts in the Southeast US better and exposes the need to prepare better to mitigate the economic, social and environmental effects of droughts.

Chapter 4

How would frequency, severity and spatial extent of future droughts change in the

Apalachicola-Chattahoochee-Flint River Basin?

4.1 Abstract

Droughts are natural disasters that cannot be prevented, but forecasting and quantifying them before their occurrence can reduce their impacts. Recurring droughts in the Southeast US have called for a more pragmatic approach to manage their consequences. The focus of this study was to analyze how droughts in the Apalachicola-Chattahoochee-Flint (ACF) River Basin will change in future as a result of projected climate change. Commonly used drought indices were computed to quantify the change in droughts.

Two commonly used drought indices, Standardized Precipitation Index (SPI) and Standardized Precipitation Evapotranspiration Index (SPEI) were used to quantify and assess historical and future droughts. The change in frequency, severity and spatial extent of future droughts were analyzed. Precipitation and temperature data, regionally downscaled for the Southeast US for high emission scenario (A2) by Regional Spectral Model (RSM) at the Florida State University (FSU) - Florida Climate Institute (FCI), from three General Circulation Models, Hadley Centre Coupled Model Version 3 (HadCM3), Geophysical Fluid Dynamics Laboratory (GFDL) Model and Community Climate System Model (CCSM), from the Third Coupled Model Inter-comparison Project (CMIP3) archive were used for this study. Data from 1969 to 1999 was used for historical simulation and that from 2039 to 2069 was used for future projections.

Severity-Area-Frequency (SAF) curves were analyzed for droughts with different recurrence intervals. SPI from HadCM3 and GFDL model indicated droughts in future to be more severe, frequent and widespread. SPI from CCSM suggested more moderate droughts in the future but fewer severe and extreme ones. The model also indicated that severity and spatial extent didn't change much. SPEI from CCSM suggested increased extreme droughts in the future but the overall severity and spatial extent was again seen to be similar. Again, SPEI from HadCM3 and GFDL model indicated increase frequency, severity and spatial extent of future droughts.

The results of this research helps us understand projected changes in the nature of droughts in the ACF River Basin. The analysis of drought trends can be applied in a drought monitoring or early warning system and can be used to mitigate the effects of droughts proactively. If droughts can be projected well ahead of time, their consequences can be tackled more appropriately and socioeconomic and environmental impacts can be lessened.

4.2 Introduction

The problems of droughts are on the rise, mainly due to increasing population and alarming effects of climate change. It is often considered to be the costliest environmental disaster and, hence, draws the attention of people from various walks of life. Farmers get affected as droughts reduce agricultural production. Economists are concerned because droughts often hampers economical growth in the region where it occurs. Environmentalists are concerned because of the enormous harm it causes to the environment and the diverse species. Drought is a disaster that affects millions directly or indirectly, causing a global annual average loss between \$6 and \$8 billion.

Droughts directly affects water resources, reduce food availability and may lead to famine, desertification and loss of biodiversity. The severity of a drought is heavily influenced by the water demand in the region. Managing and mitigating the effects of

droughts is dependent on managing water resources efficiently. The extensive losses caused by droughts speak volume about the necessity to manage them better.

Droughts are a feature of the North American climate. They will continue to exist in the future as they have in the past. The losses they bring about are in billions and hence are considered to be the costliest natural disaster in economic terms. Plenty of resources are at stake because of droughts. The problems of droughts have increased significantly over the last few decades in the US. Almost 81 percent area of contiguous US were under at least abnormally dry condition when the 2012 drought was peaking. The total loss from this disaster was estimated to be around $30 billion.

Considering the droughts in Western and Central US, which often last decades, southeastern droughts are relatively short. However, the Southeast US has been witnessing extreme weather and climate events since centuries ago. Severe thunderstorms, floods, tornadoes and droughts are not uncommon in the region. The effects of climate change are often distinct in the region and have been quantified by some studies and reported already (KC et al, 2015; NCA, 2013). Projected data predict water resource problems to be more pronounced due to changing climate.

ACF has 16 dams present in its mainstem rivers and these regulate the flow in the rivers. As these rivers in the region fulfill most of its water resource demands, the dams control the hydrology of the entire region to a great extent. The population of the region, which was 2.64 million in 1990, has increased enormously over the last couple of decades. Also, the irrigational agricultural activities have increased in the southern part of the region. Increasing demand for water resources point towards the problems the region may face in future. The severity of the 2007 and 2012 droughts are indications that we must be prepared for worse droughts in the future.

The unfavorable consequences droughts bring need to be tackled well to minimize the socioeconomic losses. The fact that extreme droughts are not frequent in the region does not mean that they won't be in the future either. The changing nature of

droughts in the recent years questions our knowledge about droughts suggesting that more research is needed to know them better. More studies can definitely assist in developing models and information systems that can correctly forecast droughts and analyze its properties. There are huge gaps that need to be filled regarding droughts in the Southeast US. The problems of increasing droughts can be mitigated with more research that can help stakeholders and policymakers make wise decisions. There are many questions that need to be answered with regards to droughts and only extensive research can help us answer them.

4.3 Objective

Analyze the changes in frequency, severity and spatial extent of droughts in the Apalachicola-Chattahoochee-Flint River Basin using Severity-Area-Frequency Curves.

4.4 Study Area

The area under consideration for this study is the Apalachicola-Chattahoochee-Flint (ACF) River Basin. It sprawls across the southeastern states of Alabama, Florida and Georgia covering about 5 degrees of latitude. The basin drains across an area of about 19,800 square miles. About 75 percent of the basin is in Georgia and the remaining 25 percent is shared by Alabama and Florida roughly equally. The mainstem of the three rivers consists of 16 dams that cause a large portion of river to be in the form of backwater, hence, influencing water quality and quantity in the basin. Water issues frequently trouble the region.

The Chattahoochee River originates in northeast Georgia in the Blue Ridge Mountains and runs along the southern half of Alabama-Georgia border. It is about 430 miles long and drains an area of about 8770 square miles. The Flint River is about 344 miles long and drains a total area of about 8460 square miles. These two rivers join to form the Apalachicola River, which is approximately 112 miles long.
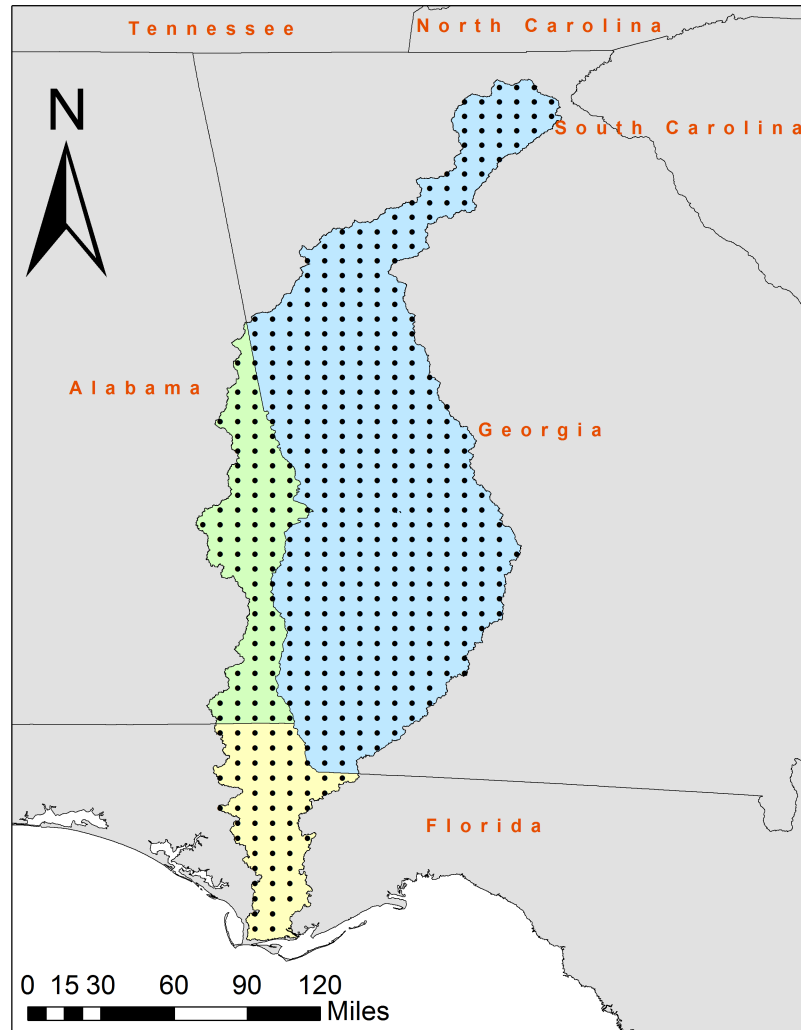
Figure 4.1: Apalachicola-Chattahoochee-Flint River Basin with all the locations for which the indices were calculated.

The confluence of the rivers lies close to the Georgia-Florida state line and it is submerged in Lake Seminole. The Apalachicola River flows into the Apalachicola Bay and then the Gulf of Mexico.

The climate in the basin is warm and humid, typically portraying temperate conditions. The annual rainfall for the region is about 55 inches. The northern part of the basin receives orographic rainfall because of the mountains and the southern side receives convective rainfall because of its proximity to the Gulf of Mexico (Couch et al., 1996). The average temperature is about 60°F in the north and about 70°F

in the south. Evapotranspiration generally increases from north to south, basically because of increasing temperatures. It ranges between 32 inches to 42 inches per year. Groundwater in the basin is basically stored in six different kinds of aquifers. The crystalline-rock aquifers dominate the northern part of the basin, the Providence aquifer, the Clayton aquifer, the Claiborne aquifer and the Floridan aquifer exist in the central part and the surficial aquifer exists close to the coastal plains. Over the
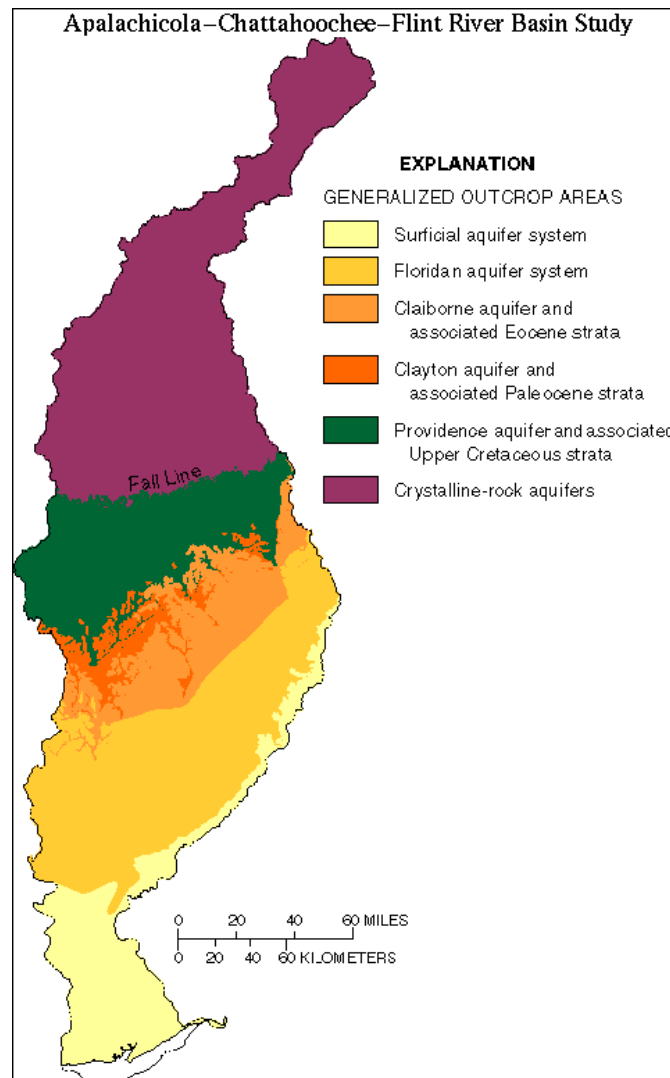
Figure 4.2: Aquifers contained in the ACF River Basin.
Source: http://ga.water.usgs.gov/nawqa/basin/gw-hydrology.html

last 50 years across the region, the average precipitation decreased between 9 percent

and 16 percent, soil moisture declined between 3 percent and 6 percent, the water-shed runoff decreased between 16 percent and 27 percent and the evapotranspiration increased between 1 percent and 3 percent causing intensification of droughts. Between 1986 and 2007, the Apalachicola-Chattahoochee-Flint River Basin witnessed 8 drought years out of which 4 were severe drought years (USCoE, 2011). The record-low precipitation received by northern Georgia coupled with increasing temperatures in 2007 gave rise to a massive reduction of water quantity in the lakes and rivers in the region. Lake Lanier was only about half of its capacity in spring 2008. Projected climate data indicate water problems in the basin to deepen over the next few decades.

The enormity of water issues in the region is vividly exemplified by the tri-state water wars going on since decades between Alabama, Florida and Georgia regarding water usage in the basin. Out of 16 dams in the region, 13 exist along the Chattahoochee River. These dams mostly regulate the flow along both Chattahoochee and Apalachicola rivers. Damming the Chattahoochee River by Buford Dam created Lake Lanier. Most of the water demand of Atlanta and Columbus metros is met from the Chattahoochee River, its tributaries and Lake Lanier. As the basin is subject of riparian water rights, Alabama and Florida filed lawsuit in early 1990s against the US Army Corps of Engineers (USCOE) and Georgia for diverting water from Lake Lanier for consumption in Atlanta. Also, increasing irrigated agriculture consumes copious amount of water in southwest Georgia. Most of this demand is met from the Upper Floridan Aquifer, which is connected to the Flint River. This regulates flow along Flint River and its tributaries as well. The dispute is still going on and the lawsuits are still pending in courts (as of June 2015).

4.5   Data and Methodology

Many climate variables from three different models were downscaled to 10 km resolution over the Southeast US by the Regional Spectral Model (RSM) at Florida State University (FSU) - Florida Climate Institute (FCI) with the methods adapted from Kanamitsu et al. (2010). As part of the COAPS Land-Atmosphere Regional Ensemble Climate Change Experiment for Southeast US at 10 km resolution (CLAREnCE10), three Coupled Model Inter-comparison Project (CMIP3) coupled General Circulation Models (GCMs) were downscaled for the A2 emissions scenario of the Fourth Assessment Report (IPCC, 2007). The models used were Community Climate System Model (CCSM), Geophysical Fluid Dynamics Laboratory (GFDL) Model and Hadley Centre Coupled Model Version 3 (HadCM3). Precipitation and temperature data were used from these three general circulation models to compute the indices.

In this study, droughts were quantified by the use of SPI and SPEI for timescales of 1, 3, 6 and 12 months. Both appear to be rational choices, as both possess the capability of to monitor and forecast droughts effectively.

4.5.1   Standardized Precipitation Index (SPI)

Long-term precipitation data for duration lasting at least 30 years is required to compute the SPI. First, the mean and standard deviation for the long record of precipitation at any given location is calculated. The data is then transformed into lognormal values to obtain the U-statistic, shape and scale parameter. Using these parameters, the cumulative gamma probability distribution can be calculated. The cumulative probabilities are obtained from this distribution. This probability is further transformed to standardized normal probability distribution using probability transformation techniques suggested by Abramowitz and Stegun, 1965. A step-by-step procedure to calculate the index is described in Appendix A.

SPI was computed for timescales of 1, 3, 6 and 12 months using precipitation data from CLAREnCE-10 dataset. A total of 529 points existed across ACF River Basin for which the time series of SPI values were calculated.

4.5.2 Standardized Precipitation Evapotranspiration Index (SPI)

SPEI calculation procedure is very much similar to that applied in calculating SPI. Besides precipitation, this index considers evapotranspiration too. This index is derived based on the moisture balance value at any given location. The moisture departure is obtained as the difference between the precipitation and potential evapotranspiration. Moisture departure is then transformed into log-logistic probability distribution. This probability distribution is further transformed to standardized normal probability distribution using probability transformation techniques suggested by Abramowitz and Stegun (1965) to obtain the SPEI. A step-by-step procedure to calculate the index is described in Appendix B.

SPEI was computed for timescales of 1, 3, 6 and 12 months using precipitation and temperature data from CLAREnCE-10 dataset. A total of 529 points existed across ACF River Basin for which the time series of SPEI values were calculated. PET was calculated from temperature using Thornthwaite Method. The difference between precipitation and PET was calculated as the moisture balance, which was used to compute the SPEI.

4.5.3 Potential Evapotranspiration

Potential evapotranspiration (PET) is an important component in calculation of SPEI. The PET is subtracted from the precipitation to obtain the moisture balance. It is the moisture balance that is processed to compute the SPEI. In this study, Thornthwaite method was used to calculate PET. Studies show that Penmann-Monteith is the most reliable method to compute PET. However, Mavromatis (2007) showed that

the choice of method for estimation of PET doesn't affect the drought index significantly. The primary idea of this study is to analyze drought events during two time slices. Therefore, the choice of method for PET calculation is not likely to affect the results as the method chosen would equally affect the values during both time slices. The method applied to calculate PET is described in detail in Appendix C.

4.5.4 Severity-Area-Frequency (SAF) Curves

Construction of Severity-Area-Frequency (SAF) curves enables droughts to be analyzed effectively. They are pretty informative and allow droughts to be compared across their entire spatial extent. Regional droughts can be compared with standard droughts with specific recurrence intervals to assess their severity, frequency and spatial extent at the same time. Comparison of drought indices at specific locations allows the changes in frequency and severity at that particular location to be studied. However, comparing droughts at specific locations to comment on overall drought characteristics across a region would not be considered wise. SAF curves make it easier to discern the subtle differences in drought severity across different percentage area being considered by associating them with various return intervals.

To construct SAF curves, firstly, the drought variable of a suitable timescale (3-SPI, 6-SPI or 12-SPI) must be identified. For the selected drought variable, the drought severity, which is simply the sum of negative values during a dry spell, is calculated. Then, for different areal extent of the droughts, the aggregated mean of drought severity is calculated by taking various areal thresholds into consideration. Drought severities across various areal extents are all fitted according to a probability distribution. In this study, Extreme Value Type I distribution was chosen. Then, frequency analysis is performed so that different return intervals can be quantified by respective severities across different areal extents. Finally, these severities are plotted against the areal extents to obtain SAF curves.

4.5.5 Timescale of Indices

Different kinds of droughts can be quantified and assessed from SPI and SPEI depending on the timescale used for their calculation. SPI and SPEI from shorter timescales like 2-3 months can provide information about the soil moisture condition or streamflow. Similarly, longer timescales of 12-24 months can be used to assess information about groundwater level. Droughts in the basin were assessed by SPI and SPEI from three GCMs for historical and projected simulations by the means of SAF curves. In this study, SAF curves were constructed from SPI and SPEI of 6 months timescale. Droughts usually take up 2-3 months to make a mark and can exist for periods ranging from months to years. Hence, minor temperature fluctuations over a month or two are not likely to instigate drought. It is, therefore, expected that the timescale of 6 months will include all major droughts and eliminate minor ones in the analysis.

4.6 Results and Discussion

Droughts in the ACF River Basin were quantified by SPI and SPEI from three GCMs for historical and projected simulations and analyzed using SAF curves. The results from the respective indices are discussed below:

4.6.1 SPI

As SPI less than -1 indicate drought conditions, all the values of SPI greater than this were omitted for analysis. The results of SPI from various models are presented below:

CCSM

Initially, drought incidences were studied to assess the drought frequency and duration across the basin for the two time periods in consideration. Comparison of
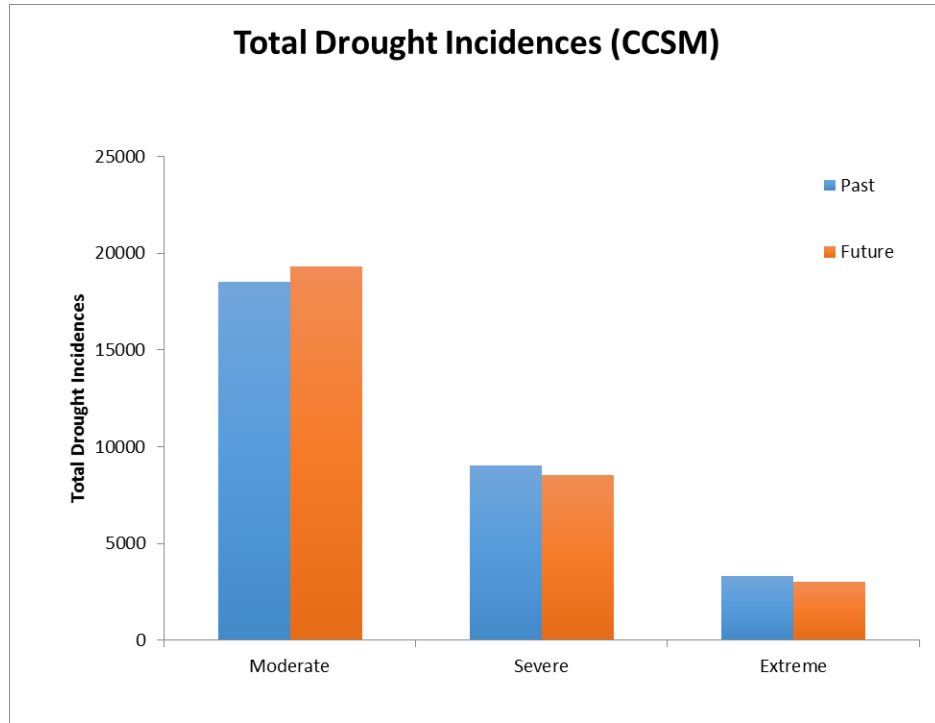
Figure 4.3: Total number of different kind of drought incidences according to SPI from CCSM.

drought incidences from 6-SPI from CCSM is shown in the Figure 4.3. In the future, moderate droughts are observed to increase by 4.3 percent and severe droughts and extreme droughts to decrease by 5.9 percent and 10.0 percent, respectively. However, the overall reduction in droughts was by a minimal 0.25 percent. The comparison of drought durations indicated them to be similar for both time periods. The longest ones in the past and future were about 14 months and 15 months, respectively.

Droughts with standard recurrence intervals of 5, 25, 50 and 100 years were compared for the two time slices. The SAF curves, shown in Figure 4.4, indicated future droughts to be very similar to the ones in the past. The results presented in Table 4.1 show slight increase in the overall severity of droughts. 2-year droughts increase in severity by 4.27 percent and 100-year droughts increase by 0.14 percent. The spatial extent of droughts appears to be very similar in the past and the future. From the SAF curves, the maximum drought severity can be observed to be around

58
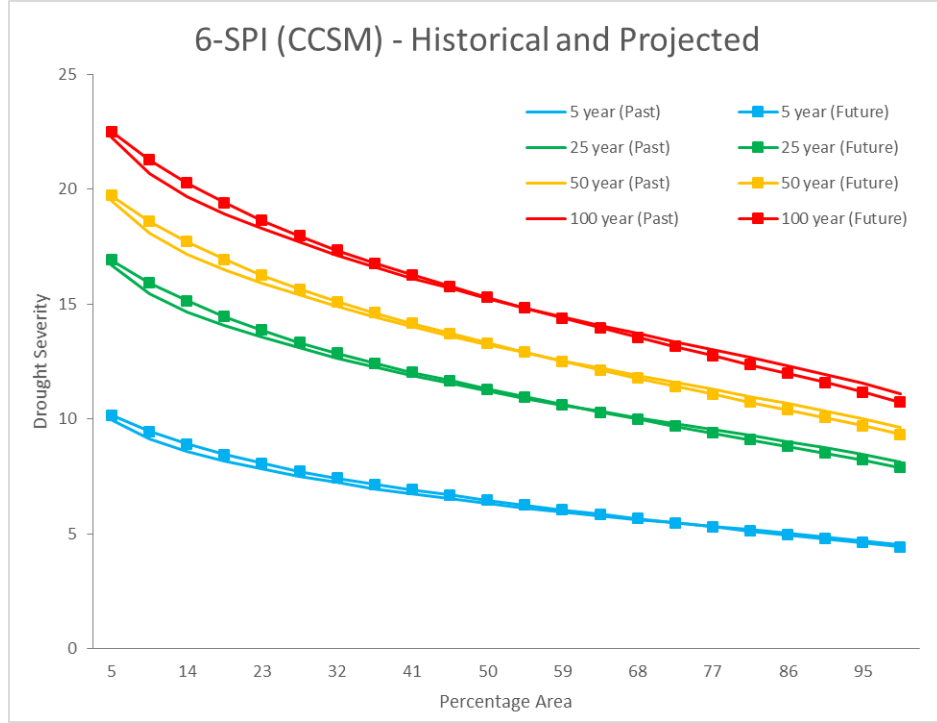
Figure 4.4: SAF curves for droughts with different recurrence intervals for future and past (SPI from CCSM).

Recurrence Interval	2 years	5 years	10 years	25 years	50 years	75 years	100 years
Percentage Increase	4.27	1.61	0.97	0.52	0.30	0.20	0.14

Table 4.1: Average percentage increase in overall drought severity according to SPI from CCSM.

22.5 for a 100-year drought in both past and future across an area of 5 percent. The decrease in severity is gradual as the area under consideration is increased.

GFDL

The results from GFDL model indicated an increase in moderate and extreme droughts but a slight decline in severe droughts in the future. The comparison is shown in Figure 4.5. Moderate droughts increased by 4.2 percent and extreme droughts increased by 49.2 percent while severe droughts decreased by 0.2 percent.

59
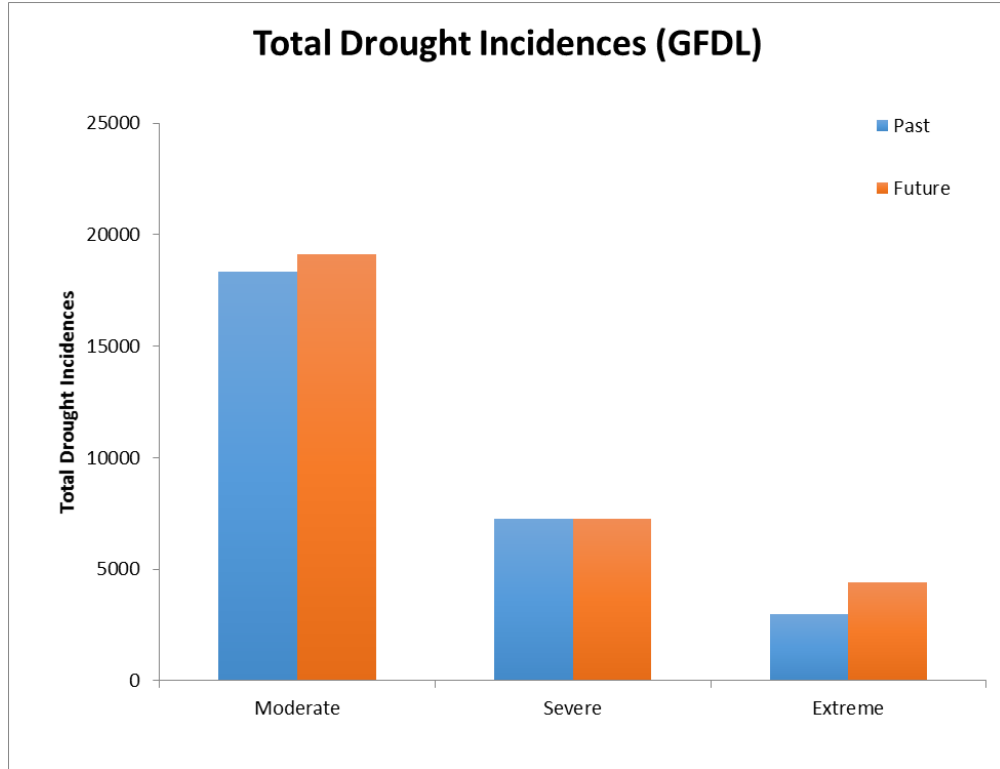
Figure 4.5: Total number of different kind of drought incidences according to SPI
from GFDL.

Overall, the droughts increased by 7.7 percent. Droughts were also observed to persist
for a longer time in the future. The droughts in the future are often as long as 21
months whereas the longest one in the past was of 15 months.

Recurrence Interval	2 years	5 years	10 years	25 years	50 years	75 years	100 years
Percentage Increase	5.93	8.59	9.28	9.79	10.04	10.15	10.22

Table 4.2: Average percentage increase in overall drought severity according to SPI
from GFDL.

The SAF curves are presented in Figure 4.6. They show future droughts to
be more severe and widespread. In general, the severity was seen to increase as the
recurrence interval of droughts increased. Table 4.2 shows average percentage increase
in drought severities for droughts with different recurrence intervals. The severity

60
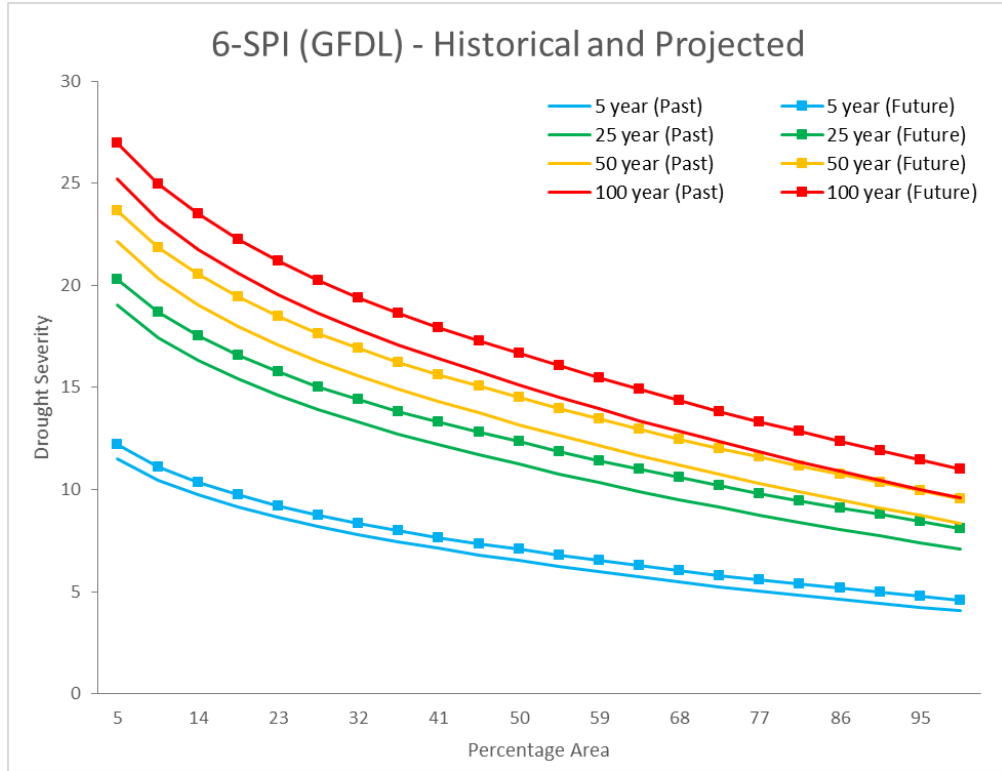
Figure 4.6: SAF curves for droughts with different recurrence intervals during historical and future periods (SPI from GFDL).

increased by about 5.9 percent for 2-year droughts and by about 10.2 percent for 100-year droughts. A 50-year drought in the future appears like a 100-year drought in the past when the entire area of the basin is considered. The overall severity, according to SPI, from GFDL was indicated to be higher than that from CCSM. This could either imply more severe droughts or similar droughts spanning a longer duration.

HadCM3

The results from HadCM3 indicated a very high increase in droughts. The general increase in drought occurrences can be observed in Figure 4.7. A slight decrease of 0.1 percent was observed among moderate droughts while severe droughts increased by 45.7 percent and extreme droughts increased colossally by 321.1 percent. In average, droughts increased by 28.9 percent. The longest drought in past was of 22 months while it was only of 13 months in the future.
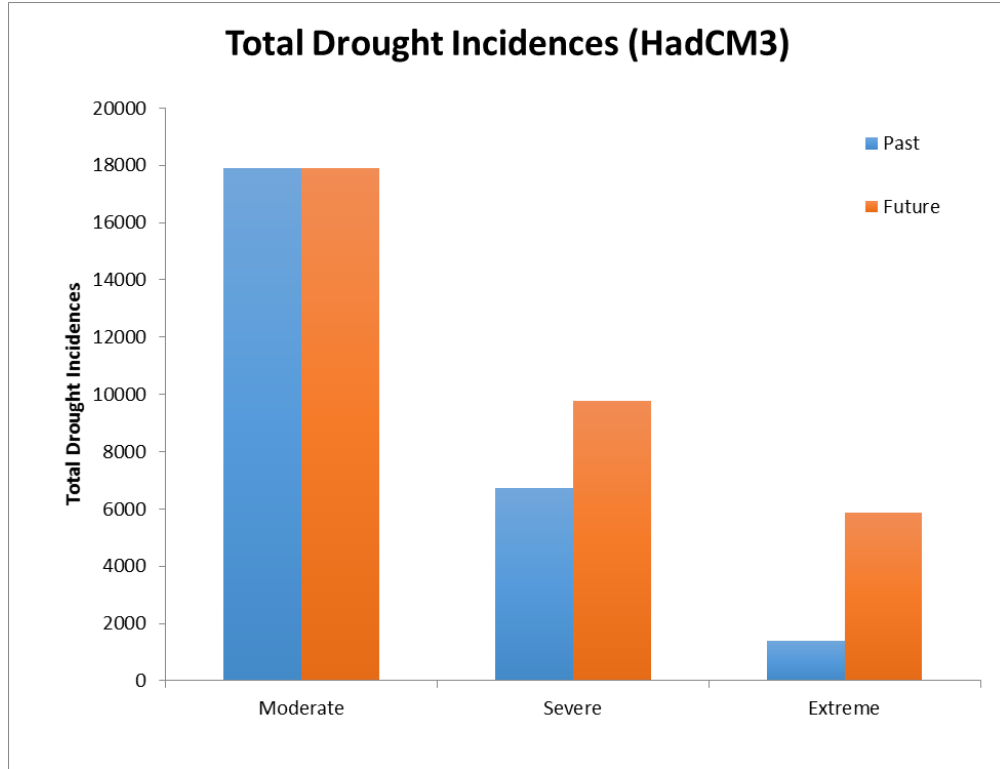
Figure 4.7: Total number of different kind of drought incidences according to SPI from HadCM3.

The SAF curves are presented in Figure 4.8. Huge increase in the severity and spatial extent of the droughts in the future can be observed. The average increase in drought severities are presented in Table 4.3. On average, 2-year droughts increase by 33.1 percent and 100-year droughts increase by 36.7 percent in the future. 25-year future drought closely resembles 100-year past drought. However, the severity is still slightly lower to that indicated from GFDL Model.

Recurrence Interval	2 years	5 years	10 years	25 years	50 years	75 years	100 years
Percentage Increase	33.11	35.25	35.87	36.31	36.55	36.62	36.70

Table 4.3: Average percentage increase in overall drought severity according to SPI from HadCM3
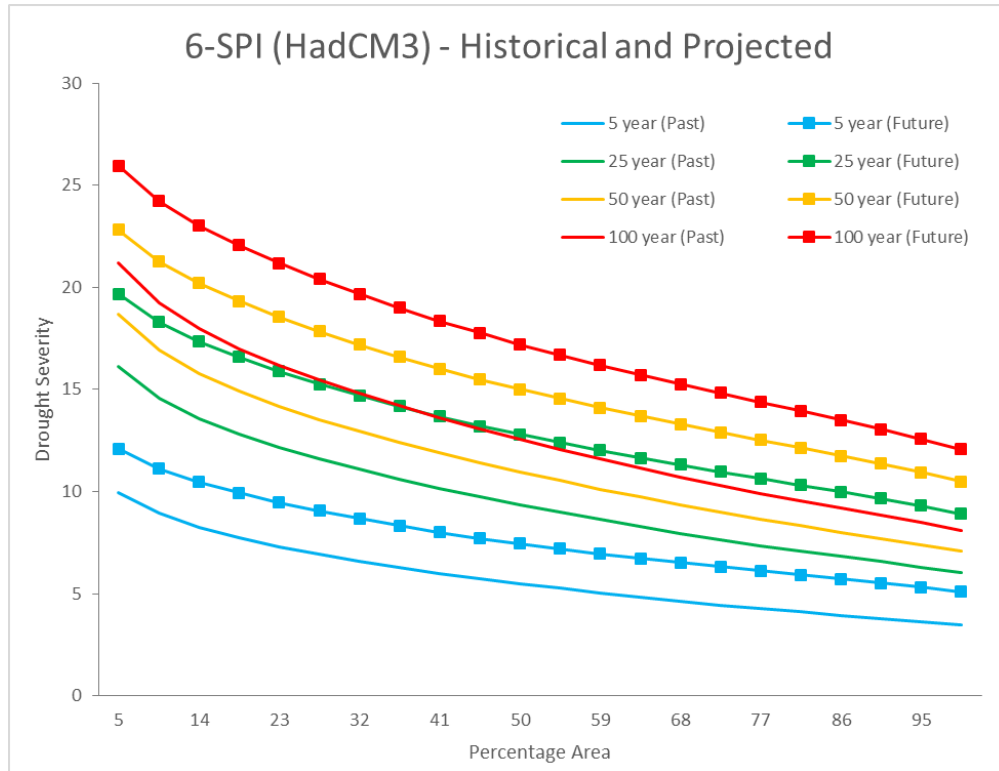
Figure 4.8: SAF curves for droughts with different recurrence intervals for future and past (SPI from HadCM3).

4.6.2 SPEI

SPEI values lesser than -1 indicate drought conditions. Values indicating non-drought conditions were omitted for analysis. The results from 6-SPEI from different models are presented below:

CCSM

SPEI from CCSM model indicated a decrease in moderate and severe droughts but an increase in extreme droughts. The bar chart is presented in Figure 4.9. Moderate and severe droughts decreased by 7.7 percent and 5.4 percent respectively. Extreme droughts increased by 72.6 percent. Overall, droughts decreased by 4.0 percent in the region. Droughts as long as 27 months lasted in the past whereas the longest drought in the future is only 13 months.
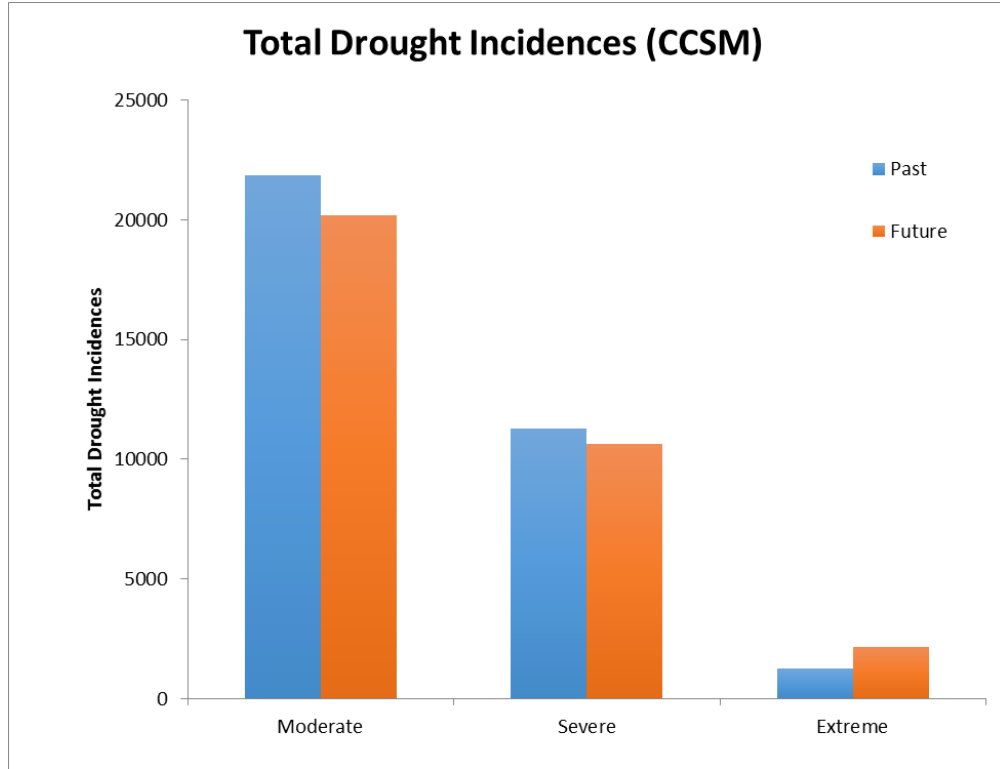
Figure 4.9: Total number of different kind of drought incidences according to SPEI from CCSM.

The SAF curves are presented in Figure 4.10. There exist vivid similarities between SAF curves for droughts of any given recurrence interval in the past and the future. Droughts with shorter return intervals can be seen to be roughly identical. The average change in severities for droughts is presented in Table 4.4. The severity for 2-year droughts increases slightly in future by about 1.58 percent. Even for more rare drought events, the differences are not drastic or distinct. The average severity for a 100-year drought is seen to decrease by 0.54 percent. This model predicts

Recurrence Interval	2 years	5 years	10 years	25 years	50 years	75 years	100 years
Percentage Increase or Decrease	1.58	0.17	-0.15	-0.35	-0.45	-0.51	-0.54

Table 4.4: Average percentage increase (+) or decrease (-) in overall drought severity according to SPEI from CCSM.

64

drought characteristics to remain similar in the future too. Besides severity, spatial extents appear to be virtually similar too. Drought incidences are fewer in the future. Both indices computed from this model indicate droughts to remain indifferent in the ACF River Basin. Although the droughts are not seen to change much, this model indicates droughts to be the most severe in both the periods considered.
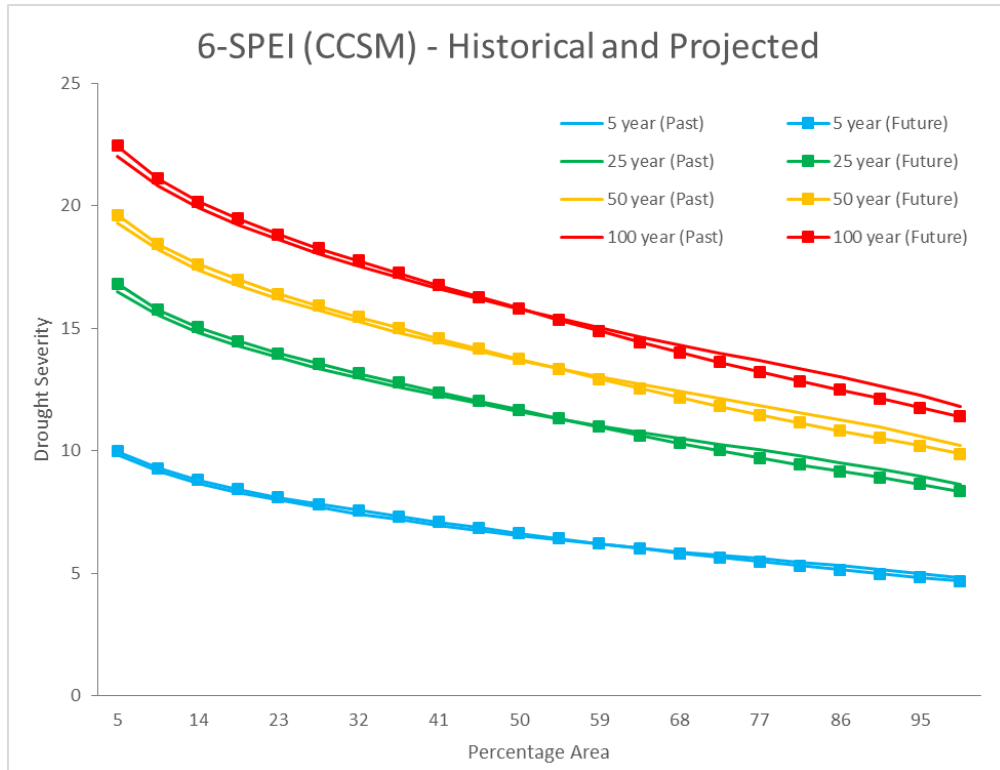
Figure 4.10: SAF curves for droughts with different recurrence intervals for future and past (SPEI from CCSM).

GFDL

GFDL indicated an increase in moderate and extreme droughts but a slight decrease in severe droughts. As evident from Figure 4.11, moderate droughts are observed to increase by 6.7 percent and extreme droughts by 28.4 percent. Severe droughts are seen to decrease by 3.3 percent. The total number of droughts increased by 5.3 percent. The longest drought in the past lasted for about 15 months. In the future, droughts as long as 19 months are projected.
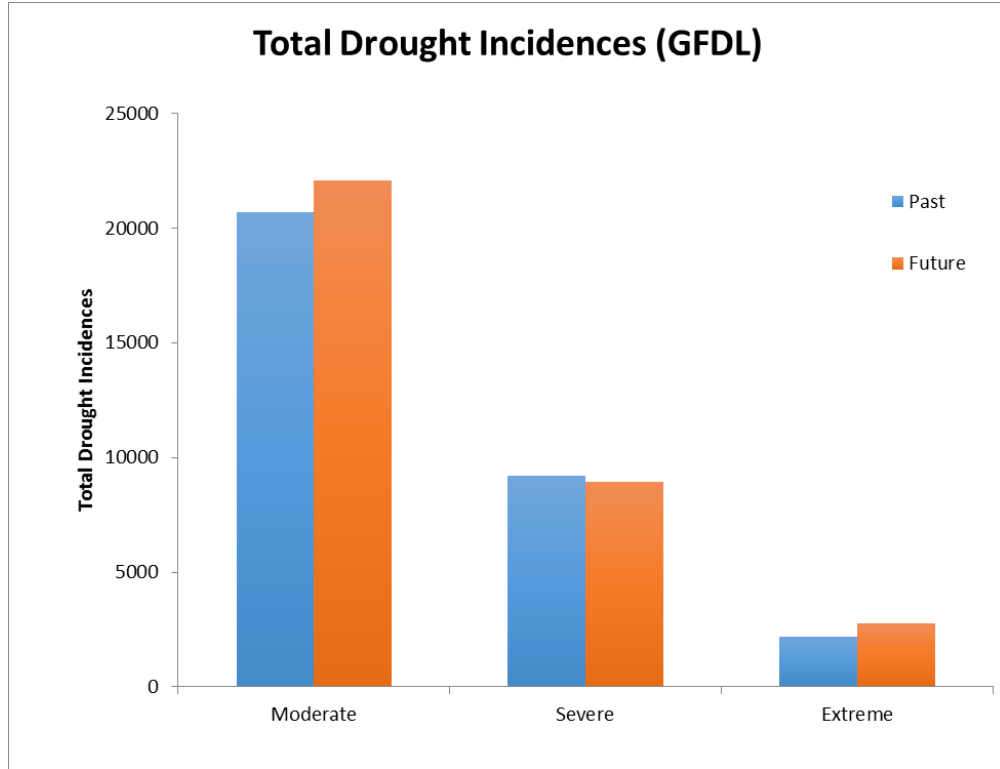
Figure 4.11: Total number of different kind of drought incidences according to SPEI from GFDL.

From the SAF curves in Figure 4.12, droughts in the future are observed to be more severe. Droughts with any chosen recurrence interval greater than 5 years are

Recurrence Interval	2 years	5 years	10 years	25 years	50 years	75 years	100 years
Percentage Increase	5.26	4.27	4.02	3.85	3.76	3.72	3.70

Table 4.5: Average percentage increase in overall drought severity according to SPEI from GFDL.

seen to be more severe and widespread in the future. The maximum severity for a 100-year future drought at 5 percent threshold area is as high as 26.1. For any chosen percentage area, the respective severity will be higher in the future. Table 4.5 summarizes the average increase in drought severities in the future. Average severity

66
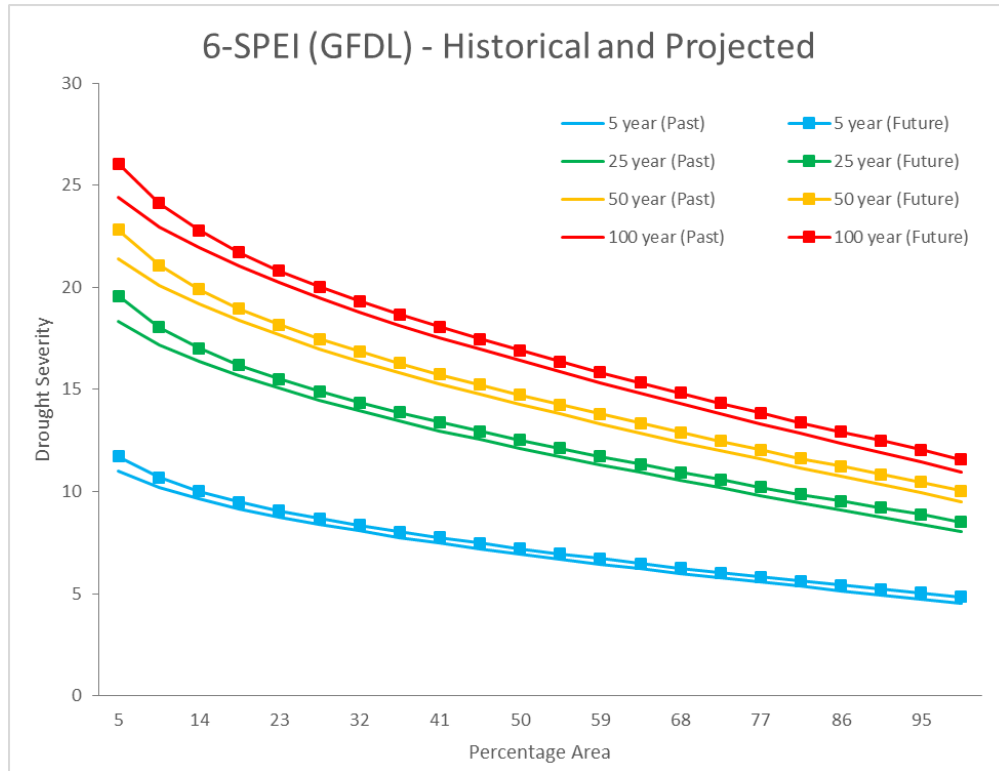
Figure 4.12: SAF curves for droughts with different recurrence intervals for future and past (SPEI from GFDL).

increases by about 2.3 percent for 2-year drought and by 3.7 percent for more extreme 100-year droughts.

HadCM3

HadCM3 indicated an increase in moderate and severe droughts but a decrease in extreme droughts in the future. As shown in the bar chart in Figure 4.13, moderate and severe droughts increased by 13.0 percent and 24.4 percent, respectively, and extreme droughts decreased by 29.1 percent. The total number of drought incidences across the ACF increased by 13.5 percent. The longest drought in past was observed to be of 20 months duration whereas the longest drought in future are seen to last as long as 16 months.

Again, the SAF curves in Figure 4.14 indicate future droughts to be more severe than those in the past. The change in severity, however, is not as high as SPI from
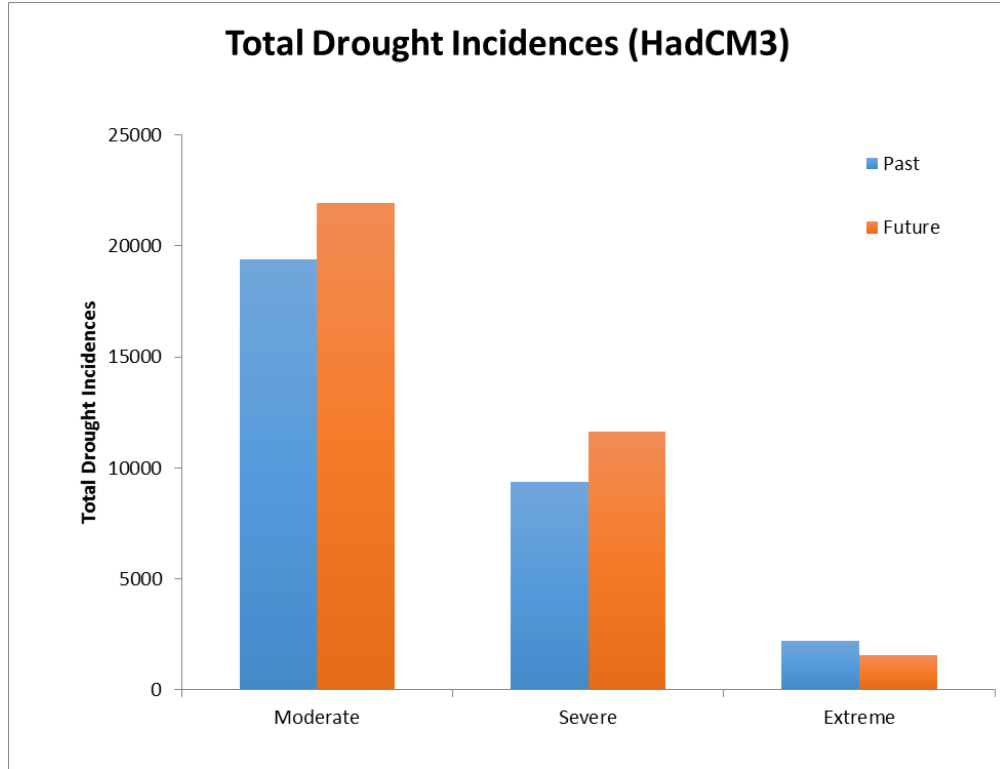
Figure 4.13: Total number of different kind of drought incidences according to SPEI from HadCM3.

this model predicts. The maximum severities for past and future droughts appear to be similar in the SAF curves. The gradual decrease in severity with increase in areal extent is faster in past droughts as compared to future droughts. Across the total spatial extent of droughts in the basin, the severity of a 50-year future drought is similar to that of a 100-year past drought and 25-year future drought to 50-year past drought. This indicates that although the maximum severities of droughts are unlikely to change, the average severity will change across the region. The average

Recurrence Interval	2 years	5 years	10 years	25 years	50 years	75 years	100 years
Percentage Increase	7.78	8.50	8.69	8.82	8.88	8.91	8.93

Table 4.6: Average percentage increase in overall drought severity according to SPEI from HadCM3.
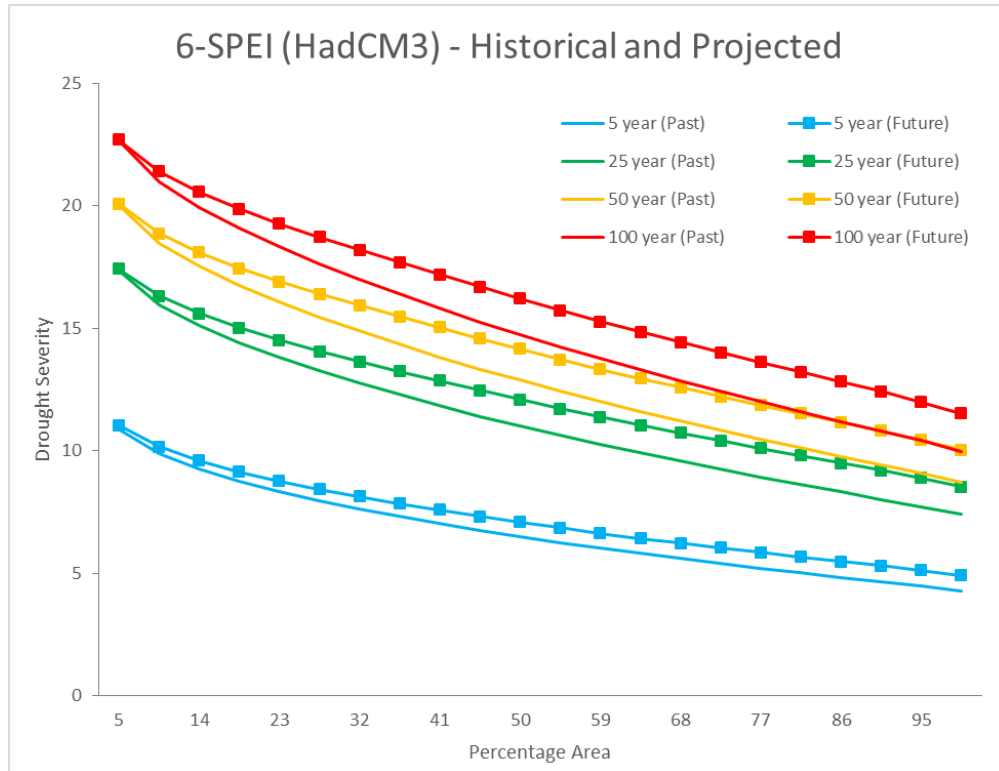
Figure 4.14: SAF curves for droughts with different recurrence intervals for future and past (SPEI from HadCM3).

increase in drought severities are given in Table 4.6. The average severity increases in future by 7.8 percent for 2-year droughts and by 8.9 percent for 100-year droughts. In general, droughts will be more severe in the future. Similarly, for any chosen severity, droughts in the future will be more widespread. Also, it can be observed that the predicted future increase in severity is proportional to the increase in return interval of the droughts.

4.7 Summary and Conclusion

The characteristics of extreme events are evidently changing in the recent years. More frequent flood and drought events have been observed in the recent years in the ACF River Basin. The plausibility of these changes in characteristics of natural calamities because of climate change cannot be denied. It has been widely predicted

69

that climate change shows its effects on water resources the fastest. Climate change is aiding the inability to fulfill water supply demands and hence, it can be predicted that the characteristics of droughts are likely to change too because of climate change.

It can be concluded from the results of this study that the characteristics of droughts in the ACF are expected to change over the future. The frequency and severity of drought events are expected to increase in general and it can also be said that droughts will increase in spatial extent too. Both indices from two out of three GCMs (GFDL and HadCM3) indicate a general increase in the frequency and severity of the droughts. These also indicate that for any given severity, the spatial extent will be much higher for future droughts. Both indices from CCSM indicate similarity in droughts in past and future. Slight reduction in the frequency of droughts can be observed according to CCSM. ACF needs to have better preparations for droughts. Climate change is influencing droughts to change their characteristics to a certain extent. To assure protectiveness against droughts, it would be beneficial if we can prepare against the worst of predicted droughts.

The results from this study can be used to increase our understanding of droughts in the ACF. Policymakers and stakeholders can use the results to come up with better plans for drought management. Accurate drought forecasting can alleviate the plausible effects from droughts. The results also give us an understanding about the expected changes in drought characteristics, which can be used to prepare better against droughts and reduce their socioeconomic and environmental impacts.

Chapter 5

Applicability of Standardized Precipitation Index for monitoring groundwater
conditions in the lower ACF River Basin

5.1 Abstract

Groundwater is a very important water source supplying a large proportion of the
total water demand in the United States. Groundwater quenches most of the water
needs in the Apalachicola-Chattahoochee-Flint (ACF) River Basin too. The river
basin has been characterized by water wars amongst Alabama, Florida and Georgia
because of water allocation from the basin. Frequent hydrological droughts in the
region worsens the situation. Monitoring groundwater levels can prove to be a part
of the strategy to manage water resources in the region.

The goal of this study is to determine the association of groundwater levels to
Standardized Precipitation Index (SPI) and find if it can be used as an index to
monitor groundwater conditions in the lower ACF River Basin. Long term historical
precipitation data were obtained from National Oceanic and Atmospheric Administra-
tion's National Centers for Environmental Information (NCEI) for various locations
in the study area. SPI was calculated at different timescales for various locations.
Daily groundwater level observations at various observation wells were obtained from
the United States Geological Survey, Georgia.

The results showed strong correlation between SPI at time scales between 9 to
12 months and the groundwater levels at the wells close to the rain gauging stations,
thereby indicating that SPI at these timescales can be used to monitor groundwater

conditions in the region. Accurate gridded observed precipitation forecasts and projections can be used to estimate groundwater levels in the corresponding locations. This can also be extended to monitoring hydrologic droughts in the region.

As most of the irrigation water demand in the lower ACF River Basin is met from groundwater resources, keeping track of groundwater conditions is of utmost importance to monitor droughts and mitigate their effects. The results of this study can be applied to monitor groundwater levels and hydrologic droughts in the region.

5.2 Introduction

Groundwater is the water that exists beneath the ground surface in pores, cracks and crevices in soil and rocks, which is often considered a large subsurface reservoir. The geologic formations containing groundwater are called aquifers. More than 90 percent of the total freshwater supply on earth exists in the form of groundwater (USGS, 2009). It occurs almost everywhere on earth in varying amounts beneath the ground surface. Almost half of the water demands in the US is met from groundwater. It is also a major source for recharge of surface water bodies and wetlands. Precipitation is the biggest source of recharge for groundwater.

The ACF River Basin is about 19,800 square miles in area and sprawls across the states of Alabama, Florida and Georgia. Alabama, Florida and Georgia have equal rights to water from the basin because of riparian water rights in the basin. The states have been involved in a tristate water war regarding the allocation of the basin's water resources. The water war, which was primarily initiated because of Georgia's inability to maintain fair streamflow levels in the rivers and tributaries of the ACF River Basin during droughts, has been going on for more than two decades now with a number of failed negotiations and litigations still pending in courts (as of June 2015).

Population is burgeoning in the region and so is the agriculture and industries. This has increased the water demand in the ACF River Basin by many folds. The increasing frequency and severity of droughts in the region in recent years exacerbates the already serious problems relating to water resources across the entire basin. Droughts directly restrict water and food availability in any region they occur. They often cause loss of wetlands and biodiversity. Decrease in groundwater levels signify hydrologic droughts. It is essential to monitor and forecast the groundwater levels early to predict droughts and mitigate their consequences.

Agriculture is a flourishing activity in southwest Georgia. Most of the water demands to sustain the requirements of this massive agricultural region is met from groundwater resources. The region contains more groundwater wells than surface water wells. The lower ACF contains a lot of land area, which contributes to the recharge of groundwater in the area. Groundwater is contained mostly in the Upper Floridan Aquifer in this region. The Upper Floridan Aquifer possesses about 100,000 cubic miles of karst limestone wherein most of the groundwater is stored. The aquifer is hydraulically connected to the principal rivers and the tributaries in the lower ACF River Basin and hence, reduction in the groundwater level in the region is often associated with decrease in streamflow levels along the Flint River and its tributaries. The interdependency of groundwater and surface water systems are worsened during drought conditions in the region (Mosner, 2002).

This goal of this study is to check the association of SPI at different timescales to the groundwater levels at various wells in the lower ACF River Basin. SPI has gained popularity as an effective drought index especially because of its capability to be used in drought early warning systems and to assess droughts. Its relative simplicity and ease to calculate compared to other drought indices makes it able to be used as an index that can be used in real time monitoring of droughts. This index when computed at long timescales has shown significant correlation to groundwater

levels in the area for which it is computed. If the index can be applied to estimate groundwater conditions in the region, forecasted precipitation data can be used to get early information about groundwater levels. It can also be used to monitor hydrologic droughts.

The urgency to effectively manage the water resources in this area is increasing every day. To better manage the detrimental consequences of droughts, there should be efficient methods and techniques to monitor and forecast water resource availability during any given time. The interconnection between groundwater and surface water systems in the region necessitate monitoring both groundwater and surface water conditions to develop better understanding of the relationship between the streams and the aquifers and use results from those for water-budgeting in the region.

5.3 Objective

Determine the applicability of Standardized Precipitation Index for monitoring groundwater conditions in the lower Apalachicola-Chattahoochee-Flint (ACF) River Basin.

5.4 Study Area

The area for which this study is based is the lower Apalachicola-Chattahoochee-Flint (ACF) River Basin. The lower ACF drains across an area of about 4632 square miles. Most of it lies in southwestern Georgia and small parts lie in southeastern Alabama and northwestern Florida as shown in Figure 5.1.

The climate in the lower ACF is warm and humid with subtropical conditions. Summers are long and winters are short and mild in the region. The average annual precipitation received by the region is about 50 inches and the average temperature is about 64°F. Precipitation is roughly equally distributed throughout the year. However, most of the recharge to the aquifer occurs between the months of December
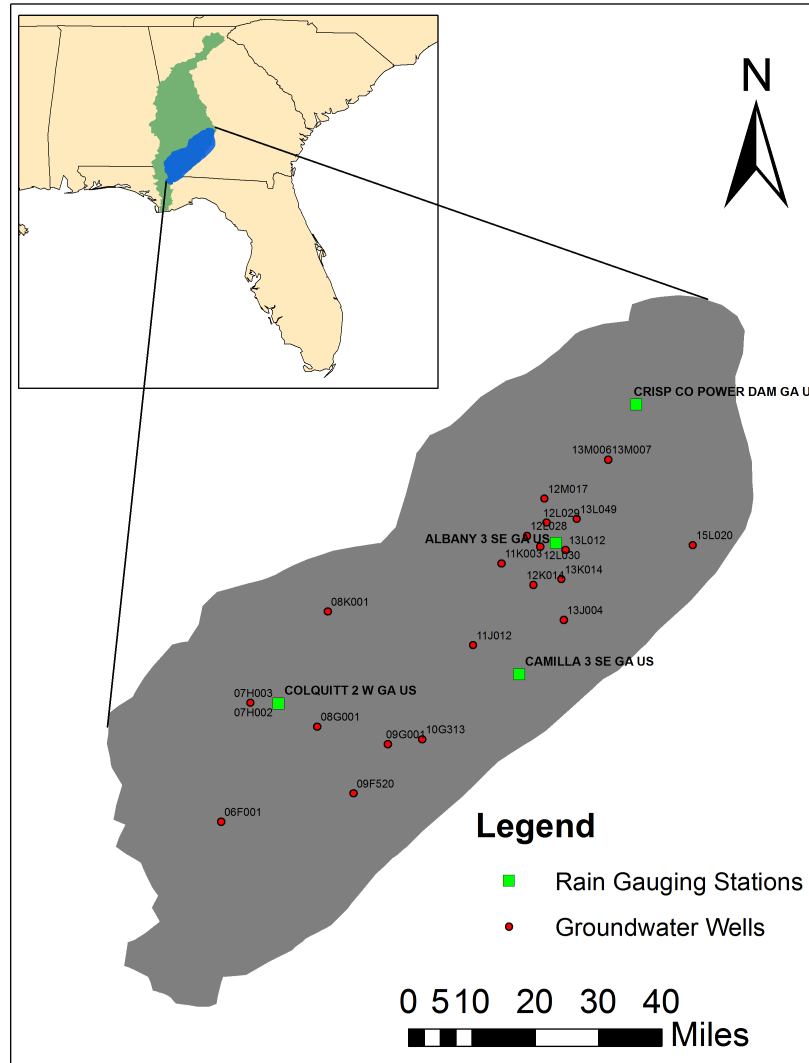
Figure 5.1: The lower Apalachicola-Chattahoochee-Flint River Basin with the location of the groundwater observation wells and the rain gauging stations.

and March. Winter rainfall are associated with high infiltration rate and low surface runoff.

The stream-lake-aquifer flow system in this part of the basin comprises of the surficial aquifer system, upper semiconfining unit, Upper Floridan Aquifer and lower semiconfining unit. The thickness of upper semiconfining unit ranges from a few feet to about 400 feet. Groundwater levels in this unit have been observed to respond to infiltration of precipitation. Water in the Upper Floridan Aquifer is mostly held

in over 100,000 cubic miles of karst limestone and it is used for agricultural use and public supply in the region.

Water management is a huge problem in the basin that is clearly exemplified by the tristate water wars that has been going on for decades between Alabama, Florida and Georgia. This region has obtrusively witnessed decreasing groundwater levels due to increased agricultural pumpage since mid-1970s and frequent droughts since the 80s. Mostly groundwater fulfills the irrigation demand in this region for the irrigation of almost half a million acres. Hence, the importance of monitoring groundwater conditions cannot be stressed enough.

5.5 Data and Methodology

Rainfall data from Global Historical Climatology Network maintained by NOAA were obtained at four rain gauging stations in the lower ACF River Basin. The climatology network is a collection of data from 30 sources. Monthly precipitation time series was obtained for the four gauging stations from beginning of 1970 to May 2015.

Daily groundwater data for observation wells in the lower ACF River Basin were obtained from United States Geological Survey, Georgia. The observation wells were all located in the Upper Floridan Aquifer. The data used was between 1975 and 2012 for a total of 38 years. From the available daily data, time series of average monthly groundwater levels for each of the well was calculated.

5.5.1 Standardized Precipitation Index

Standardized Precipitation Index was computed at four rain gauging stations for various timescales. The rain gauging stations are Colquitt 2 W GA, Camilla 3 SE GA, Albany 3 SE GA and Crisp Co Power Dam GA. Long-term monthly precipitation data from January 1970 to May 2015 was used to compute the SPI. SPI is computed

by transforming long-term precipitation data into gamma probability distribution and further transforming this into standard normal probability distribution. The stepwise method to compute the SPI is given in Appendix A. SPI between January 1975 and December 2012 was used to correlate to the groundwater levels.

5.5.2   Pearson's Correlation

Pearson's product-moment correlation was used to study the strength of association between the SPI at various timescales to the groundwater levels. The values can range from +1 to -1. Positive values imply positive correlation and negative values imply negative correlation between the variables. The strength of association implied by different values of Pearson's correlation coefficient are shown in Table 5.1.

Value of correlation coefficient	Strength of correlation
0.70 and above	Very strong (positive)
0.40 to 0.69	Strong (positive)
0.30 to 0.39	Moderate (positive)
0.20 to 0.29	Weak (positive)
0.19 to -0.19	Negligible
-0.20 to -0.29	Weak (negative)
-0.30 to -0.39	Moderate (negative)
-0.40 to -0.69	Strong (negative)
-0.70 and less	Very strong (negative)

Table 5.1: Range of correlation coefficients and their strengths.

5.6   Results and Discussion

SPI at timescales of 6, 9, 12, 15 and 18 months were correlated with the groundwater levels for different rain gauging stations and the observation wells close to it. All the stations for which the SPI was computed lie in Georgia. The groundwater levels at the wells close to the location of these gauging stations was correlated with

the SPI values. Strong correlation was observed between SPI and monthly groundwater levels at most of the locations and nearby wells. Very strong correlation was observed in a few places.

Groundwater levels were plotted as a function of SPI at timescales of 9 and 12 months for various locations. All of the plots, in general, depict a positive slope, indicating that groundwater table rose higher with increasing SPI.

SPI at different timescales at Albany 3 SE GA was correlated with groundwater levels in wells 12L028, 13L049, 12L030, 13L012, 11K003, 12K014 and 13K014. The values of the Pearson's r coefficient along with 95 percent confidence interval is presented in Table 5.2. Very strong correlation was observed in many wells and strong correlation was observed in the remaining ones. In most of the cases, the correlation was seen to be maximum for SPI timescales between 9 and 12 months.

Groundwater levels in each of the wells were plotted as a function of SPI for timescales of 9 and 12 months. Figures 5.2, 5.3, 5.4, 5.5, 5.6, 5.7 and 5.8 show groundwater levels plotted as a function of SPI of 9 and 12 month timescales at Albany in Wells 12L028, 13L049, 12L030, 13L012, 11K003, 12K014 and 13K014, respectively. A positive slope can be observed in the trend for all cases. This indicates that as SPI increases, the groundwater water level increases.

All the plots imply that groundwater levels show significant association with the SPI at both timescales of 9 and 12 months. Upon checking the Pearson product-moment correlation coefficient, we can see that the two have strong association in most cases.

SPI at different timescales at Camilla 3 SE GA was correlated with groundwater levels in wells 11J012, 13J004, 10G313 and 12K014. Very strong correlation was observed in for groundwater level in well 10G313 and 12 month SPI. The correlation was strong in all the other wells. Here, SPI of timescales between 9 and 15 months show strong correlation. Figures 5.9, 5.10, 5.11 and 5.12 show groundwater levels

plotted as a function of SPI of 9 and 12 month timescales at Camilla 3 SE GA in Wells 11J012, 13J004, 10G313 and 12K014, respectively.

Again, a positive slope can be observed for all cases at Camilla, indicating that as SPI increases, the groundwater water level increases. The values of Pearson product-moment correlation coefficient indicates that the two have a very strong association in Well 10G313 and strong correlation at Wells 13J004 and 12K014. Well 11J012 doesn't show strong correlation at SPI timescale of 12 months.

SPI at different timescales at Colquitt 2 W GA was correlated with groundwater levels in wells 08G001, 09G001, 09F520 and 06F001. The values of the coefficient along with 95 percent confidence interval are presented in Table 5.4. All the wells show significant strong correlation between SPI and groundwater levels.

Figures 5.13, 5.14, 5.15 and 5.16 show groundwater levels plotted as a function of SPI of 9 and 12 month timescales at Colquitt 2 W GA in Wells 08G001, 09G001, 09F520 and 06F001, respectively. Again a positive slope can be observed in all cases signifying the correlation between groundwater level and SPI.

SPI at different timescales at Crisp Co Power Dam GA were correlated with groundwater levels in Well 13M007. Table 5.5 shows the coefficient of correlation and the confidence intervals for different correlations at Crisp County Power Dam. It can be seen that the correlation is pretty strong.

Groundwater at Well 13M007 is plotted as a function of SPI at different timescales in Crisp County Power Dam in Figures 5.17. The positive trend is visible indicating rise of groundwater level with increasing SPI.

All of the locations for which the association of the two parameters was checked indicate a significant strong correlation with at least one of the nearby wells. Hence, it can be concluded that an increase in SPI calculated at a timescale between 9 and 12 indicates rising groundwater tables in the region.

Well ID	SPI	Pearson's r Coefficient	95 % confidence interval		p-value
			Upper Limit	Lower Limit	
12L028	6-SPI	0.7042	0.7579	0.6411	0.0000
	9-SPI	0.7630	0.8073	0.7103	0.0000
	12-SPI	0.7517	0.7978	0.6968	0.0000
	15-SPI	0.7119	0.7644	0.6500	0.0000
	18-SPI	0.6661	0.7256	0.5967	0.0000
13L049	6-SPI	0.6930	0.7456	0.6318	0.0000
	9-SPI	0.7621	0.8042	0.7124	0.0000
	12-SPI	0.7700	0.8109	0.7217	0.0000
	15-SPI	0.7412	0.7865	0.6878	0.0000
	18-SPI	0.7106	0.7606	0.6522	0.0000
12L030	6-SPI	0.6439	0.7030	0.5759	0.0000
	9-SPI	0.7574	0.8000	0.7073	0.0000
	12-SPI	0.7701	0.8109	0.7217	0.0000
	15-SPI	0.7412	0.7865	0.6878	0.0000
	18-SPI	0.7106	0.7606	0.6522	0.0000
13L012	6-SPI	0.6358	0.6894	0.5753	0.0000
	9-SPI	0.6412	0.6941	0.5813	0.0000
	12-SPI	0.6142	0.6703	0.5512	0.0000
	15-SPI	0.5754	0.6359	0.5079	0.0000
	18-SPI	0.5639	0.6256	0.4952	0.0000
11K003	6-SPI	0.6495	0.7027	0.5891	0.0000
	9-SPI	0.7485	0.7886	0.7021	0.0000
	12-SPI	0.7847	0.8196	0.7440	0.0000
	15-SPI	0.7890	0.8233	0.7490	0.0000
	18-SPI	0.7802	0.8158	0.7388	0.0000
12K014	6-SPI	0.6258	0.6843	0.5593	0.0000
	9-SPI	0.6438	0.7001	0.5797	0.0000
	12-SPI	0.6236	0.6824	0.5568	0.0000
	15-SPI	0.5753	0.6400	0.5025	0.0000
	18-SPI	0.5515	0.6189	0.4760	0.0000
13K014	6-SPI	0.6479	0.7041	0.5836	0.0000
	9-SPI	0.6335	0.6916	0.5673	0.0000
	12-SPI	0.5890	0.6527	0.5172	0.0000
	15-SPI	0.5392	0.6087	0.4616	0.0000
	18-SPI	0.5159	0.5879	0.4357	0.0000

Table 5.2: Pearson's r coefficient for SPI at different well locations and Albany Station.

Well ID	SPI	Pearson's r Coefficient	95 % confidence interval		p-value
			Upper Limit	Lower Limit	
	6-SPI	0.5091	0.5801	0.4304	0.0000
	9-SPI	0.5076	0.5787	0.4288	0.0000
11J012	12-SPI	0.4657	0.5411	0.3830	0.0000
	15-SPI	0.4345	0.5128	0.3491	0.0000
	18-SPI	0.4269	0.5059	0.3408	0.0000
	6-SPI	0.4625	0.5349	0.3833	0.0000
	9-SPI	0.5423	0.6069	0.4706	0.0000
13J004	12-SPI	0.5840	0.6441	0.5168	0.0000
	15-SPI	0.5994	0.6578	0.5340	0.0000
	18-SPI	0.6131	0.6700	0.5493	0.0000
	6-SPI	0.5741	0.6338	0.5077	0.0000
	9-SPI	0.6751	0.7231	0.6206	0.0000
10G313	12-SPI	0.7022	0.7468	0.6513	0.0000
	15-SPI	0.6829	0.7300	0.6294	0.0000
	18-SPI	0.6575	0.7079	0.6006	0.0000
	6-SPI	0.5515	0.6189	0.4760	0.0000
	9-SPI	0.5475	0.6154	0.4716	0.0000
12K014	12-SPI	0.5047	0.5773	0.4243	0.0000
	15-SPI	0.4617	0.5386	0.3771	0.0000
	18-SPI	0.4510	0.5290	0.3655	0.0000

Table 5.3: Pearson's r coefficient for SPI at different well locations and Camilla Station.

Well ID	SPI	Pearson's r Coefficient	95 % confidence interval		p-value
			Upper Limit	Lower Limit	
08G001	6-SPI	0.5870	0.6459	0.5213	0.0000
	9-SPI	0.6020	0.6592	0.5380	0.0000
	12-SPI	0.5768	0.6368	0.5099	0.0000
	15-SPI	0.5365	0.6008	0.4654	0.0000
	18-SPI	0.5143	0.5808	0.4410	0.0000
09G001	6-SPI	0.4917	0.5642	0.4117	0.0000
	9-SPI	0.5314	0.5998	0.4554	0.0000
	12-SPI	0.5303	0.5987	0.4541	0.0000
	15-SPI	0.5065	0.5775	0.4279	0.0000
	18-SPI	0.4794	0.5531	0.3982	0.0000
09F520	6-SPI	0.5346	0.5985	0.4640	0.0000
	9-SPI	0.5795	0.6389	0.5133	0.0000
	12-SPI	0.5637	0.6249	0.4955	0.0000
	15-SPI	0.5195	0.5855	0.4466	0.0000
	18-SPI	0.4813	0.5510	0.4049	0.0000
06F001	6-SPI	0.6014	0.6617	0.5334	0.0000
	9-SPI	0.5909	0.6525	0.5216	0.0000
	12-SPI	0.5406	0.6078	0.4656	0.0000
	15-SPI	0.4957	0.5677	0.4162	0.0000
	18-SPI	0.4588	0.5344	0.3759	0.0000

Table 5.4: Pearson's r coefficient for SPI at different well locations and Colquitt Station.

Well ID	SPI	Pearson's r Coefficient	95 % confidence interval		p-value
			Upper Limit	Lower Limit	
13M007	6-SPI	0.6504	0.7096	0.5958	0.0000
	9-SPI	0.6602	0.7129	0.6001	0.0000
	12-SPI	0.6326	0.6888	0.5688	0.0000
	15-SPI	0.5739	0.6371	0.5031	0.0000
	18-SPI	0.5190	0.5882	0.4423	0.0000

Table 5.5: Pearson's r coefficient for SPI at different well locations and Crisp County Power Dam Station.

Figure 5.2: Groundwater level at Well 12L028 as a function of (a) 9-SPI and (b) 12-SPI at Albany.

Figure 5.3: Groundwater level at Well 13L049 as a function of (a) 9-SPI and (b) 12-SPI at Albany.
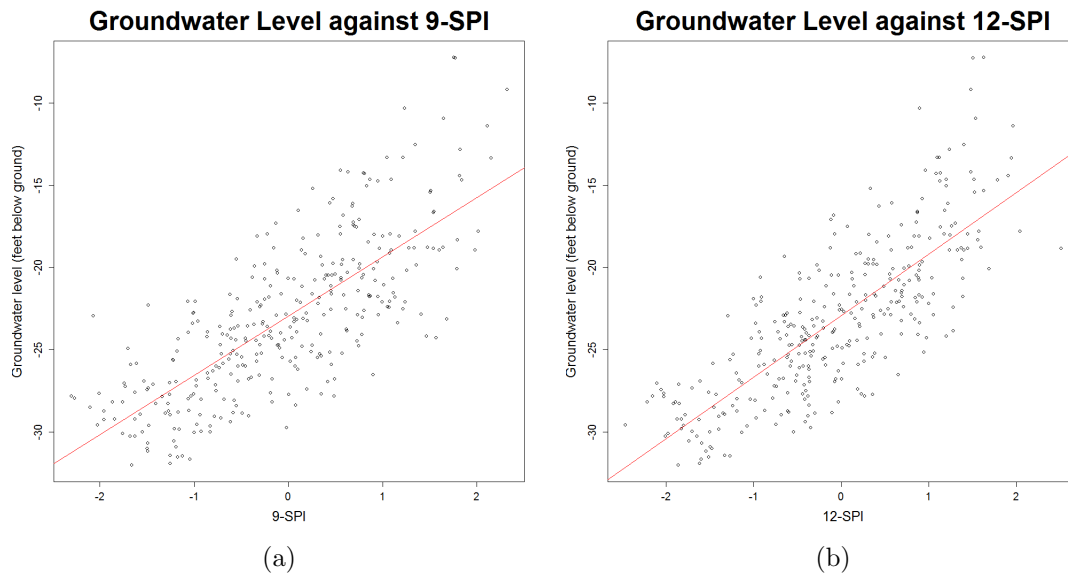
Figure 5.4: Groundwater level at Well 12L030 as a function of (a) 9-SPI and (b) 12-SPI at Albany.
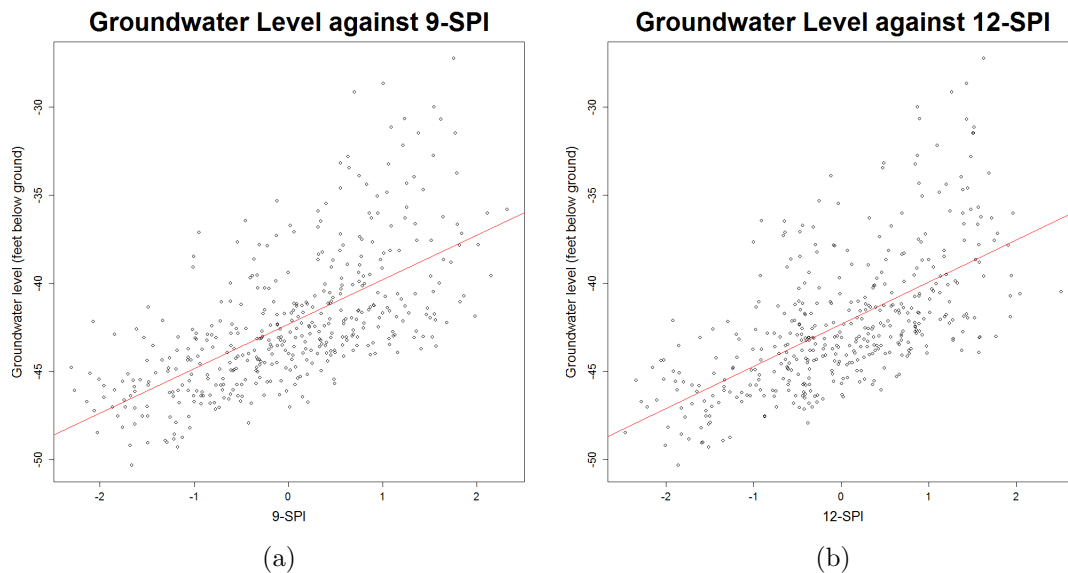
Figure 5.5: Groundwater level at Well 13L012 as a function of (a) 9-SPI and (b) 12-SPI at Albany.
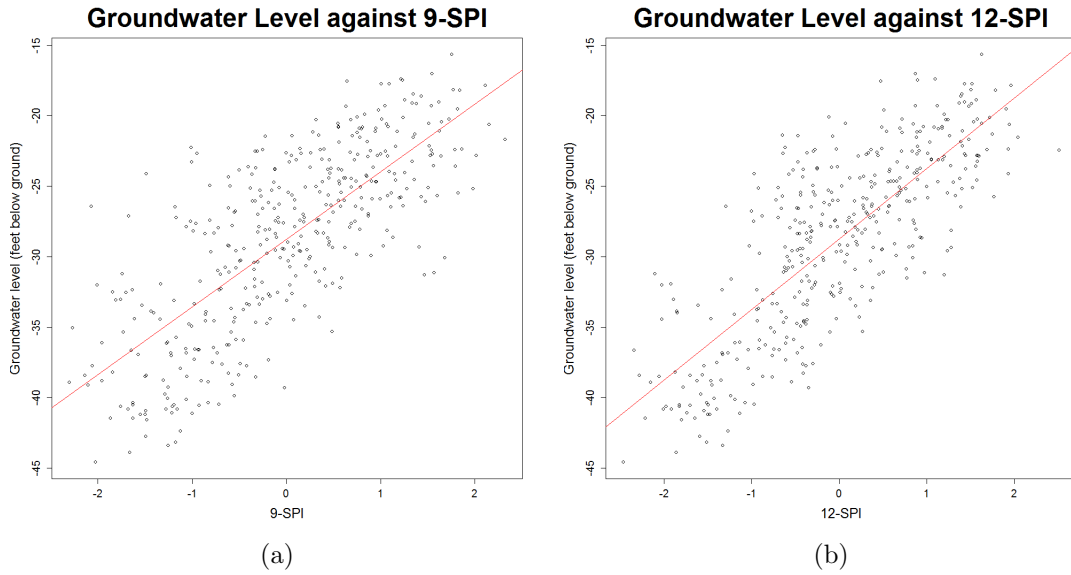
Figure 5.6: Groundwater level at Well 11K003 as a function of (a) 9-SPI and (b) 12-SPI at Albany.
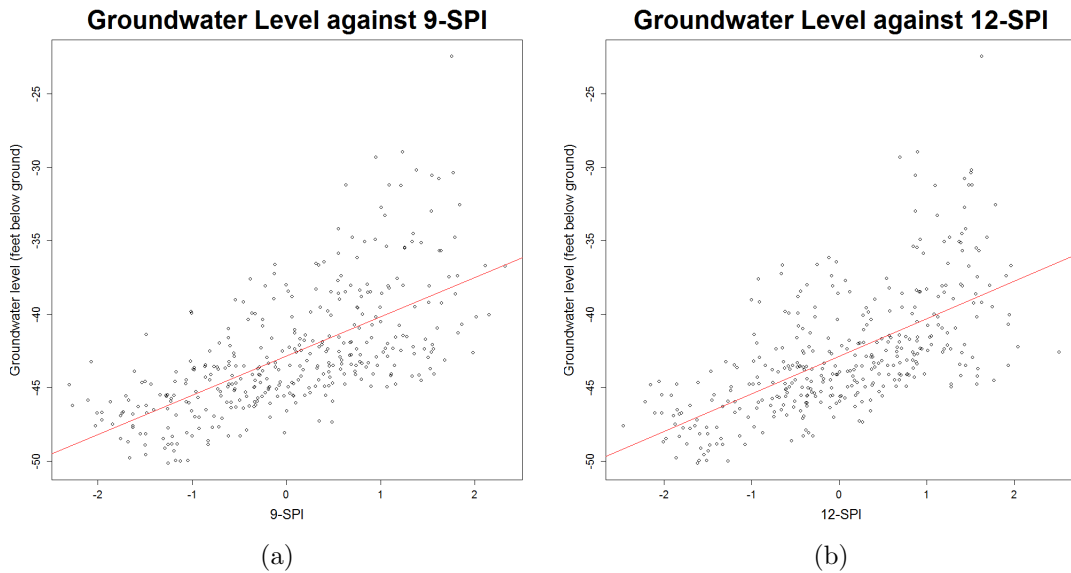
Figure 5.7: Groundwater level at Well 12K014 as a function of (a) 9-SPI and (b) 12-SPI at Albany.
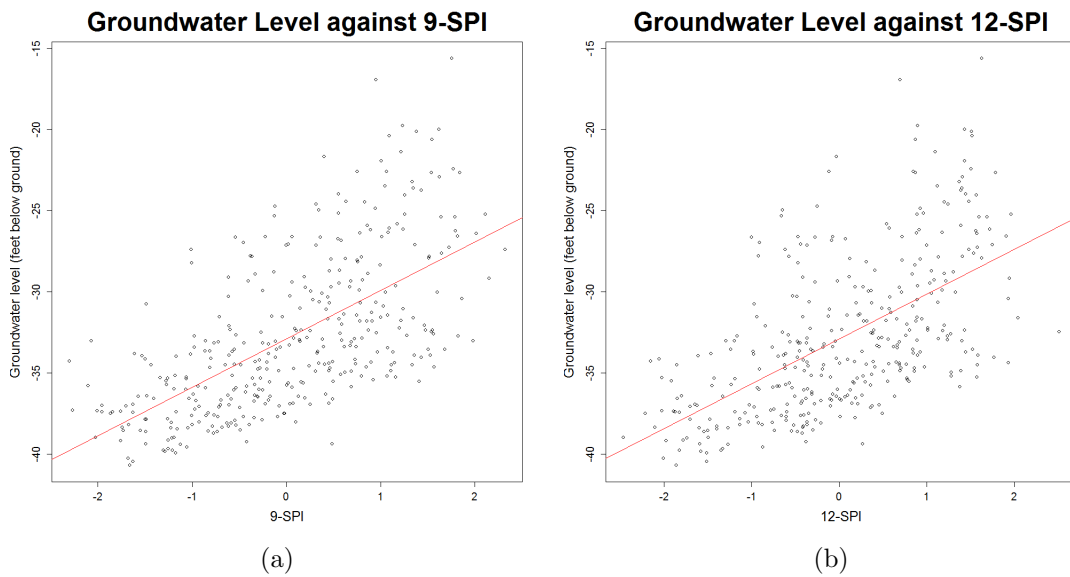
Figure 5.8: Groundwater level at Well 13K014 as a function of (a) 9-SPI and (b) 12-SPI at Albany.
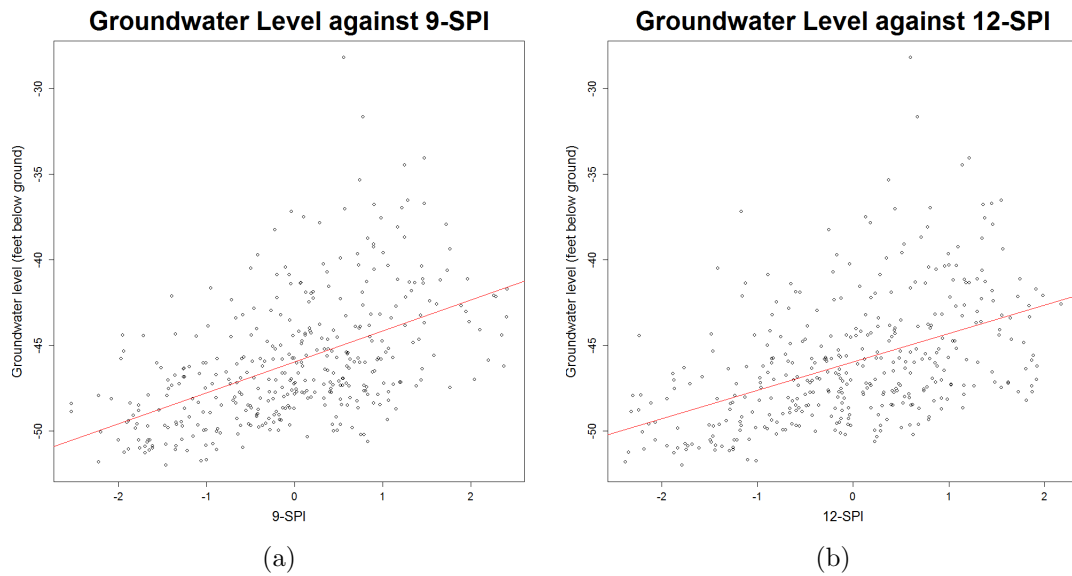
Figure 5.9: Groundwater level at Well 11J012 as a function of (a) 9-SPI and (b) 12-SPI at Camilla.
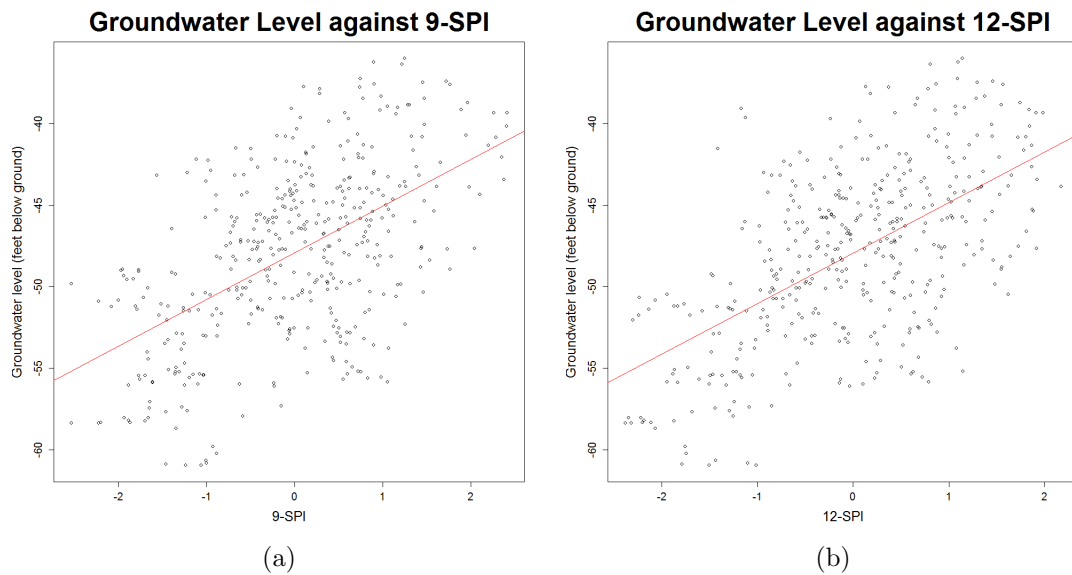
Figure 5.10: Groundwater level at Well 13J004 as a function of (a) 9-SPI and (b) 12-SPI at Camilla.

87
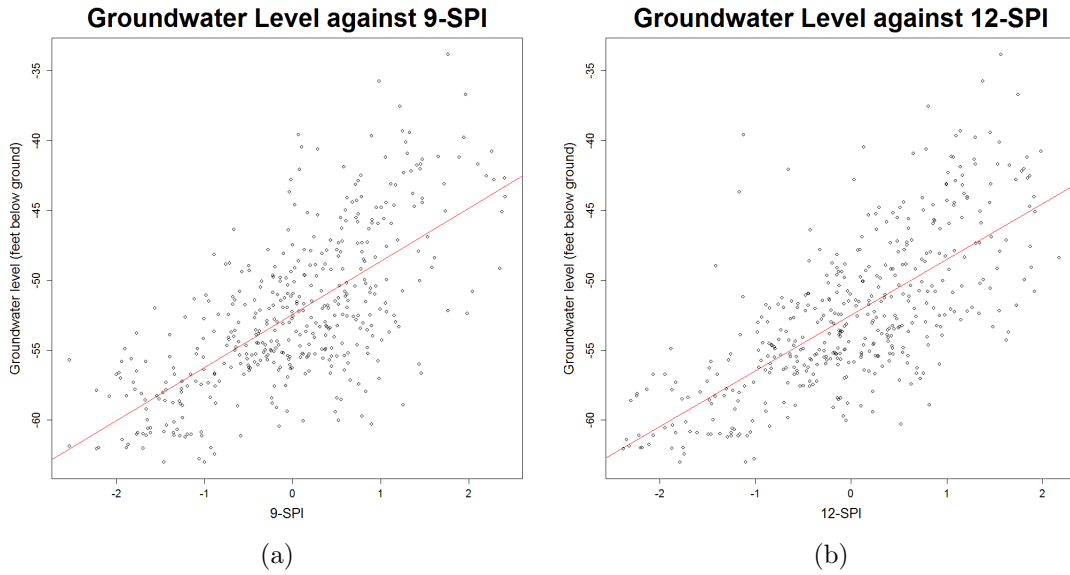
Figure 5.11: Groundwater level at Well 10G313 as a function of (a) 9-SPI and (b) 12-SPI at Camilla.
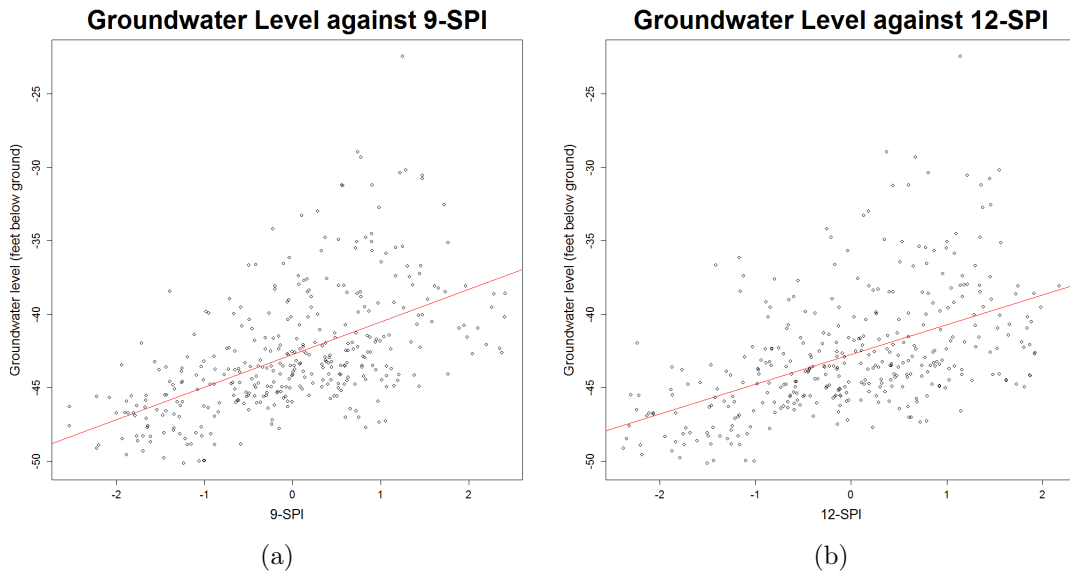
Figure 5.12: Groundwater level at Well 12K014 as a function of (a) 9-SPI and (b) 12-SPI at Camilla.
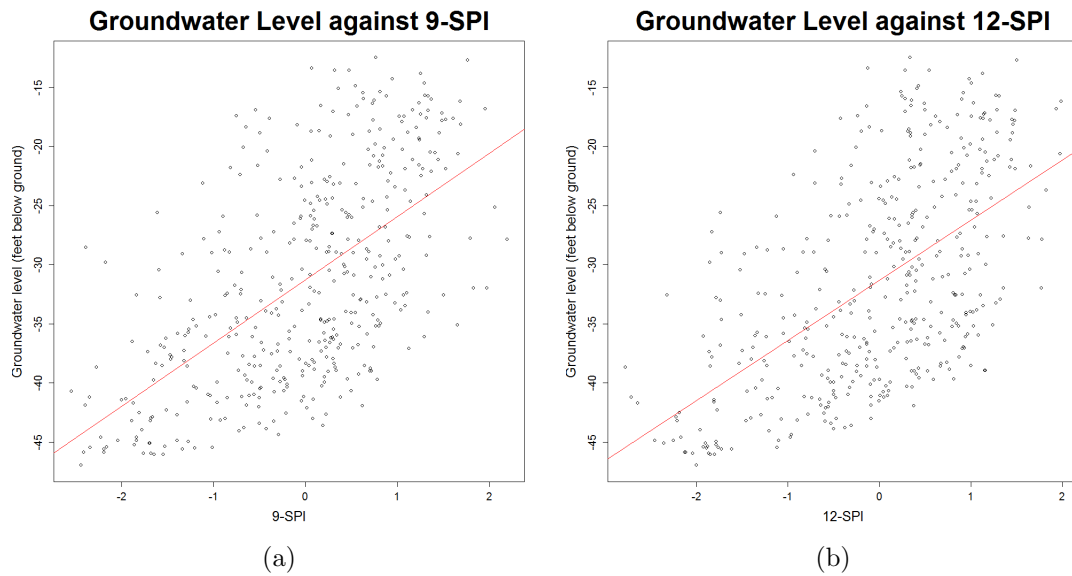
Figure 5.13: Groundwater level at Well 08G001 as a function of (a) 9-SPI and (b) 12-SPI at Colquitt.
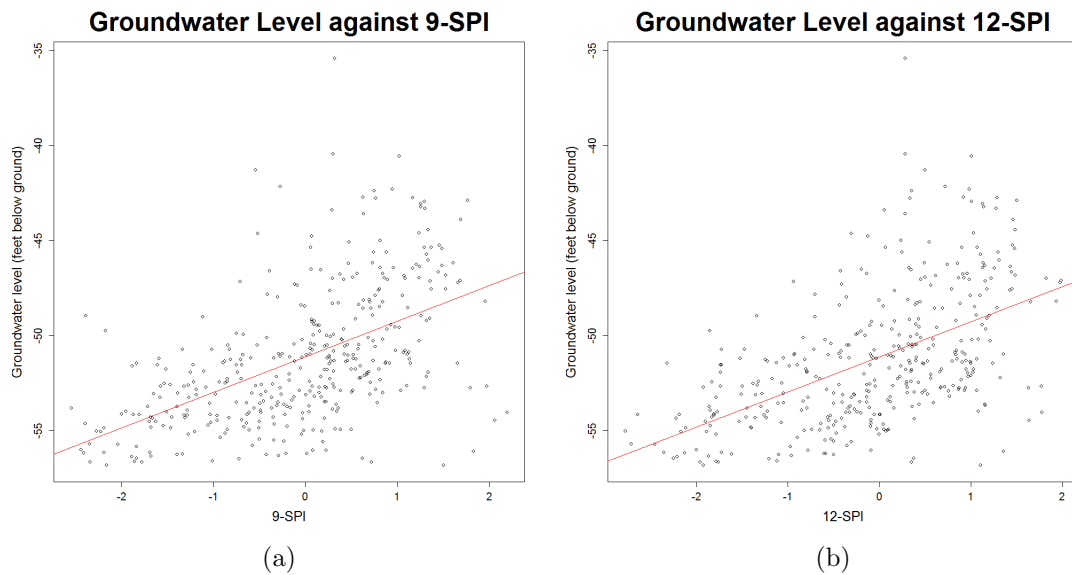
Figure 5.14: Groundwater level at Well 09G001 as a function of (a) 9-SPI and (b) 12-SPI at Colquitt.
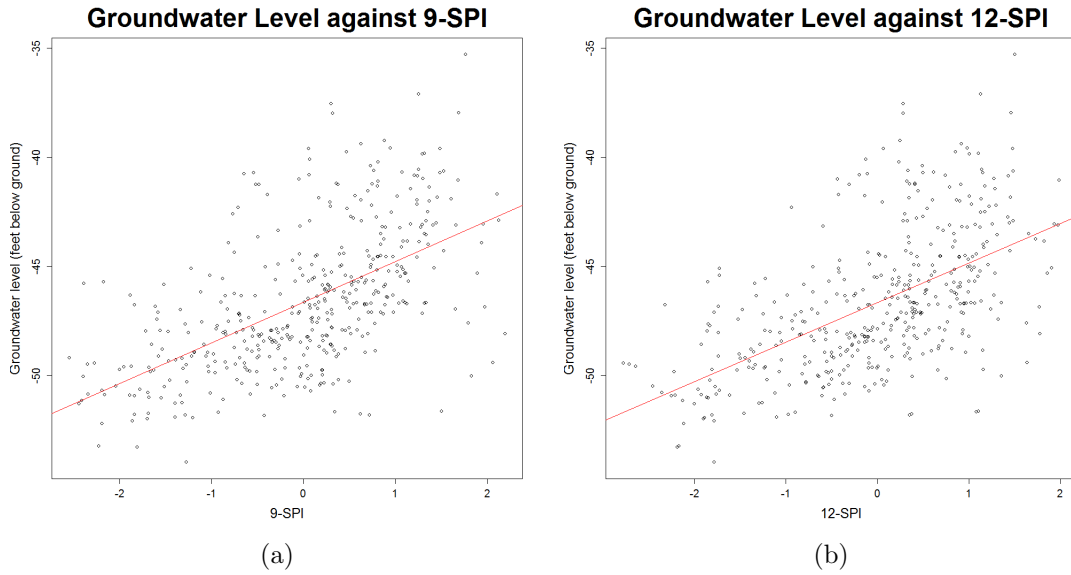
Figure 5.15: Groundwater level at Well 09F520 as a function of (a) 9-SPI and (b) 12-SPI at Colquitt.
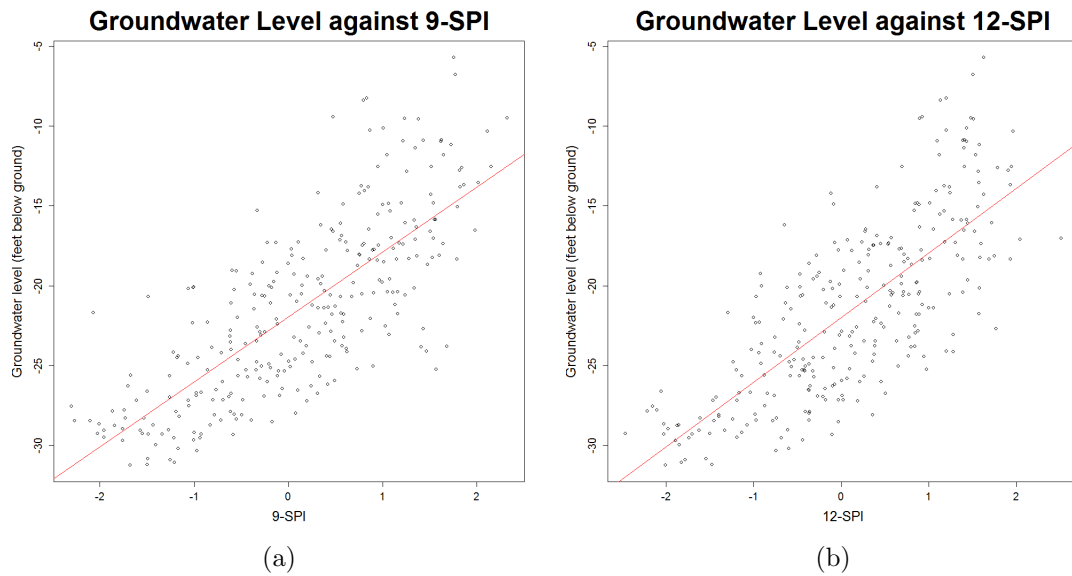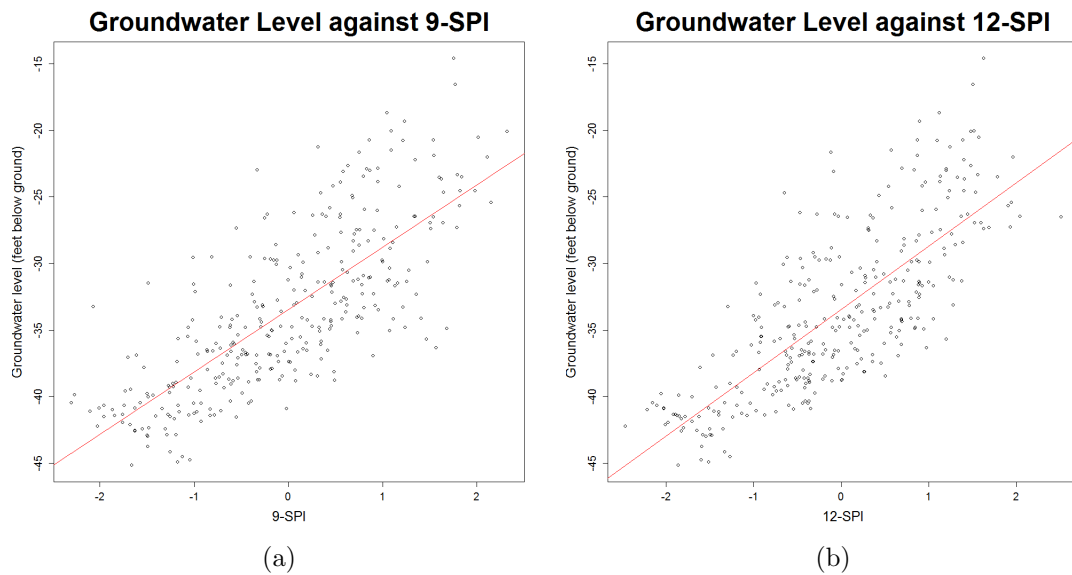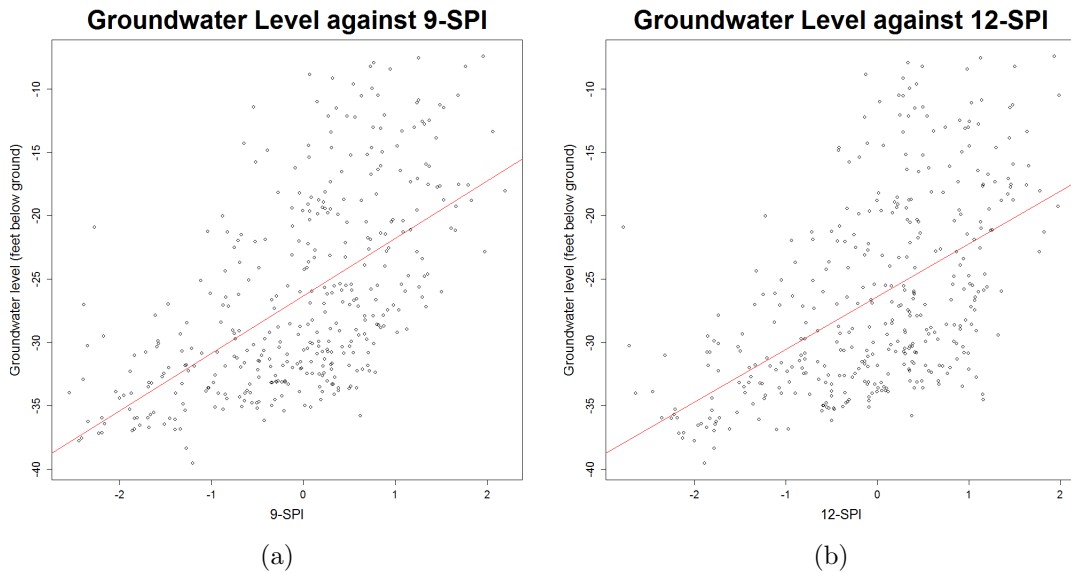

Figure 5.16: Groundwater level at Well 06F001 as a function of (a) 9-SPI and (b) 12-SPI at Colquitt.
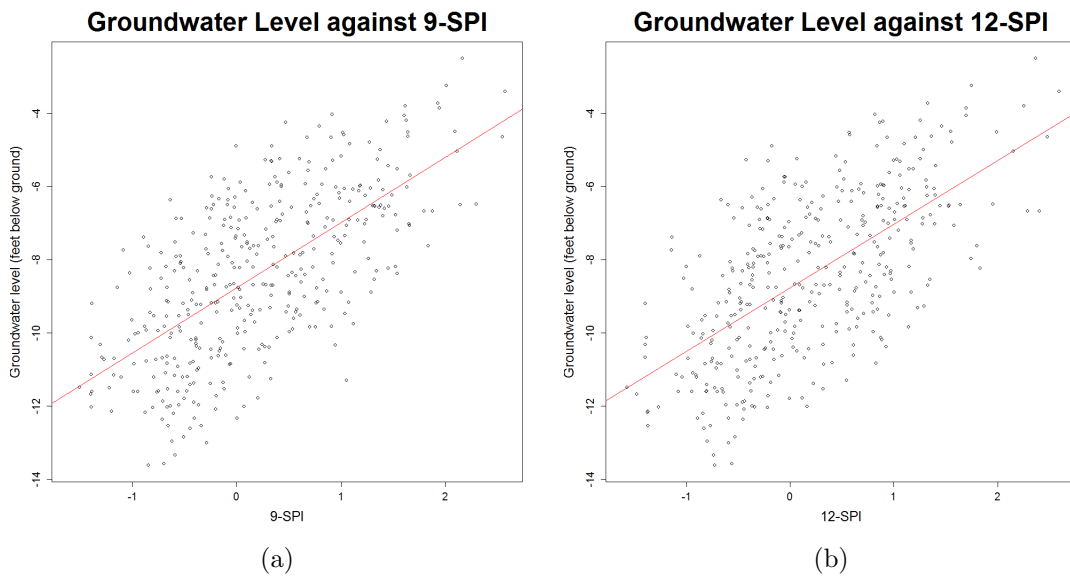
Figure 5.17: Groundwater level at Well 13M007 as a function of (a) 9-SPI and (b) 12-SPI at Crisp County Power Dam.

5.7   Summary and Conclusion

SPI at timescales of 6, 9, 12, 15 and 18 months were correlated with the groundwater levels at different observation wells. Strong correlations of varying strengths were observed at all locations. This suggests that SPI can be used to monitor groundwater conditions in this region of the basin. SPI trends at a timescale between 9 and 12 months can be analyzed to draw conclusions about groundwater conditions at any particular location in the region.

Besides monitoring groundwater conditions, SPI can also be used to monitor hydrological droughts in the region. Droughts are a major problem in the region and precipitation forecasts and projections can be used to compute the SPI and predict hydrological droughts much earlier. SPI has been used widely to assess and monitor meteorological droughts. This study can be extended further with more analyses to develop a tool that can make reasonable estimates of groundwater levels from the SPI. Water resource managers can use SPI at long timescales to monitor hydrologic droughts in the region.

Chapter 6

Conclusions

6.1 Summary and Conclusions

Recurring droughts in the Southeast US are one of the biggest problems in the region considering the agricultural, economic and environmental damage it does. Frequent droughts in the recent years have consistently questioned water management strategies in the region and questioned the abilities of the region to easily subdue the impacts of a major drought event in the future. In this study, future droughts were quantified and compared with past droughts using two drought indices calculated based on high-resolution climate data derived from regional climate models. These indices have successfully been used for assessment of droughts elsewhere. The data were processed to construct SAF curves to assess past and future droughts.

6.1.1 Objective 1

Analyze the changes in frequency, severity and spatial extent of droughts in Alabama using Severity-Area-Frequency Curves.

Drought incidences during two time slices, one in past (1969-1999) and the other in future (2039-2069), were studied to assess the frequency, severity and spatial extent of future droughts that are projected to occur. Three GCMs were used and two drought indices were computed and studied. Number of drought incidences was compared and SAF curves were constructed to study drought characteristics in past and future. The major conclusions are:

1. Both SPI and SPEI from CCSM model suggested that droughts are not likely to change their characteristics significantly in the future. Both the indices showed slight reduction in drought occurrences in the future. The severity of future droughts was slightly less according to the SPI. Other than that, other drought characteristics weren't projected to change by much.

2. SPI from GFDL model indicated droughts to relatively increase in frequency, severity and spatial extent in the future.

3. SPEI from GFDL model shows that the frequency of droughts will increase in the future. Also, the severity and spatial extent are expected to increase more than that indicated by SPI from this model.

4. SPI from HadCM3 shows droughts are expected to change their characteristics significantly. The severity, frequency and spatial extent are all projected to increase in the future.

5. The frequency, severity and spatial extent of droughts are expected to increase in the future from the results of SPEI from HadCM3. However, the maximum drought severity is not seen to change by much.

6. Overall, both indices from two out of three climate models suggest increase in frequency, severity and spatial extent of future droughts in Alabama.

6.1.2   Objective 2

Analyze the changes in frequency, severity and spatial extent of droughts in the Apalachicola-Chattahoochee-Flint River Basin using Severity-Area-Frequency Curves.

ACF region recently suffered from some of the worst drought events of the century. Droughts are more frequent in the region than ever. Water management is a

very critical issue in the region, and during times when resources are scarce, management becomes more difficult. Droughts in this region were analyzed according to the process applied for analysis of droughts in Alabama. The major conclusions are listed below.

1. SPI from CCSM indicates drought characteristics to remain similar in the future. The frequency, severity and spatial extent are all seen to be highly similar during both time slices.

2. SPI from GFDL model indicates a mild increase in the frequency of future droughts. The severity and spatial extent are projected to increase as well. The increase in these characteristics is seen to be proportional to the return interval of the droughts.

3. SPI from HadCM3 indicates the maximum increase in frequency of future droughts. The increase in severity and spatial extent is also seen to be rapid.

4. SPEI from CCSM shows a slight decrease in frequency of droughts in the future. Severity and spatial extent do not change distinctly.

5. A slight increase was projected in the frequency of future droughts from the results of SPEI from GFDL model. Slight increases are visible in severity and spatial extent as well.

6. The frequency, severity and spatial extent of droughts are projected to increase in the future according to the results of SPEI from HadCM3. However, the maximum drought severity across the entire region is not changed.

7. Overall, both indices from two out of three climate models suggest increase in frequency, severity and spatial extent of future droughts in ACF River Basin.

The findings of National Climate Assessment, 2013 suggest that the mean precipitation is projected to decrease and the mean temperature is projected to increase in future in Southeast US. However, droughts are viewed with uncertainty in the report. The projected changes in precipitation and temperature was extrapolated in this research to get information about future droughts. The results of this research for Objectives 1 and 2 are consistent with the observations presented in National Climate Assessment, 2013.

6.1.3 Objective 3

Check the applicability of Standardized Precipitation Index for monitoring groundwater conditions in the lower Apalachicola-Chattahoochee-Flint (ACF) River Basin.

SPI at higher timescales can be used to monitor hydrologic droughts. SPI at different timescales were correlated with groundwater levels in the lower ACF River Basin. Strong correlation existed among the two parameters in most parts. The general conclusions are:

1. Groundwater levels show strong correlation with SPI calculated at a timescale between 9 and 15 months in the lower ACF River Basin.

2. SPI at a timescale between 9 and 12 months would be most applicable to monitor groundwater conditions in lower ACF River Basin.

Chapter 7

Future Research

This research analyzed how the frequency, severity and spatial extent of droughts in Alabama and the ACF River Basin would change with respect to projected changes in climate. Two drought indices were computed and were analyzed by constructing SAF curves to study the changes in their characteristics. Also, groundwater levels were correlated with SPI in lower ACF River Basin. With increasing concerns due to droughts in the Southeast US, the need of more research and studies are increasing. The knowledge gaps pertaining to droughts in the Southeast US must be filled sooner than later. More parameters need to be computed, studied and statistically analyzed to make meaningful conclusions out of the primitive data we possess. More studies can lead to development of better models that can temporally and spatially predict droughts more accurately.

The technique used in the study can be used to project, monitor and assess droughts elsewhere using similar data. However, the study can still be improved by researching which GCMs best fit the climate of Southeast US. The results from those GCMs can be viewed with much higher importance. Also, droughts can be analyzed using the relatively newer data from CMIP5 projected runs. The climate change scenarios are modified in the CMIP5 data and it can be studied if results from CMIP5 archive better represent conditions in the Southeast US. Further, regional analysis can be done to pinpoint where more droughts are likely to occur. SAF curves can be constructed and analyzed for the climate divisions of Alabama for this purpose.

The changes in droughts resulting from various climate variability cycles like El Niño Southern Oscillation (ENSO), Atlantic Multidecadal Oscillation (AMO) and Pacific Decadal Oscillation (PDO) can be studied. This can be of tremendous use in early forecast of droughts. This can also help in assessing how droughts may affect the state of Alabama and the region.

As the indices used in this study possess the capability to analyze different types of droughts depending on the timescale used to calculate the index, they possess capabilities to draw conclusions about some drought triggers like streamflow and groundwater level. Hence, these triggers can be applied to study water levels across different streams in the region and the predicted changes in water levels with respect to projected changes in the indices. Groundwater levels can further be associated with more indices at various timescales. Studies can be done to associate the indices with groundwater and streamflow levels.

More analysis can be done on the computed value of the indices to know more about the nature of droughts. Construction of Severity-Area-Duration (SAD) curves is one method that can incorporate drought duration in the analysis. Similarly, other techniques can be explored to draw rigid conclusion based on available data.

Bibliography

[1] Abramowitz, Milton, and Irene A. Stegun. Handbook of mathematical functions. Vol. 1046. New York: Dover, 1965.

[2] Akhtari, R., S. R. Bandarabadi, and B. Saghafian. "Spatio-temporal pattern of drought in Northeast of Iran." In International Conference on Drought management: Scientific and Technological Innovations, Zaragoza, Spain. 2008.

[3] Akinremi, O. O., S. M. McGinn, and A. G. Barr. "Evaluation of the Palmer drought index on the Canadian prairies." Journal of Climate 9, no. 5 (1996): 897-905.

[4] Alley, William M. "The Palmer drought severity index: limitations and assumptions." Journal of climate and applied meteorology 23, no. 7 (1984): 1100-1109.

[5] Bender, Morris A., Isaac Ginis, Robert Tuleya, Biju Thomas, and Timothy Marchok. "The operational GFDL coupled hurricane-ocean prediction system and a summary of its performance." Monthly Weather Review 135, no. 12 (2007): 3965-3989.

[6] Berhanu F, Alemaw, and Kileshye-Onema JM. "Regional drought severity assessment at a basin scale in the Limpopo drainage system." Journal of Water Resource and Protection 2013 (2013).

[7] Binita, K. C., J. Marshall Shepherd, and Cassandra Johnson Gaither. "Climate change vulnerability assessment in Georgia." Applied Geography 62 (2015): 62-74.

[8] Burke, Eleanor J., and Simon J. Brown. "Regional drought over the UK and changes in the future." Journal of hydrology 394, no. 3 (2010): 471-485.

[9] Burton, I., Kates, R. W. and White, G. F.: The environment as hazard, Oxford University Press, New York, 240 pp, 1978

[10] Center for Climate and Energy Solutions. Last accessed on 12th June 2015. http://www.c2es.org/science-impacts/extreme-weather/drought.

[11] Chahine, Moustafa T. "The hydrological cycle and its influence on climate." Nature 359, no. 6394 (1992): 373-380.

[12] Chang, Tiao J., and Xenia A. Kleopa. "A proposed method for drought monitoring." (1991): 275-281.

[13] Chaudhari, K. N., and V. K. Dadhwal. "Assessment of impact of drought-2002 on the production of major kharif and rabi crops using standardized precipitation index." J Agrometeorology 6 (2004): 10-15.

[14] Collins, William D., Cecilia M. Bitz, Maurice L. Blackmon, Gordon B. Bonan, Christopher S. Bretherton, James A. Carton, Ping Chang et al. "The community climate system model version 3 (CCSM3)." Journal of Climate 19, no. 11 (2005): 2122-2143.

[15] Cook, Edward R., Richard Seager, Mark A. Cane, and David W. Stahle. "North American drought: reconstructions, causes, and consequences." Earth-Science Reviews 81, no. 1 (2007): 93-134.

[16] Cordery, Ian, and Mark McCall. "A model for forecasting drought from teleconnections." Water Resources Research 36, no. 3 (2000): 763-768.

[17] Couch, Carol Anne, Evelyn H. Hopkins, and P. Suzanne Hardy. Influences of environmental settings on aquatic ecosystems in the Apalachicola-Chattahoochee-Flint River basin. US Department of the Interior, US Geological Survey, 1996.

[18] Dai, Aiguo. "Drought under global warming: a review." Wiley Interdisciplinary Reviews: Climate Change 2, no. 1 (2011): 45-65.

[19] Delworth, T. L., R. Stouffer, K. Dixon, M. Spelman, T. Knutson, A. Broccoli, P. Kushner, and R. Wetherald. "Review of simulations of climate variability and change with the GFDL R30 coupled climate model." Climate Dynamics 19, no. 7 (2002): 555-574.

[20] Déqué, M., R. G. Jones, M. Wild, F. Giorgi, J. H. Christensen, D. C. Hassell, P. L. Vidale et al. "Global high resolution versus Limited Area Model climate change projections over Europe: quantifying confidence level from PRUDENCE results." Climate Dynamics 25, no. 6 (2005): 653-670.

[21] Dixon, Keith W., Thomas L. Delworth, Thomas R. Knutson, Michael J. Spelman, and Ronald J. Stouffer. "A comparison of climate change simulations produced by two GFDL coupled climate models." Global and Planetary Change 37, no. 1 (2003): 81-102.

[22] Domonkos, Peter. "Recent precipitation trends in Hungary in the context of larger scale climatic changes." Natural Hazards 29, no. 2 (2003): 255-271.

[23] Easterling, David R., Gerald A. Meehl, Camille Parmesan, Stanley A. Changnon, Thomas R. Karl, and Linda O. Mearns. "Climate extremes: observations, modeling, and impacts." science 289, no. 5487 (2000): 2068-2074.

[24] Edwards, Daniel C. and McKee, Thomas B. "Characteristics of 20th Century Drought in the United States at Multiple Time Scales." Atmospheric Science Paper No. 634 (1997); 1-30

[25] Ek, M. B., K. E. Mitchell, Y. Lin, E. Rogers, P. Grunmann, V. Koren, G. Gayno, and J. D. Tarpley. "Implementation of Noah land surface model advances in the National Centers for Environmental Prediction operational mesoscale Eta model." Journal of Geophysical Research: Atmospheres (1984-2012) 108, no. D22 (2003).

[26] FAO, Land and Water. Drought. 2013. Accessed June 7, 2015. `http://www.fao.org/nr/aboutnr/nrl/en/`.

[27] Feddema, Johannes J., Keith W. Oleson, Gordon B. Bonan, Linda O. Mearns, Lawrence E. Buja, Gerald A. Meehl, and Warren M. Washington. "The importance of land-cover change in simulating future climates." Science 310, no. 5754 (2005): 1674-1678.

[28] Flanders, Archie, John C. McKissick, and Tommie Shepherd: Georgia economic losses due to 2007 drought." Center for Agribusiness and Economic Development (2007).

[29] Friedman, Don G. "Prediction of Long Continuing Drought in South and Southwest Texas." (1957).

[30] Fuchs B., Svoboda M., Scott, S., Nothwehr J. "A New National Drought Risk Atlas for the U.S. from the National Drought Mitigation Center." (2012) `http://www.nws.noaa.gov/om/csd/content/seminars/semser_20130430_fuchs_brian/semser_20130430_fuchs_brian_presentation_1.pdf`.

[31] Gent, Peter R., Stephen G. Yeager, Richard B. Neale, Samuel Levis, and David A. Bailey. "Improvements in a half degree atmosphere/land version of the CCSM." Climate Dynamics 34, no. 6 (2010): 819-833.

[32] Giddings, Lorrain, MIGUEL SOTO, B. M. Rutherford, and A. Maarouf. "Standardized precipitation index zones for Mexico." Atmsfera 18, no. 1 (2005): 33-56.

[33] Gillette, H. P. "A creeping drought under way." Water and Sewage Works 104 (1950): e105.

[34] Glantz, Michael H. Climate affairs: a primer. Island Press, 2003.

[35] Gleick, Peter H. Water in crisis: a guide to the world's fresh water resources. Oxford University Press, Inc., 1993.

[36] Goldewijk, K. Klein. "Estimating global land use change over the past 300 years: the HYDE database." Global Biogeochemical Cycles 15, no. 2 (2001): 417-433.

[37] González, J., and J. B. Valdés. "The mean frequency of recurrence of in-time-multidimensional events for drought analyses." Natural Hazards and Earth System Science 4, no. 1 (2004): 17-28.

[38] Gordon, Chris, Claire Cooper, Catherine A. Senior, Helene Banks, Jonathan M. Gregory, Timonthy C. Johns, John FB Mitchell, and Richard A. Wood. "The simulation of SST, sea ice extents and ocean heat transports in a version of the Hadley Centre coupled model without flux adjustments." Climate dynamics 16, no. 2-3 (2000): 147-168.

[39] Guttman, Nathaniel B. "Accepting the standardized precipitation index: A calculation algorithm."(1999):311-322.

[40] Guttman, Nathaniel B. "Comparing the palmer drought index and the standardized precipitation index." (1998): 113-121.

[41] Hall, Forrest G., G. Collatz, S. Los, E. Brown de Colstoun, and D. Landis. ISLSCP Initiative II. NASA. DVD/CD-ROM. NASA, 2005.

[42] Hayes, Michael J., Mark D. Svoboda, Donald A. Wilhite, and Olga V. Vanyarkho. "Monitoring the 1996 drought using the standardized precipitation index." Bulletin of the American Meteorological Society 80, no. 3 (1999): 429-438.

[43] Heim Jr, Richard R. "A review of twentieth-century drought indices used in the United States." Bulletin of the American Meteorological Society 83, no. 8 (2002): 1149-1165.

[44] Henriques, A. G., and M. J. J. Santos. "Regional drought distribution model." Physics and Chemistry of the Earth, Part B: Hydrology, Oceans and Atmosphere 24, no. 1 (1999): 19-22.

[45] Hong, Song-You, and Hua-Lu Pan. "Nonlocal boundary layer vertical diffusion in a medium-range forecast model." Monthly weather review 124, no. 10 (1996): 2322-2339.

[46] Huntington, Thomas G. "Evidence for intensification of the global water cycle: review and synthesis." Journal of Hydrology 319, no. 1 (2006): 83-95.

[47] Ingram, Keith T., Kirstin Dow, Lynne Carter, and Julie Anderson, eds. Climate of the Southeast United States: Variability, change, impacts, and vulnerability. Island Press, 2013.

[48] Jackson, Robert B., Stephen R. Carpenter, Clifford N. Dahm, Diane M. McKnight, Robert J. Naiman, Sandra L. Postel, and Steven W. Running. "Water in a changing world." Ecological applications 11, no. 4 (2001): 1027-1045.

[49] Janga Reddy, M., and Poulomi Ganguli. "Application of copulas for derivation of drought severity-duration-frequency curves." Hydrological Processes 26.11 (2012): 1672-1685.

[50] Jones, Philip D., and Anders Moberg. "Hemispheric and large-scale surface air temperature variations: An extensive revision and an update to 2001." Journal of Climate 16, no. 2 (2003): 206-223.

[51] Kanamaru, Hideki, and Masao Kanamitsu. "Scale-selective bias correction in a downscaling of global analysis using a regional model." Monthly weather review 135, no. 2 (2007): 334-350.

[52] Kanamitsu, Masao, Kei Yoshimura, Yoo-Bin Yhang, and Song-You Hong. "Errors of interannual variability and trend in dynamical downscaling of reanalysis." Journal of Geophysical Research: Atmospheres (1984-2012) 115, no. D17 (2010).

[53] Kanamitsu, Masao, Wesley Ebisuzaki, Jack Woollen, Shi-Keng Yang, J. J. Hnilo, M. Fiorino, and G. L. Potter. "NCEP-DOE AMIP-II reanalysis (R-2)." Bulletin of the American Meteorological Society 83, no. 11 (2002): 1631-1643.

[54] Karl, Thomas R. "The sensitivity of the Palmer drought severity index and Palmer's Z-index to their calibration coefficients including potential evapotranspiration." Journal of Climate and Applied Meteorology 25, no. 1 (1986): 77-86.

[55] Keyantash, John A., and John A. Dracup. "An aggregate drought index: Assessing drought severity based on fluctuations in the hydrologic cycle and surface water storage." Water Resources Research 40, no. 9 (2004).

[56] Keyantash, John, and John A. Dracup. "The quantification of drought: an evaluation of drought indices." Bulletin of the American Meteorological Society 83, no. 8 (2002): 1167-1180.

[57] Keyantash, John, and John A. Dracup. "The quantification of drought: an evaluation of drought indices." Bulletin of the American Meteorological Society 83, no. 8 (2002): 1167-1180.

[58] Khadr, Mosaad, Gerd Morgenschweis, and Andreas Schlenkhoff. "Analysis of meteorological drought in the Ruhr basin by using the standardized precipitation index." World Academy of Science, Engineering and Technology 57 (2009): 607-616.

[59] Komuscu, A. U. "Using the SPI to analyze spatial and temporal patterns of drought in Turkey." Drought Network News 11, no. 1 (1999): 7-13.

[60] Łabedzki, Leszek. "Estimation of local drought frequency in central Poland using the standardized precipitation index SPI." Irrigation and Drainage 56, no. 1 (2007): 67-77.

[61] Lana, Xavier, Cesar Serra, and Augusto Burgueo. "Patterns of monthly rainfall shortage and excess in terms of the standardized precipitation index for Catalonia (NE Spain)." International Journal of Climatology 21, no. 13 (2001): 1669-1691.

[62] Li, Wenhong, Rong Fu, Robinson I. Negron Juarez, and Katia Fernandes. "Observed change of the standardized precipitation index, its potential cause and implications to future climate change in the Amazon region." Philosophical Transactions of the Royal Society B: Biological Sciences 363, no. 1498 (2008): 1767-1772.

[63] Livada, I., and V. D. Assimakopoulos. "Spatial and temporal analysis of drought in Greece using the Standardized Precipitation Index (SPI)." Theoretical and applied climatology 89, no. 3-4 (2007): 143-153.

[64] Loveland, T. R., B. C. Reed, J. F. Brown, D. O. Ohlen, Z. Zhu, L. W. M. J. Yang, and J. W. Merchant. "Development of a global land cover characteristics database and IGBP DISCover from 1 km AVHRR data." International Journal of Remote Sensing 21, no. 6-7 (2000): 1303-1330.

[65] Loveland, Thomas R., James W. Merchant, Jesslyn F. Brown, Donald O. Ohlen, Bradley C. Reed, Paul Olson, and John Hutchinson. "Seasonal land-cover regions of the United States." Annals of the Association of American Geographers 85, no. 2 (1995): 339-355.

[66] Manuel, J., 2008: Drought in the Southeast: Lessons for Water Management. Environmental Health Perspectives, 116, A168-A171.

[67] Mavromatis, T. "Drought index evaluation for assessing future wheat production in Greece." International Journal of Climatology 27, no. 7 (2007): 911-924.

[68] McEvoy, Daniel J., Justin L. Huntington, John T. Abatzoglou, and Laura M. Edwards. "An evaluation of multiscalar drought indices in Nevada and Eastern California." Earth Interactions 16, no. 18 (2012): 1-18.

[69] McKee, Thomas B., Nolan J. Doesken, and John Kleist. "Drought monitoring with multiple time scales." In Ninth Conference on Applied Climatology. American Meteorological Society, Boston. 1995.

[70] McKee, Thomas B., Nolan J. Doesken, and John Kleist. "The relationship of drought frequency and duration to time scales." In Proceedings of the 8th Conference on Applied Climatology, vol. 17, no. 22, pp. 179-183. Boston, MA: American Meteorological Society, 1993.

[71] Meehl, G. A. "Coauthors, 2007: Global climate projections. Climate Change 2007: The Physical Science Basis, S. Solomon et al., Eds."

[72] Milano, Marianne, Denis Ruelland, Sara Fernandez, Alain Dezetter, Julie Fabre, and Eric Servat. "Facing climatic and anthropogenic changes in the Mediterranean basin: What will be the medium-term impact on water stress?" Comptes Rendus Geoscience 344, no. 9 (2012): 432-440.

[73] Min, Seung-Ki, Won-Tae Kwon, E. Park, and Youngeun Choi. "Spatial and temporal comparisons of droughts over Korea with East Asia." International Journal of Climatology 23, no. 2 (2003): 223-233.

[74] Mishra, A. K., and V. P. Singh. "Development of drought SAF curves." Hydrology and hydraulics. Water Resources Publications, Highlands Ranch (2008): 811-831.

104

[75] Mishra, A. K., and V. R. Desai. "Drought forecasting using stochastic models." Stochastic Environmental Research and Risk Assessment 19, no. 5 (2005): 326-339.

[76] Mishra, A. K., and V. R. Desai. "Spatial and temporal drought analysis in the Kansabati river basin, India." International Journal of River Basin Management 3, no. 1 (2005): 31-41.

[77] Mishra, A. K., and Vijay P. Singh. "Analysis of drought severity-area-frequency curves using a general circulation model and scenario uncertainty." Journal of Geophysical Research: Atmospheres (1984-2012) 114, no. D6 (2009).

[78] Mishra, Ashok K., and Vijay P. Singh. "A review of drought concepts." Journal of Hydrology 391, no. 1 (2010): 202-216.

[79] Mishra, Ashok K., and Vijay P. Singh. "Drought modeling - A review." Journal of Hydrology 403, no. 1 (2011): 157-175.

[80] Misra, Vasubandhu, Lauren Moeller, Lydia Stefanova, Steven Chan, James J. O'Brien, Thomas J. Smith, and Nathaniel Plant. "The influence of the Atlantic Warm Pool on the Florida panhandle sea breeze." Journal of Geophysical Research: Atmospheres (1984-2012) 116, no. D21 (2011).

[81] National Oceanic and Atmospheric Administration. "Responding to Extreme Weather and Climate Events." Accessed June 7, 2015. http://cpo.noaa.gov/sites/cpo/Projects/SARP/Extreme_Weather_Factsheet_Compendium.final7.19.13.pdf.

[82] Pai, D. S., Latha Sridhar, Pulak Guhathakurta, and H. R. Hatwar. "District-wide drought climatology of the southwest monsoon season over India based on standardized precipitation index (SPI)." Natural hazards 59, no. 3 (2011): 1797-1813.

[83] Pan H.-L., W.-S. Wu. "Implementing a mass-flux convective parameterization package for the NMC Medium Range Forecast Model." Preprints, 10th Conference on Numerical Weather Prediction, Portland, OR, American Meteorological Society, pp96-98. , 1994

[84] Pan, H-L., and L. Mahrt. "Interaction between soil hydrology and boundary-layer development." Boundary-Layer Meteorology 38, no. 1-2 (1987): 185-202.

[85] Paulo, Ana A., and Luis S. Pereira. "Prediction of SPI drought class transitions using Markov chains." Water resources management 21, no. 10 (2007): 1813-1827.

[86] Paulson, R.W., E.B. Chase, R.S. Roberts, and D.W. Moody. National Water Summary 1988-89: Hydrologic Events and Floods and Droughts. Water Supply Paper. Washington, D.C., 1991. USGS Publications Warehouse. http://pubs.er.usgs.gov/publication/wsp2375.

[87] Postel, Sandra L., Gretchen C. Daily, and Paul R. Ehrlich. "Human appropri-
ation of renewable fresh water." Science-AAAS-Weekly Paper Edition 271, no.
5250 (1996): 785-787.

[88] Ross, Tom, and Neal Lott. A climatology of 1980-2003 extreme weather and
climate events. US Department of Commerce, National Ocanic and Atmospheric
Administration, National Environmental Satellite Data and Information Service,
National Climatic Data Center, 2003.

[89] Ruhl, J. B. "Water Wars, Eastern Style: Divvying Up the Apalachicola-
Chattahoochee-Flint River Basin." Journal of Contemporary Water Research
& Education 131, no. 1 (2005): 47-54.

[90] S. Solomon et al., Eds. "Climate Change 2007: The Physical Science Basis.
Contribution of Working Group I to the Fourth Assessment Report of the Inter-
governmental Panel on Climate Change." (Cambridge Univ. Press, Cambridge,
2007).

[91] Seager, Richard, Alexandrina Tzanova, and Jennifer Nakamura. "Drought in the
southeastern United States: causes, variability over the last millennium, and the
potential for future hydroclimate change*." Journal of Climate 22, no. 19 (2009):
5021-5045.

[92] Sheffield, Justin, and Eric F. Wood. "Projected changes in drought occurrence
under future global warming from multi-model, multi-scenario, IPCC AR4 sim-
ulations." Climate dynamics 31, no. 1 (2008): 79-105.

[93] Sheffield, Justin, Eric F. Wood, and Michael L. Roderick. "Little change in global
drought over the past 60 years." Nature 491, no. 7424 (2012): 435-438.

[94] Slingo, J. M. "The development and verification of a cloud prediction scheme
for the ECMWF model." Quarterly Journal of the Royal Meteorological Society
113, no. 477 (1987): 899-927.

[95] Sohn, Soo-Jin, Chi-Yung Tam, and Joong-Bae Ahn. "Development of a
multimodel-based seasonal prediction system for extreme droughts and floods:
a case study for South Korea." International Journal of Climatology 33, no. 4
(2013): 793-805.

[96] Solomon, Susan, ed. Climate change 2007-the physical science basis: Working
group I contribution to the fourth assessment report of the IPCC. Vol. 4. Cam-
bridge University Press, 2007.

[97] Soulé, Peter T. "Spatial patterns of drought frequency and duration in the con-
tiguous USA based on multiple drought event definitions." International Journal
of Climatology 12, no. 1 (1992): 11-24.

[98] Stefanova, Lydia, Vasubandhu Misra, Steven Chan, Melissa Griffin, James J. O'Brien, and Thomas J. Smith III. "A proxy for high-resolution regional reanalysis for the Southeast United States: assessment of precipitation variability in dynamically downscaled reanalyses." Climate dynamics 38, no. 11-12 (2012): 2449-2466.

[99] Steinemann, Anne. "Drought indicators and triggers: A stochastic approach to evaluation." (2003): 1217-1233.

[100] Stooksbury, David Emory. "Historical droughts in Georgia and drought assessment and management." (2003).

[101] Tannehill, Ivan Ray. "Drought, its causes and effects." Soil Science 64, no. 1 (1947): 83.

[102] Thomas R. Karl, Jerry M. Melillo, and Thomas C. Peterson, (eds.).: Global Climate Change Impacts in the United States. Cambridge University Press, 2009.

[103] Tsakiris, G., and H. Vangelis. "Establishing a drought index incorporating evapotranspiration." European Water 9, no. 10 (2005): 3-11.

[104] Tsakiris, G., and H. Vangelis. "Towards a drought watch system based on spatial SPI." Water Resources Management 18.1 (2004): 1-12.

[105] Tsakiris, G., D. Pangalou, and H. Vangelis. "Regional drought assessment based on the Reconnaissance Drought Index (RDI)." Water resources management 21, no. 5 (2007): 821-833.

[106] U.S. Army Corps of Engineers, South Atlantic Division, Mobile District. Drought contingency plan for Apalachicola-Chattahoochee-Flint River Basin (Buford Dam and Lake Lanier, West Point Dam and Lake Walter F. George Lock and Dam and Reservoir, Jim Woodruff Lock and Dam and Lake Seminole. March 2011.

[107] U. S. Geological Survey. "Droughts in Georgia." U.S. Geological Open-File Report 00-380. October 2000.
http://pubs.usgs.gov/of/2000/0380/pdf/ofr00-380.pdf.

[108] U. S. Geological Survey. "Extreme Drought to Extreme Floods: Summary of Hydrologic Conditions in Georgia, 2009." Fact Sheet 2010-3101. October 2010.
http://pubs.usgs.gov/fs/2010/3101/pdf/fs2010-3101.pdf.

[109] Uppala, Sakari M., P. W. Kllberg, A. J. Simmons, U. Andrae, V. Bechtold, M. Fiorino, J. K. Gibson et al. "The ERA-40 re-analysis." Quarterly Journal of the Royal Meteorological Society 131, no. 612 (2005): 2961-3012.

[110] Vicente-Serrano, Sergio M., and J. M. Cuadrat-Prats. "Trends in drought intensity and variability in the middle Ebro valley (NE of the Iberian Peninsula) during the second half of the twentieth century." Theoretical and Applied Climatology 88, no. 3-4 (2007): 247-258.

[111] Vicente-Serrano, Sergio M., Santiago Beguería, and Juan I. López-Moreno. "A multiscalar drought index sensitive to global warming: the standardized precipitation evapotranspiration index." Journal of Climate 23, no. 7 (2010): 1696-1718.

[112] Weakly, Harry E. "Recurrence of drought in the Great Plains during the last 700 years." Agricultural Engineering 46 (1965): 85.

[113] Weber, Lena, and Lawrence Nkemdirim. "Palmer's drought indices revisited." Geografiska Annaler: Series A, Physical Geography 80, no. 2 (1998): 153-172.

[114] Wells, Nathan, Steve Goddard, and Michael J. Hayes. "A self-calibrating Palmer drought severity index." Journal of Climate 17, no. 12 (2004): 2335-2351.

[115] Wilhite, Donald A. Drought assessment, management and planning: theory and case studies. Kluwer Academic Publishers, 1993.

[116] Wilhite, Donald A., and Michael H. Glantz. "Understanding: the drought phenomenon: the role of definitions." Water international 10, no. 3 (1985): 111-120.

[117] Wilhite, Donald A., and Michael J. Hayes. "Drought planning in the United States: Status and future directions." In The arid frontier, pp. 33-54. Springer Netherlands, 1998.

[118] Wilhite, Donald A., ed. Drought and water crises: science, technology, and management issues. CRC Press, 2014.

[119] Wilhite, Donald A., ed. Drought: a global assessment. Routledge, 2001.

[120] Wolf JF, Abatzoglou J. 2011. "The suitability of drought metrics historically and under climate change scenarios." 47th Annual Water Resources Conference, Albuquerque, NM, 7 - 10 November 2011.

[121] Wolf, Jacob W. "Evaluation of Drought Metrics in Tracking Streamflow in Idaho" (Master's Thesis, University of Idaho, 2012)

[122] Wood, Andrew W., Edwin P. Maurer, Arun Kumar, and Dennis P. Lettenmaier. "Long-range experimental hydrologic forecasting for the eastern United States." Journal of Geophysical Research: Atmospheres (1984-2012) 107, no. D20 (2002): ACL-6.

[123] World Meteorological Organization, 1975a, Drought and Agriculture, 127 pp. (Geneva: WMO).

[124] Wu, Hong, Michael J. Hayes, Albert Weiss, and Qi Hu. "An evaluation of the Standardized Precipitation Index, the China-Z Index and the statistical Z-Score." International journal of climatology 21, no. 6 (2001): 745-758.

[125] Yoshimura, Kei, Masao Kanamitsu, and Michael Dettinger. "Regional downscaling for stable water isotopes: A case study of an atmospheric river event." Journal of Geophysical Research: Atmospheres (1984-2012) 115, no. D18 (2010).

[126] Yu, Meixiu, Qiongfang Li, Michael J. Hayes, Mark D. Svoboda, and Richard R. Heim. "Are droughts becoming more frequent or severe in China based on the standardized precipitation evapotranspiration index: 1951-2010?" International Journal of Climatology 34, no. 3 (2014): 545-558.

[127] Zhang, Qiang, Chong-Yu Xu, and Zengxin Zhang. "Observed changes of drought/wetness episodes in the Pearl River basin, China, using the standardized precipitation index and aridity index." Theoretical and Applied Climatology 98, no. 1-2 (2009): 89-99.

Appendices

<center>Appendix A</center>

<center>Standardized Precipitation Index</center>

A.1 Stepwise procedure to calculate the SPI

1. The mean of the precipitation is computed.

$$Mean, \overline{X} = \frac{\sum X}{N}$$

   N is the number of precipitation observations.

2. The standard deviation of the precipitation is calculated.

$$StandardDeviation, s = \sqrt{\frac{\sum (X - \overline{X})^2}{N}}$$

3. Then, the skewness of the precipitation is computed.

$$Skew = \frac{N}{(N-2)(N-1)} \sum \left(\frac{X - \overline{X}}{s}\right)^3$$

4. The precipitation is converted into log-normal values to compute the statistic U and shape parameter β and scale parameter α.

$$Logmean = \overline{X}_{ln} = ln\overline{X}$$

$$U = \overline{X}_{ln} - \left(\frac{\sum ln(X)}{N}\right)$$

$$ShapeParameter, \beta = \frac{1 + \sqrt{1 + \frac{4U}{3}}}{4U}$$

$$ScaleParameter, \alpha = \frac{\overline{X}}{\beta}$$

5. From these parameters, the cumulative probability is calculated.

<center>111</center>

$$G(x) = \frac{\int_0^x x^{\alpha-1} e^{\frac{-x}{\beta}} dx}{\beta^\alpha \Gamma(\alpha)}$$

6. As the cumulative probability will be undefined for x=0 and there may exist precipitation with values consisting 0, the cumulative probability is modified as:

$$H(x) = q + (1 - q)G(x)$$

Where, q is the probability of no rainfall in the timescale used.

7. From H(x), the SPI is calculated as:

$$SPI = -\left(t - \frac{c_0 + c_1 t + c_2 t^2}{1 + d_1 t + d_2 t^2 + d_3 t^3}\right) \qquad For\, 0 < H(x) < 1$$

$$SPI = +\left(t - \frac{c_0 + c_1 t + c_2 t^2}{1 + d_1 t + d_2 t^2 + d_3 t^3}\right) \qquad For\, 0.5 < H(x) < 1$$

Where,

$$t = \sqrt{ln\left(\frac{1}{(1 - H(x))^2}\right)} \qquad For\, 0 < H(x) < 0.5$$

$$t = \sqrt{ln\left(\frac{1}{H(x)^2}\right)} \qquad For\, 0.5 < H(x) < 1$$

$$c_0 = 2.515517 \qquad c_1 = 0.802583 \qquad c_2 = 0.010328$$

$$d_1 = 1.432788 \qquad d_2 = 0.189269 \qquad d_3 = 0.001308$$

Appendix B

Standardized Precipitation Evapotranspiration Index

B.1 Stepwise procedure to calculate the SPEI

1. Moisture departure (D) is calculated as the difference between the monthly values of potential evapotranspiration and precipitation.

$$D_i = P_i - PET_i$$

2. In the calculation of SPI, gamma distribution was used to model precipitation probability. For the calculation of SPEI, log-logistic distribution is used. To start off with modeling the distribution, probability-weighted moments, w, for various orders s, is calculated.

$$w_s = \frac{1}{N} \sum_i^N (1 - F_i)^s D_i$$

F_i is calculated as:

$$F_i = \frac{i - 0.35}{N}$$

N is the number of data points and i is the range of observations arranged in increasing order. From the values of w_s, the L-moments λ_1, λ_2, λ_3 and λ_4 can be calculated as:

$$\lambda_1 = w_0$$

$$\lambda_2 = w_0 - 2w_1$$

$$\lambda_3 = w_0 - 6w_1 + 6w_2$$

$$\lambda_4 = w_0 - 12w_1 + 30w_2 - 20w_3$$

3. The probability density function of a three parameter Log-logistic distributed variable is expressed as:

$$f(x) = \frac{\beta}{\alpha} \left(\frac{x - \gamma}{\alpha} \right)^{\beta - 1} \left(1 + \left(\frac{x - \gamma}{\alpha} \right)^{\beta} \right)^{-2}$$

Where α, β and γ are scale, shape and origin parameters respectively. They can be calculated as:

$$\beta = \frac{\lambda_2}{\lambda_3}$$

$$\alpha = \frac{}{\Gamma(1 + \frac{1}{\beta})\Gamma(1 - \frac{1}{\beta})}$$

$$\gamma = w_0 - \alpha\Gamma\left(1 + \frac{1}{\beta}\right)\Gamma\left(1 - \frac{1}{\beta}\right)$$

4. Now, the probability distribution function of the D series according to the log-logistic distribution is given by the following formula:

$$F(x) = \left[1 + \left(\frac{\alpha}{x - y}\right)^{\beta}\right]^{-1}$$

5. The SPEI can now be calculated by the following formula:

$$SPEI = W - \left(\frac{c_0 + c_1 W + c_2 W^2}{1 + d_1 W + d_2 W^2 + d_3 W^3}\right) \qquad For\, 0.5 < H(x) < 1$$

$W = \sqrt{-2 ln P}$, Where, the probability P of exceeding a given D value is given by $P = 1 - F(x)$ for $P0.5$. If $P > 0.5$, P is replaced by $1 - P$ which in turn reverses the sign of the calculated value of SPEI.

$$c_0 = 2.515517 \qquad c_1 = 0.802583 \qquad c_2 = 0.010328$$

$$d_1 = 1.432788 \qquad d_2 = 0.189269 \qquad d_3 = 0.001308$$

Appendix C

Potential Evapotranspiration

C.1   Thornthwaite Method to compute PET

Potential evapotranspiration is computed as:

$$PE = 16K \left(\frac{10T}{I} \right)^m$$

Where, T is the monthly mean temperature in °C; I is a heat index (the sum of 12 monthly index values i, which is derived from mean monthly temperature)

$$i = \left(\frac{T}{5} \right)^{1.514}$$

m is a coefficient calculated as:

$$m = 6.75E^{-7}I^3 - 7.71E^{-5}I^2 + 1.79E^{-2}I + 0.49239$$

K is the correction coefficient, which is a function of the latitude and month. It is calculated as:

$$K = \left(\frac{N}{12} \right) \left(\frac{NDM}{30} \right)$$

N is the maximum number of sun hours and NDM is the number of days in the month being considered.

$$N = \left(\frac{24}{\pi} \right) \overline{\omega_s}$$

$\overline{\omega_s}$ is the hourly angle of sun rising given by $\overline{\omega_s} = \arccos(-\tan\phi\tan\delta)$
ϕ is the latitude in radians and δ is the solar declination in radians calculated as:

$$\delta = 0.4093 \sin\left(\frac{2\pi J}{365} - 1.405 \right)$$

J is the average Julian Day of the month.

Appendix D

Probability Distributions

D.1 Gamma Distribution

The gamma distribution is a continuous probability distributions with shape and scale parameters.

D.1.1 Probability Density Function

The general formula for the probability density function of the gamma distribution is

$$f(x) = \frac{\left(\frac{x-\mu}{\beta}\right)^{\gamma-1} e^{-\frac{x-\mu}{\beta}}}{\beta \Gamma(\gamma)}$$

$$x \geq \mu \text{ and } \gamma, \beta > 0$$

Where, γ is the shape parameter, μ is the location parameter, β is the scale parameter, and Γ is the gamma function.

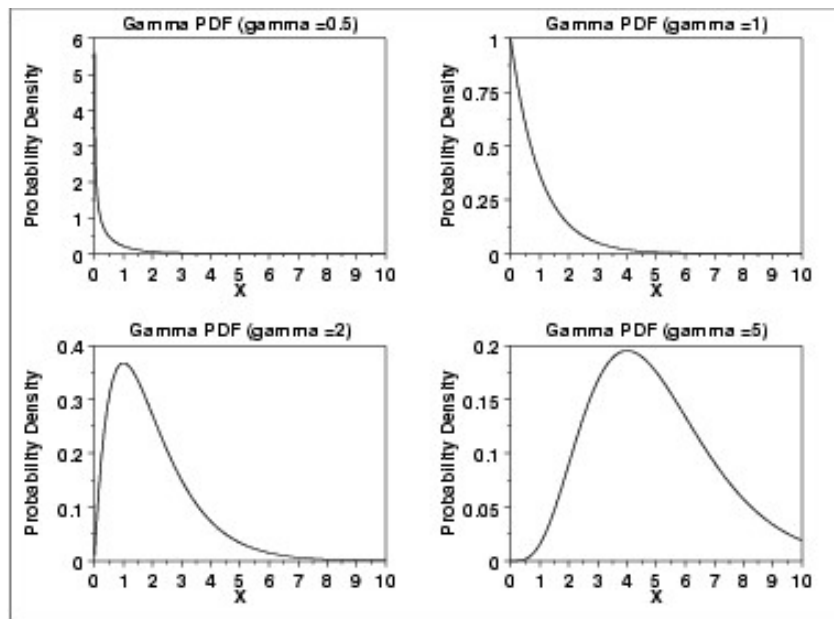The plot for gamma probability density function is given below:

Figure D.1: Gamma probability density function for different values of gamma.

The gamma function has the following formula:

$$\Gamma(a) = \int_0^\infty t^{a-1} e^{-t} dt$$

The case where $\mu = 0$ and $\beta = 1$ is called the standard gamma distribution. The equation for the standard gamma distribution reduces to

$$f(x) = \frac{x^{\gamma-1} e^{-x}}{\Gamma(\gamma)}$$

$$x \geq 0 \text{ and } \gamma > 0$$

D.1.2   Cumulative Distribution Function

The formula for the cumulative distribution function of the gamma distribution is

$$F(x) = \frac{\Gamma_x(\gamma)}{\Gamma(\gamma)}$$

$$x \geq 0 \text{ and } \gamma > 0$$

Where Γ is the gamma function defined above and $\Gamma_x(\gamma)$ is the incomplete gamma function.

The following is the plot of the gamma cumulative distribution function with the same values of γ as the probability density function plots above.
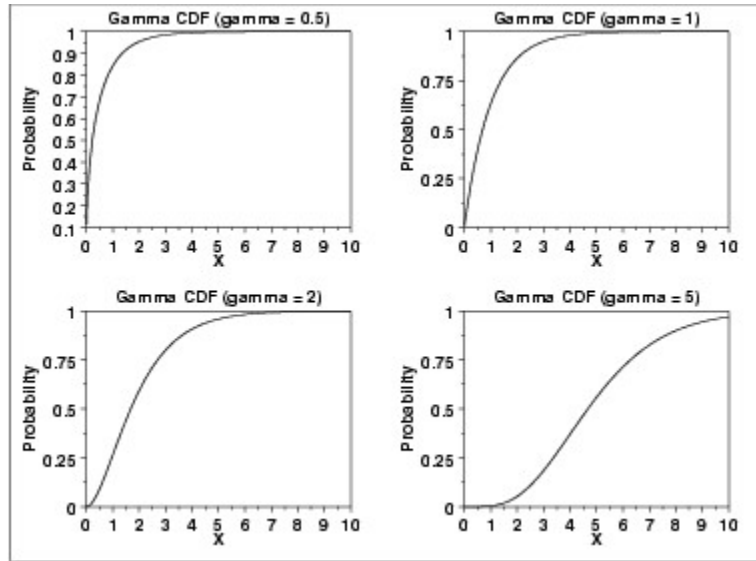

Figure D.2: Gamma cumulative distribution function plots for different values of gamma.

The incomplete gamma function has the formula

$$\Gamma_x(a) = \int_0^x t^{a-1} e^{-t} dt$$

D.2   Three Parameter Log-logistic Distribution

The log-logistic distribution is a probability distribution in which the logarithm has a logistic distribution.

D.2.1   Probability Density Function

The general formula for the probability density function of three parameter log-logistic distribution is

$$f(x) = \frac{\beta}{\alpha}\left(\frac{x-\gamma}{\alpha}\right)^{\beta-1}\left(1+\left(\frac{x-\gamma}{\alpha}\right)^{\beta}\right)^{-2}$$

$$\alpha > 0 \ , \ x > \gamma \ , \ \gamma, \beta \geq 1$$

Where α, β and γ are scale, shape and origin parameters respectively. They can be calculated as:

$$\beta = \frac{\lambda_2}{\lambda_3}$$

$$\alpha = \frac{}{\Gamma(1+\frac{1}{\beta})\Gamma(1-\frac{1}{\beta})}$$

$$\gamma = w_0 - \alpha\Gamma\left(1+\frac{1}{\beta}\right)\Gamma\left(1-\frac{1}{\beta}\right)$$

Probability-weighted moments, w, for order s, are calculated as:

$$w_s = \frac{1}{N}\sum_i^N (1-F_i)^s D_i$$

F_i is calculated as:

$$F_i = \frac{i-0.35}{N}$$

N is the number of data points and i is the range of observations arranged in increasing order. From the probability-weighted moments of w_s, the L-moments λ_1, λ_2, λ_3 and λ_4 can be calculated as:

$$\lambda_1 = w_0$$

$$\lambda_2 = w_0 - 2w_1$$

$$\lambda_3 = w_0 - 6w_1 + 6w_2$$

$$\lambda_4 = w_0 - 12w_1 + 30w_2 - 20w_3$$

D.2.2 Cumulative Distribution Function

The formula for the cumulative distribution function of three-parameter log-logistic distribution is:

$$F(x) = \left[1 + \left(\frac{\alpha}{x - y} \right)^{\beta} \right]^{-1}$$

$$x \geq 0 \text{ and } \gamma > 0$$

D.3 Extreme Value Type-I Distribution

Extreme Value Type I distribution can either be based on the smallest extreme (minimum case) or the largest extreme (maximum case). The distribution is also commonly known as the Gumbel distribution.

D.3.1 Probability Density Function

The probability density function of the Gumbel (minimum) distribution is generalized by:

$$f(x) = \frac{1}{\beta} e^{\frac{x - \mu}{\beta}} e^{-e^{\frac{x - \mu}{\beta}}}$$

Where, μ is the location parameter and β is the scale parameter.
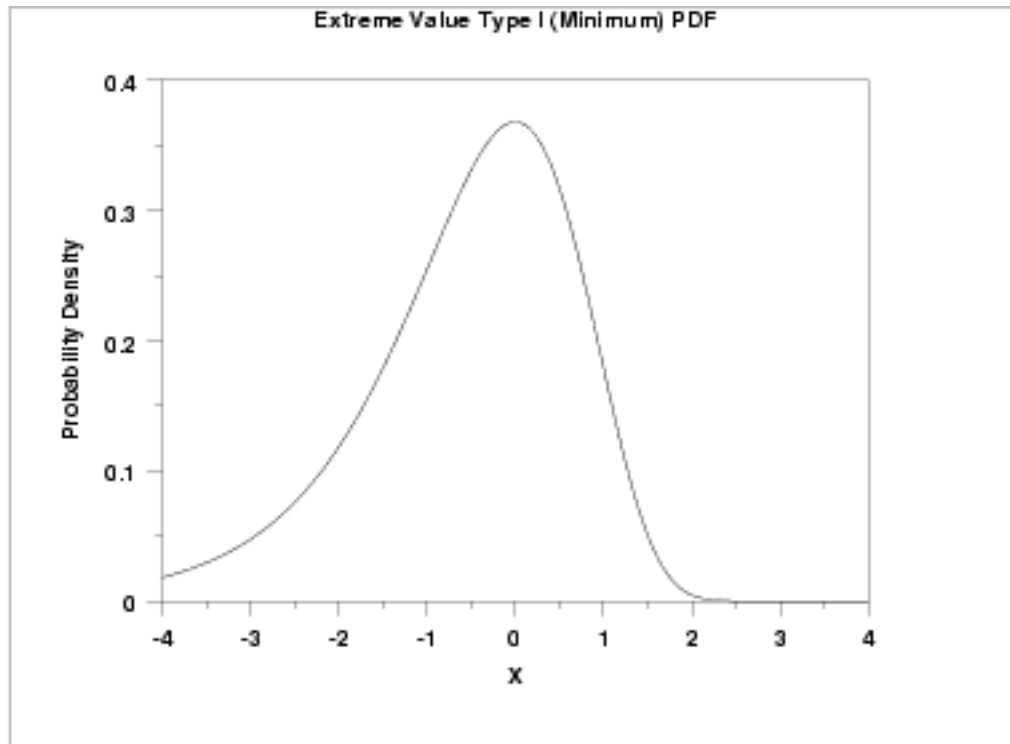

Figure D.3: The plot of Gumbel probability density function for minimum case.

When $\mu = 0$ and $\beta = 1$, it is called the standard Gumbel distribution. Upon substitution of the values, the general equation for the standard Gumbel distribution (minimum) reduces to:

$$f(x) = e^x e^{-e^x}$$

The probability density function of the Gumbel (maximum) distribution is generalized by:

$$f(x) = \frac{1}{\beta} e^{-\frac{x-\mu}{\beta}} e^{-e^{\frac{x-\mu}{\beta}}}$$

Where, μ is the location parameter and β is the scale parameter. When $\mu = 0$ and $\beta = 1$, the distribution is called the standard Gumbel distribution. Substitution of these values reduce the equation for the standard Gumbel distribution (maximum) to:

$$f(x) = e^{-x} e^{-e^x}$$

D.3.2 Cumulative Distribution Function

The cumulative distribution function of the Gumbel distribution (minimum) is given by:

$$F(x) = 1 - e^{-e^x}$$

The plot of Gumbel cumulative distribution function for minimum case is shown below:
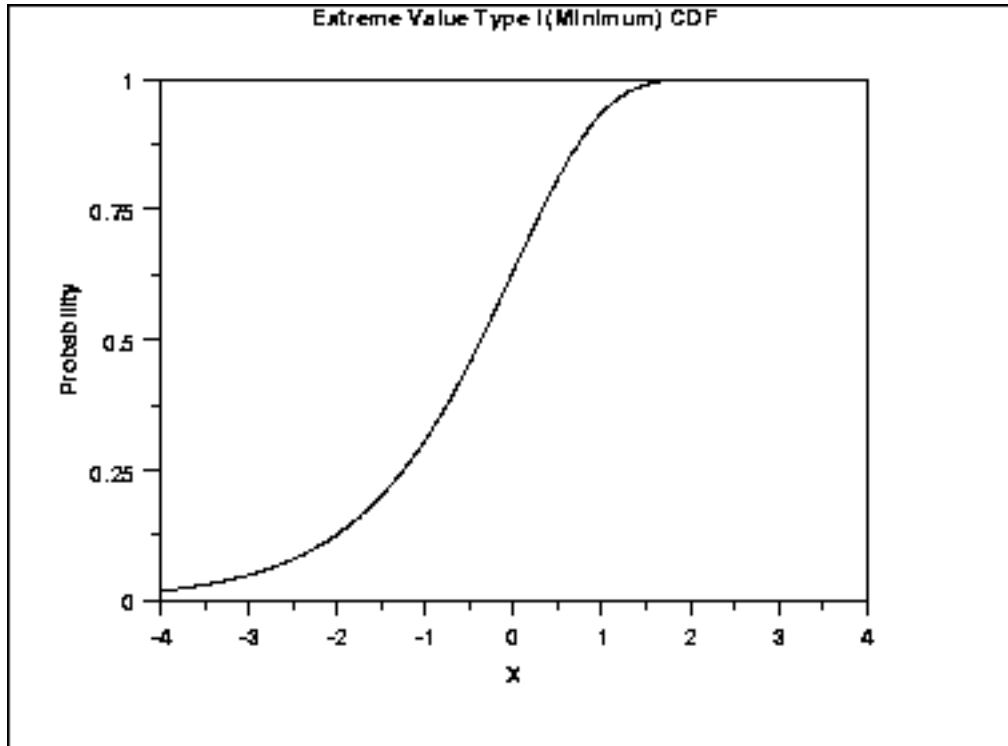

Figure D.4: Gumbel cumulative distribution function for minimum case.

The cumulative distribution function of the Gumbel distribution (maximum) is given by:

$$F(x) = e^{-e^{-x}}$$

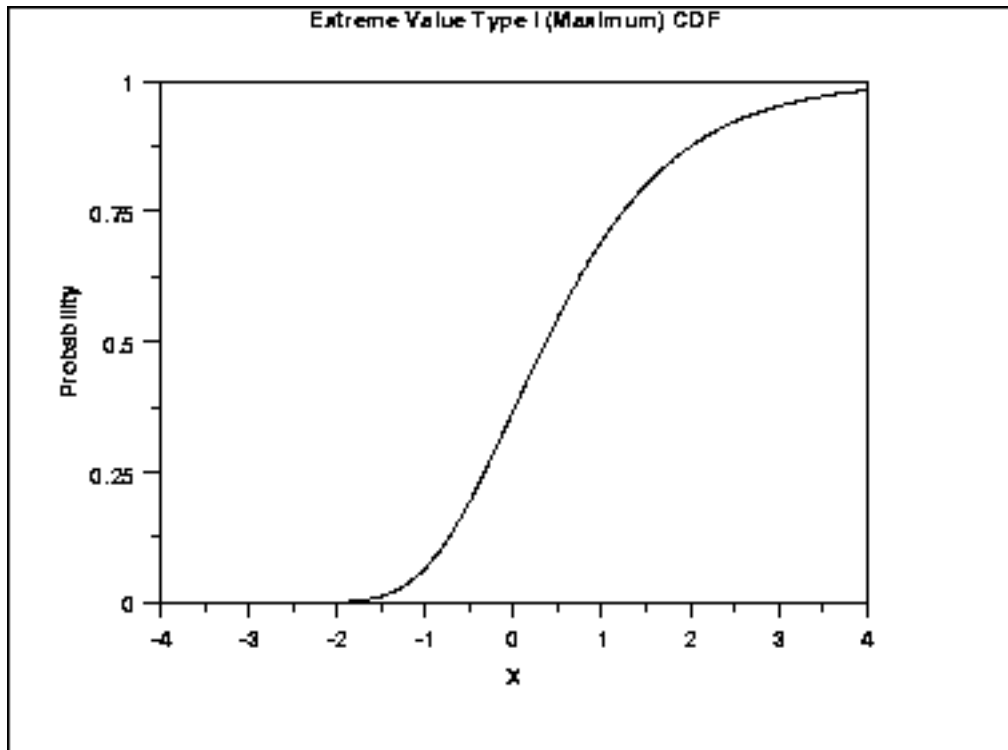The plot of Gumbel cumulative distribution function for the maximum case is shown below.

Figure D.5: Gumbel cumulative distribution function for the maximum case.